4-2024

Eureka Littoral Cell Updated Tributary Sand Loads and Sand Budget

Northern Hydrology & Engineering

Eureka Littoral Cell

Updated Tributary Sand Loads and Sand Budget

Prepared for

Friends of the Dunes

California State Coastal Conservancy

April 2024

Prepared by

Northern Hydrology & Engineering

Northern
Hydrology &
Engineering

Table of Contents

1 Introduction 1
1.1 Objectives 1
1.2 Acknowledgements 2
2 Study Area 3
3 Methods 5
3.1 Fluvial Sand Loads 5
3.1.1 Data 5
3.1.2 Analysis 7
3.1.2.1 Suspended Sand Loads 7
3.1.2.2 Bedload Flux 10
3.1.2.3 Uncertainty Estimation 10
3.2 ELC Sand Budget Analysis 11
3.2.1 General Sediment Budget Equation 11
3.2.2 ELC Sand Budget Unit Locations and Extents 12
3.2.3 ELC Sand Budget Term Definitions 13
3.2.4 Sand Budget Process Equations 14
3.2.5 ELC Sand Budget Uncertainty 15
3.2.6 ELC Sand Budget Analysis and Time Periods 16
3.2.6.1 Sand Budget for 1966-2001 Period 16
3.2.6.2 Time-Dependent Sand Budget for 1911-2018 Period 16
3.2.7 Common Sand Budget Variables 16
3.2.8 Relative Sea-Level Change Rate and Acceleration 17
3.2.9 Sand Budget Input Terms 19
3.2.9.1 Fluvial Sand Load (Q_R) 19
3.2.9.2 Bluff Erosion (Q_B) 19
3.2.10 Sand Budget Output Terms 20
3.2.10.1 Shoreline Sand Loss from Sea-Level Rise (Q_{SLS}) 20
3.2.10.2 Estuary Sand Loss from Sea-Level Rise (Q_{SLE}) 20
3.2.11 Sand Budget Storage Change Terms 20
3.2.11.1 Shoreline Volume Change (ΔS_S) 20
3.2.11.2 Inner-Shelf Volume Change (ΔS_{IS}) 22
3.2.12 Sand Budget Removal/Extraction Terms 26
3.2.12.1 Fluvial Sand/Gravel Extraction (R_R) 26
3.2.12.2 Humboldt Bay Sand Dredging (R_{HB}) 28
3.2.13 Sand Budget Placement Terms 29
3.2.13.1 Sand Placement (P_B) 29
4 Results and Discussion 31
4.1 Fluvial Sand Loads 31

4.1.1 Trends in Fluvial Sand Loads 32
4.1.2 Dynamic vs. Static Rating Curves 33
4.1.3 Uncertainty in Fluvial Sand Loads 33
4.1.4 Comparison of Bedload Approaches 34
4.2 Fluvial Sand/Gravel Extraction and Humboldt Bay Dredging 35
4.3 ELC Sand Budget 36
4.3.1 Sand Budget for 1966-2001 Period 36
4.3.1.1 Sand Budget Inputs and Placed Material (+ Terms) 38
4.3.1.2 Sand Budget Outputs, Material Removed, and Volume Change (- Terms) 38
4.3.1.3 1966-2001 Sand Budget Uncertainty 38
4.3.1.4 Comparison to Other ELC Sand Budgets 40
4.3.1.5 Sand Loss from the ELC 41
4.3.2 Time-Dependent Sand Budget for 1911-2018 Period 44
4.3.2.1 Time-Dependent Sand Budget Analysis with Sand Disposal at HOODS (Existing Conditions) 44
4.3.2.2 Time-Dependent Sand Budget Analysis with No HOODS Disposal (Hypothetical Case) 47
4.3.2.3 Comparison of Cumulative Mean Annual Sand Residual 49
5 Summary 51
6 References 53

List of Figures

Figure 1. Map indicating the location of the Eureka Littoral Cell, nine coastal subbasins and stream gages used in this study. Colored circles indicate the flow and sediment data available at each gage. 4

Figure 2. Annual frequency of flow and suspended sediment sampling in the study subbasins. 6

Figure 3. Relations between area-normalized river discharge and fluvial suspended sediment concentration for the sand fraction (>= 125μm) for the Eel River, Van Duzen River, Mad River and Redwood Creek. 8

Figure 4. A) Relation between river discharge and suspended sediment concentration for the sand fraction (>=125μm) for the Eel River at the Scotia Station (11477000). Additional flow and SSC data from Goni et al. (2013) is depicted by black squares. LOESS fit curve is solid black line. Red and grey dashed lines represent block-bootstrapped 95% confidence and 90% prediction intervals, respectively. Solid light blue lines represent the 95% block-bootstrapped confidence interval iterations. Dashed grey vertical line indicates the highest observed discharge applied to the LOESS rating curve. B) Median residual ratios from the LOESS regression computed for each water year for the period 1950-2018. Dashed line represents an exponential decay model used to predict residual ratios for years with no data. C) Gap-filled residual ratios for the period 1910-2018. Dotted line represents period of no data for which residual ratios were computed as the mean of post-2000 ratios. 9

Figure 6. Sketch of materials (mass) balance 11

Figure 7. Location map of Eureka Littoral Cell (ELC) showing the extent of the littoral cell from Trinidad Head to False Cape; the location and extents of the shoreline, inner-shelf, and sandy estuaries; Humboldt Bay dredge disposal sites; and the nine tributaries used in the ELC sand budget 13

Figure 8. A) Annual regional sea level (ReSL) for the Humboldt Bay region fit with second-order polynomial resulting in a rate = 1.757 mm/yr and acceleration = 1.008E-6 m/yr^2 (2 x quadratic term). Results for single iteration of 10,000 Monte Carlo simulations for determining the relative sea-level (RSL) rate for the ELC; B) probability distribution of vertical land motion (VLM) for ELC; C) ensemble of RSL rates by combining the ReSL rate and acceleration, and VLM; and D) resulting probability distributions of RSL for 1910, 1965 and 2021. 18

Figure 9. Linear model fit of the median end point uncertainties versus the span in years between images used in the McDonald (2017) shoreline analysis. 22

Figure 10. Location of the five inner-shelf sub-environment zones (A, D/E, H/I/L, O/P, R/T) as defined by Crockett and Nittrouer (2004). These five zones were digitized (based on Figure 10 in Crockett and Nittrouer, 2004) between the -14 m (depth of closure) and the -50 m contour lines (referenced to NAVD88), which covers the inner-shelf area defined in this work. To cover the entire ELC inner-shelf we extended zone A (A-EXT) and zone R/T (RT-EXT) to the south and north ends of the ELC, respectively. 23

Figure 11. Linear model fit of the mean sand deposition rate (cm/yr) versus the mean mud deposition rate (cm/yr) for the inner-shelf zones A, D/E and H/I/L. 25

Figure 12. Power regression model fits of annual sand/gravel extraction volume fits for the Eel River and Mad River (A), and the Van Duzen River and Mad River (B) for the 1997 to 2018 period. 27

Figure 13. Annual fluvial sand/gravel extraction volumes (>= 125µm) for the Mad, Eel and Van Duzen Rivers for the 1997 to 2018 period, with CHERT oversight beginning in 1992. 27

Figure 14. Annual Humboldt Bay dredging volumes for sand (>= 125µm) for the 1911 to 2018 period. Dredge disposal to HOODS began in 1990, and the dredge deepening project started in 1999. 29

Figure 15. Gross fluvial sand flux (>= 125µm) to the Eureka Littoral Cell from the Eel, Van Duzen, Mad and Little Rivers from water years 1911-2018. Red line represents the gravel extraction rates (no extraction on Little River). Shaded region represents 90% prediction interval uncertainty bounds. Note the different vertical axis scales. 31

Table 12. Percent of total mean annual sand flux 32

Figure 16. Cumulative sand loads (>= 125µm) from all nine coastal subbasins in the ELC watershed computed using static and dynamic rating curves (both suspended sand load and bedload); as well as the bedload approach of 4% of the total suspended load (Slagel and Griggs, 2006), and the bedload as 100% of the total suspended sand load (Willis and Griggs, 2003). 34

Figure 17. Annual fluvial (fluvial) sand/gravel extraction, Humboldt Bay dredging, and combined extraction and dredging volumes for sand (>= 125µm) for the 1911 to 2018 period. The black dashed lines is the running 10-yr centered average for the combined volumes. Also shown are key dates for CHERT oversight of fluvial extraction (1992), dredge disposal to HOODS and outside the ELC (1990), and the dredge deepening project (1999) which increased annual dredge volumes. 36

Figure 18. Schematic diagram of Eureka littoral cell sand budget terms (sand >= 125µm) for mean annual volumes ± standard error (SE) for the 1966 to 2001 period. 37

Figure 19. Bar chart of the 1966-2001 the Eureka littoral cell sand budget (sand >= 125µm) showing mean annual volumes and 95% confidence intervals (CI) for all budget terms. Blue bars represent input or positive terms; brown are output or negative terms; and dune growth (red) is the residual from the sum of the input and output terms. 39

Figure 20. Simplified bar chart of Figure 19 for the 1966 to 2001 Eureka littoral cell sand budget (sand >= 125µm) showing mean annual volumes and 95% confidence intervals (CI). In this plot, Humbold Bay Dredging (HumBay Dredging) and River Extraction were combined into Dredging/Extraction; and Shoreline and Estuary relative sea-level (RSL) were combined into Shoreline/Estuary RSL. Blue bars are input or positive terms; brown is output or negative terms; and dune growth (red) is the residual from the sum of the input and output terms. 43

Figure 21. Time-dependent annual mean sand residual for the 1911-2018 sand budget analysis with the existing Humboldt Bay dredged sand disposal practices. The grey line is the annual mean residual, the red line is the 10-year centered average annual mean residual, and the 95% CI on the annual mean residual is the light red band. Also shown is the period of minimal SSC data (1911 to 1954), when dredge disposal to HOODS (out of the ELC) begins (1990), and the Humboldt Bay dredge deepening project (1999). 45

Figure 22. Time-dependent annual mean sand residual for the 1911-2018 sand budget analysis for the hypothetical case of Humboldt Bay dredged sand placement within the ELC after 1990 and no HOODS disposal. The grey line is the annual mean residual, the green line is the 10-year centered average annual mean residual, and the 95% CI is the light green band. Also shown is the period of minimal SSC data (1911 to 1954), when dredge disposal to HOODS (out of the ELC) begins (1990), and the Humboldt Bay dredge deepening project (1999). 48

Figure 23. Cumulative time-dependent annual mean sand residual for the 1911-2018 sand budget analysis for the two cases: (1) existing conditions with dredged sand placement within the ELC prior to 1990 and disposal at HOODS out of the ELC after 1990 (green line and fill), and (2) hypothetical case of Humboldt Bay dredged sand placement within the ELC after 1990 and no HOODS disposal (red line and brown fill). Also shown is the period of minimal SSC data (1911 to 1954), when dredge disposal to HOODS (out of the ELC) begins (1990), and the Humboldt Bay dredge deepening project (1999). 50

List of Tables

Table 1. USGS gaging stations and gaging data used in this study. Apart from Redwood Creek, fluvial sediment flux was computed only for the ELC coastal subbasins. 6

Table 2. Miscellaneous sand budget probability distribution (PD) variables used in Monte Carlo simulation. 17

Table 3. Tide station relative sea level (RSL) and vertical land motion (VLM) rates and standard errors (SE) from Patton et al. (2023); VLM determined by differencing RSL and the regional (or absolute) sea level (ReSL) rate of 1.99 ± 0.16 mm/yr (Montillet et al., 2018); and the alongshore measured distance and SE (coefficient of variation = 0.5%) between stations in the ELC. Trinidad is at the north end of the ELC, and Crescent City is not in the ELC. 18

Table 4. Bluff erosion probability distribution (PD) variables used in Monte Carlo simulation. 20

Table 5. Estuary area probability distribution (PD) variables used in Monte Carlo simulation. 20

Table 6. Shoreline rate probability distribution (PD) variables used in Monte Carlo (MC) simulation for the period 1966-2001. 21

Table 7. Inner-shelf mud and sand probability distribution (PD) variables used in Monte Carlo simulation to determine deposition rates for the 1966-2001 period (36-years). Inner-shelf zone data from Table 1 in Crockett and Nittrouer (2004). Total Eel River loads estimated from Eel River rating curve and Van Duzen River stated annual loads in Sommerfield and Nittrouer (1999), and mud/sand fractions from Crockett and Nittrouer (2004). 24

Table 8. Inner-shelf sand storage probability distribution variables used in the Monte Carlo (MC) simulation for the period 1966-2001. Sand deposition rates were determined from an intermediate MC simulation using data from Table 7. Inner-shelf zone areas A and R/T were expanded (A-EXP, R/T-EXP) to cover the entire ELC (Figure 10). 26

Table 9. Fluvial sand/gravel extraction volume probability distribution (PD) variables used in Monte Carlo simulation. 28

Table 10. Interior channel probability distribution variables for an intermediate Monte Carlo (MC) simulation to determine the interior channel's sand fraction greater than 125µm. 30

Table 11. Humboldt Bay dredged sand volume probability distribution (PD) variables used in Monte Carlo simulation. 30

Table 12. Percent of total mean annual sand flux (>= 125µm) for tributary subbasins draining to the Eureka Littoral Cell during the periods 1911-2018 and 2009-2018. 32

Table 13. Average sand yields (>= 125µm) during select periods for the Eel, Van Duzen, Mad and Little Rivers from this study, as well as CRSMP (2017). CRSMP reported annual volumes converted to mass using 1,600 kg/m^3 32

Table 14. Total mean annual sand loads (>= 125µm) to the Eureka Littoral Cell computed using static vs. dynamic rating curves over select time periods. Percent (%) difference is relative to dynamic curve. 33

Table 15. Comparison of total mean annual sand loads (>= 125µm) from select subbasins for the period 1911 – 2018, where bedload was computed via regional bedload rating curve vs. 100% of the suspended sand load (Willis and Griggs, 2003). 35

Table 16. Total fluvial (Mad, Eel and Van Duzen Rivers) extraction volume per year, and the Humboldt Bay dredged sand volume per year for sand (>= 125μm) for select time periods. 36

Table 17. Eureka littoral cell sand budget (sand >= 125μm) results for the 1966 to 2001 period for each term. Results are provided for the mean annual volume, standard error (SE), coefficient of variation (CV), the 90% and 95% confidence intervals (CI), and the mean percent of each term to the total positive or negative terms. 37

Table 18. Comparison of Eureka Littoral Cell sand budgets for sand >= 125μm. Left side sand budget (white columns) is a combination of the Patsch and Griggs (2007) (PG2007) and CSMW (2017) (CSMW) information. Right side (grey columns) is the sand budget developed in this study (subset of Table 17). 41

Table 19. Eureka littoral cell sand budget (sand >= 125μm) results for the 1966 to 2001 period (Table 17) that combined shoreline change from RSL and estuary change from RSL into a single Estuary/Shoreline *RSL* term; and combined Humboldt Bay dredging and fluvial extraction to Dredging/Extraction term. Results are provided for the mean annual volume, standard error (SE), coefficient of variation (CV), the 90% and 95% confidence intervals (CI), and the mean percent of each term to the total positive or negative terms. 42

Table 20. Time-dependent annual mean sand residual (>= 125μm) for specific/combined terms from the 1911-2018 sand budget analysis for select time periods with the existing Humboldt Bay dredged sand disposal practices. 45

Table 21. Time-dependent annual mean sand residual (>= 125μm) for specific/combined terms from the 1911-2018 sand budget analysis for select time periods with the hypothetical case of Humboldt Bay dredged sand placement within the ELC after 1990 and no HOODS disposal. 48

1 INTRODUCTION

Coastal zones are dynamic environments that are home to a disproportionately large and ever-increasing human population (44% of the global population live within 150 kilometers of the coast, United Nations Atlas of the Oceans, n.d.). Not only do coastal regions represent centers of industry, commerce, and tourism, but they also support a host of important ecosystem services such as fisheries, recreation, and coastal storm protection (U.S. Global Change Research Program, 2018).

Unfortunately, the health and resilience of coastal zones are increasingly threatened by a host of human activities and related impacts, including sea level rise, shoreline armoring, and alteration of sediment supplies associated with river engineering and watershed alteration. Collectively, these unprecedented threats not only jeopardize highly productive coastal ecosystems, but also imperil vital socio-economic systems that are concentrated in coastal margins. For example, as a result of SLR alone, Thorne et al. (2018) project a loss of 60% of middle and 95% of high marsh habitats along the Pacific Coast by the end of the century due to low vertical accretion rates and limited upland migration. Moreover, studies such as those by Wills and Griggs (2003) and Vasilopoulos et al. (2021) indicate that anthropogenic reductions in fluvial sediment supply are significant drivers of beach and coastal river delta loss, raising serious concerns about the long-term sustainability and resilience of these critical areas.

Our ability to predict and adapt to these threats hinges on an accurate understanding and quantification of sediment flux pathways. These pathways play a pivotal role in shaping key coastal morphodynamics that influence rates of coastal erosion, dune loss, as well as marsh accretion and resiliency in the face of accelerating sea level rise. This is especially the case for the Eureka Littoral Cell (ELC), as portions of it are subject to the highest relative sea-level (RSL) rise rates in California and indeed the entire west coast of the U.S. due to vertical land motion (VLM) from regional tectonics (Patton et al., 2023).

Fluvial sediment input, which constitutes 75%–90% of beach material in California (Bowen and Inman 1966; Best and Griggs 1991), is a key component of littoral cell sediment budgets. This is particularly the case in steep coastal watersheds along California's tectonically active North Coast, which have been shown to generate sediment yields greatly disproportionate to their drainage area (Warrick et al., 2013). Despite the importance of fluvial sediments in the construction of well-constrained littoral sediment budgets, conventional approaches for estimating fluvial sediment flux rely on static sediment rating curves that often over or underestimate sediment discharge – particularly in rivers that have experienced significant change through time (Klein and Anderson, 2012; Warrick et al., 2013).

Indeed, the only published study calculating a littoral cell sediment budget for the ELC, assumed time-invariant fluvial sediment flux (Patsch and Griggs, 2006). Moreover, as it was a statewide effort with broad geographic scope, a simplified sand budget methodology was used that relied on existing data sources that limited quantification of key budget variables. Additionally, no attempt was made to quantify uncertainty in the various sediment budget terms, such as gravel mining, dredging and fluvial sediment inputs. These limitations hindered budget closure and restricted the utility of findings, emphasizing the critical need for uncertainty quantification to enhance reliability, inform decision-making, identify knowledge gaps, facilitate communication, and manage risks associated with coastal dynamics and human activities.

1.1 Objectives

Here, we develop a refined sand budget for the Eureka Littoral Cell (ELC), along California's North Coast, that reflects time-dependent changes in fluvial sediment yields, fluvial sand extraction, Humboldt

Bay dredging, and relative sea-level rise; and incorporates comprehensive estimates of shoreline change (erosion and storage), inner-shelf storage, shoreline and estuary sand losses from RSL rise, and ultimate dune growth (storage). We also seek to: 1) quantify uncertainty in our fluvial sediment flux and sand budget estimates, 2) examine the implications of long-term trends in fluvial sediment loading estimated via static vs. dynamic rating curves, and 3) elucidate different sand pathways in the ELC.

1.2 Acknowledgements

This work was completed by Northern Hydrology and Engineering (NHE) as part of the Humboldt Coastal Resilience Project. Funding was provided by California Ocean Protection Council and the California State Coastal Conservancy grants, as administered by the Conservancy. NHE was contracted with Friends of the Dunes, who is the fiscal receiver and oversees community outreach for the Project.

2 STUDY AREA

The Eureka littoral cell, located in northern California, is roughly 67 km long and is bounded to the north and south by Trinidad Head and False Cape, respectively (Figure 1). The watershed draining to the ELC is approximately 11,700 km^2 and is comprised primarily of the Eel, Van Duzen, and Mad Rivers – as well as several smaller coastal subbasins, including the Little River, Luffenholtz Creek, Strawberry Creek, Norton Creek, Elk River, Freshwater Creek and Guthrie Creek (Figure 1). In addition to an extensive coastal dune field, the ELC also contains Humboldt Bay, the second largest natural bay in California. The Eel Submarine Canyon lies east of the ELC inner-shelf and shoreline in deeper shelf waters. Although Redwood Creek does not contribute to the ELC, we included it in our analyses as it is the most proximal, data-rich catchment in the study area.

The region is known for its high erosion rates and fluvial sediment supply, which is generally attributed to its unique combination of unique land use, climate, geology and tectonics (Kelsey, 1980; Mackey et al., 2011; Warrick et al., 2013). Current land cover is predominated by evergreen and mixed forest with the bulk of remaining land in a mixture of shrub and grassland. Principle land uses across the region consist of timber harvest, which peaked in the 1950s and 1960s, as well as cattle grazing that has remained relatively stable over time (Warrick et al., 2013). Although the region's climate is relatively moderate (cool temps with moderate precipitation of 30-40 inches/yr), the wave climate is quite extreme with large frequent swells emanating from both the North and South Pacific (Wheatcroft and Borgeld, 2000; Patsch and Griggs, 2007; George and Hill, 2008).

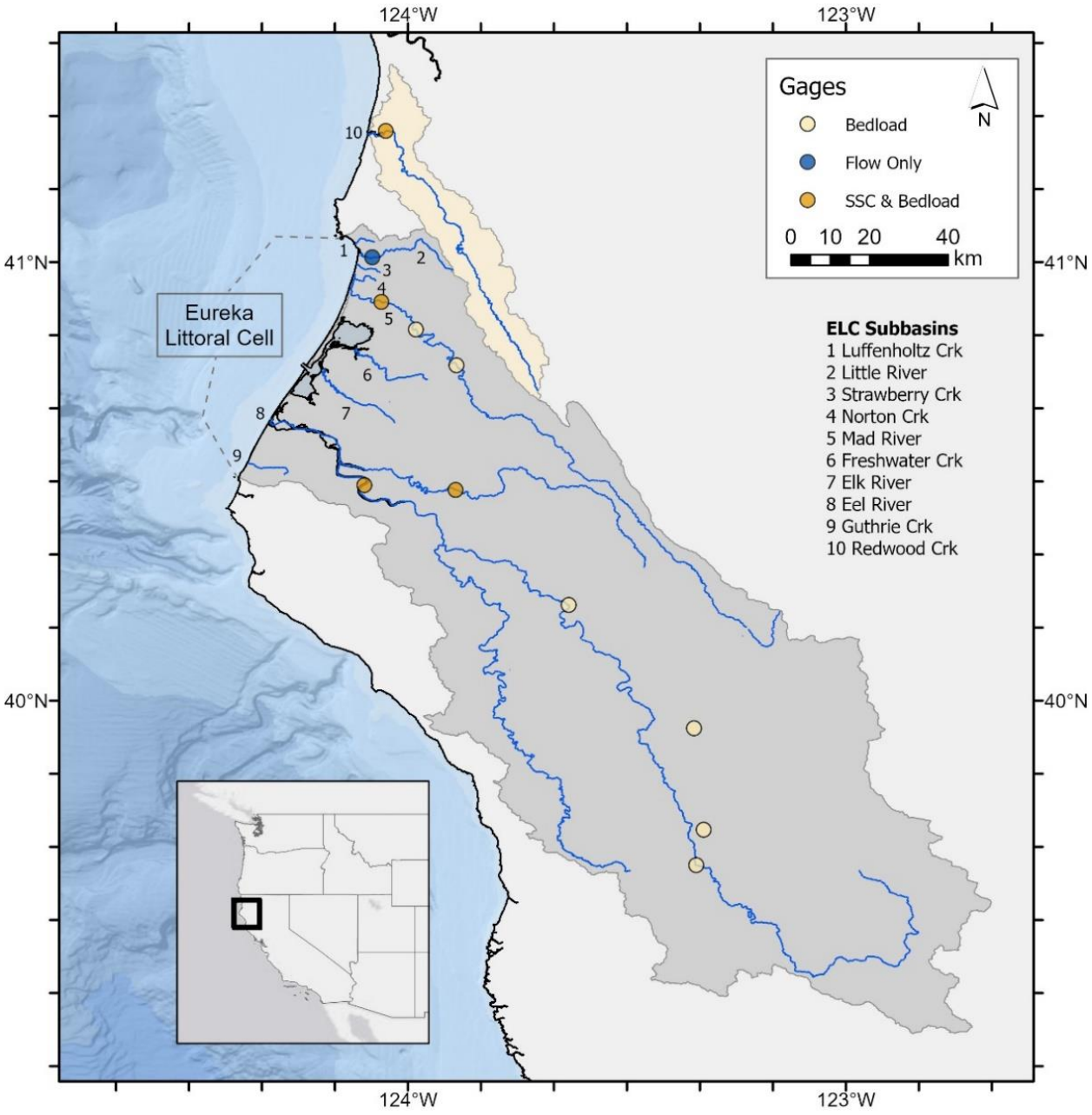

Figure 1. Map indicating the location of the Eureka Littoral Cell, nine coastal subbasins and stream gages used in this study. Colored circles indicate the flow and sediment data available at each gage.

3 METHODS

The framework for our analysis consisted of the following principal steps: 1) estimate fluvial sand loads via static and dynamic regional and river-specific LOESS regression rating curves and quantify load uncertainty via a percentile block bootstrap method, 2) estimate additional ELC sand budget inputs, outputs and storage terms from available literature data and assign uncertainty by assuming or quantifying probability distributions, and 3) compute the ELC sand budget and propagate input/output uncertainties using Monte Carlo (MC) simulation. As we were interested in examining long-term trends in various sand budget input/output sources, we extended records back to the earliest date of available data. For example, we constructed annual fluvial sediment discharge, fluvial sand/gravel extraction, and Humboldt Bay sand dredging volumes spanning WY 1911 to 2018. We also developed an annual RSL change series from 1900 to 2021 for the ELC that accounted for regional sea-level change and VLM.

3.1 Fluvial Sand Loads

This section describes the development of time-dependent sand loads for the ELC. Two key assumptions for fluvial sand loads are as follows:

- Temporal trends in SSC observed in the Eel River, Van Duzen River, Redwood Creek and Mad River are applicable to other coastal subbasins in the ELC.
- Fluvial sediment concentrations post-2000 provides a reasonable approximation of pre-disturbance levels (i.e. prior to intense mid-century logging and flooding; Warrick, 2014).

3.1.1 Data

Suspended and bedload sand flux to the ELC were computed using rating curves based on suspended sediment concentration (SSC) data obtained from multiple USGS gage locations within the ELC watershed (Table 1). All SSC, bedload, grain size distribution, and discharge data were obtained via automated download from the USGS National Water Information System (NWIS; https://waterdata.usgs.gov/nwis) website using the dataRetrival package in R (De Cicco et al., 2018). NWIS grain size distribution data for the sand fraction was supplemented with records obtained through manual download from the USGS Sediment Data Portal website (https://cida.usgs.gov/sediment/). The grain size distribution data was used to assess the sand and gravel fraction of the suspended sediment concentration using a littoral cutoff diameter of 125μm, which was shown to be appropriate for northern California beaches (Glogoczowski and Wilde, 1971; Limber et al., 2008). The bulk of SSC sampling occurred during the 1960's and 1970's in response to major floods (Figure 2). The NWIS flow and SSC records for the Eel and Mad Rivers were extended with field data from Goni et al. (2013) and GMA (2007), respectively. The GMA (2007) data were collected using standard discharge-integrated sampling techniques employed by the USGS (Edwards and Glysson, 1999), and thus, integrate well with the USGS NWIS data. The Goni et al. (2013) data were collected via surface water grab samples, which have been shown to provide reasonable, albeit somewhat conservative estimates of discharge-weighted fine grained sediment concentrations (< 0.63mm; Warrick, 2014). Here, we assume the Goni et al. (2013) data would again provide reasonable, but likely less conservative estimates of the coarser grained sand fraction (>= 125μm).

Maintenance of Variance Extension Type 1 (MOVE1) regression (Hirsch, 1982) was used to transfer streamflows from the Eel River to the other partial-record stations in the ELC watershed (e.g. Van Duzen

flows from 1910-1950 were back-filled using the MOVE1 Eel River flows). Flows for the six ungaged ELC subbasins were estimated via area-ratio adjustment of the MOVE1 Little River flows.

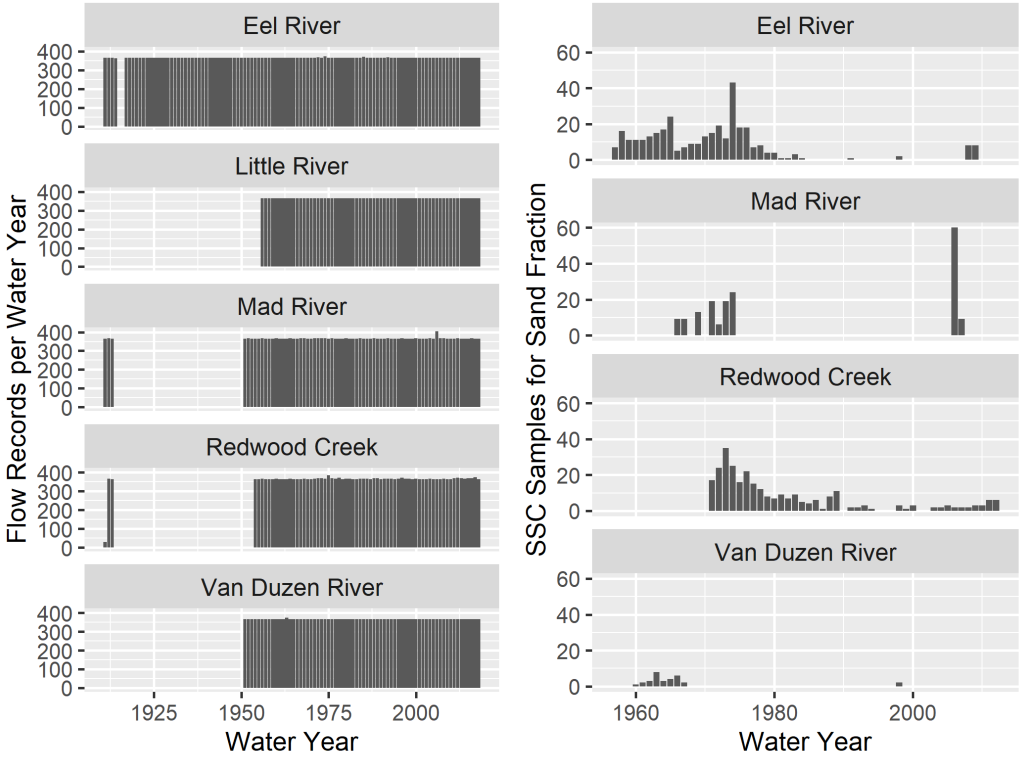

Figure 2. Annual frequency of flow and suspended sediment sampling in the study subbasins.

Table 1. USGS gaging stations and gaging data used in this study. Apart from Redwood Creek, fluvial sediment flux was computed only for the ELC coastal subbasins.

Available Data	Station Name	USGS Station #	USGS Station Name	Drainage Area (km^2)	Suspended Sediment		Discharge	
					Period of Record (WY)	# Records	Period of Record (WY)	# Records
SSC & Flow	Eel River	11477000	Eel R. at Scotia	8063	32	341	106	38,737
	Mad River	11481000	Mad R. near Arcata	1256	10	168	70	25,980
	Van Duzen	11478500	Van Duzen R nr Bridgeville	575	9	31	68	24,848
	Redwood Creek	11482500	Redwood C. at Orick	717	35	287	67	24,602
Flow Only	Little River	11481200	Little R nr Trinidad	117	--	--	63	23,011
Ungaged	Luffenholtz Creek	--	--	50	--	--	--	--
	Strawberry Creek	--	--	11	--	--	--	--
	Norton Creek	--	--	12	--	--	--	--
	Freshwater Creek	--	--	127	--	--	--	--
	Elk River	--	--	145	--	--	--	--
	Guthrie Creek	--	--	54	--	--	--	--

3.1.2 **Analysis**

We chose a data-driven approach that leveraged the somewhat sparse and episodic fluvial sediment data to estimate sediment flux. Separate LOESS rating curves for the sand fraction were constructed for the bed and suspended load components. However, we found that the bedload data in the study area was insufficient to create robust time-dependent bedload rating curves, and bedload sand flux was estimated as a percentage of the suspended sand load. Suspended sand loads were computed via time-dependent LOESS rating curves of suspended sediment concentration (Warrick, 2013). Data constraints precluded the construction of unique SSC rating curves for each coastal subbasin contributing to the ELC. Thus, apart from suspended sediment concentrations for the Eel River, suspended loads were computed via regional rating curves. To ascertain the importance of capturing temporal patterns in sediment flux we estimated sand flux via static vs. dynamic rating curves that incorporated time-varying residual ratios. Upper and lower uncertainty bounds on our estimates of sand flux were quantified via a percentile block bootstrap method (Hirsch et al., 2015).

3.1.2.1 Suspended Sand Loads

Fluvial suspended sand loads were computed using both river specific and regional rating curves based on bias-corrected locally-weighted regression (LOESS; Cleveland and Devlin, 1988) on $\log_{10}$-transformed discharge and SSC data. LOESS regression was chosen to accommodate observed curvature (non-linearity) in the SSC-Q relationships (Hicks et al., 2000; Warrick et al., 2013; Helsel et al., 2020). Notably, LOESS regression is sensitive to several hyperparameters – especially the span parameter (*f*), which controls how the fit at a specific point in the series weights the data nearest to it. We employed an automated technique to objectively determine the span parameter for all LOESS fits using a bias-corrected Akaike Information Criterion (AIC_C) method as implemented in the *fANCOVA* package in R (Wang and Ji, 2020). The choice of *f* was further constrained to ensure monotonic SSC-Q rating curves. River-specific rating curves utilized non-area normalized flows, whereas the regional SSC curve employed discharge values normalized to drainage area.

As previously mentioned, prior research has demonstrated strong time-dependent trends in sediment loads across the region, and particularly in the Eel River, Mad River and Redwood Creek. Temporal trends in these curves were captured by incorporating time-varying residual ratios (observed SSC – predicted SSC) into the computation of daily sediment flux (Eq.1; Warrick et al., 2013; Warrick, 2014). As SSC measurements are relatively sparse and episodic in the ELC watershed, it was necessary to impute median residual ratio values for water years with insufficient data via an exponential decay function (Figure 4A; Hicks and Basher, 2008; Warrick, 2014). Additionally, the nonparametric smearing method of Duan (1983) was used to correct for the systematic bias associated with back-transforming from log to arithmetic space.

Similar to Cohn (1995), Wheatcroft and Borgeld (2000), and Warrick et al. (2013), daily suspended sand flux (*Qss*; Mt) was computed as follows:

$$Qss_t = Q_t \times \widehat{SSC_t} \times R_y \times BCF_d \times cf \qquad \text{Eq. 1}$$

where *Q* is the mean daily discharge ($m^3 s^{-1}$ for the Eel River curve vs. $m^3 s^{-1}/km^2$ for the regional curve) at time *t* (days), $\widehat{SSC_t}$ is the suspended sand concentration predicted from the *SSC-Q* rating curve, R_y is the time-dependent correction factor computed as the median of the rating curve residuals for the corresponding water year (*y*), BCF_d is Duan's (1983) bias correction factor for log back-transformations, and *cf* is a unit conversion factor. Daily SSC values for mean daily flows that were above or below the sampled discharge domain used in the construction of the rating curve were extrapolated using the LOESS fitted curve. Daily sand loads at the outlets of all gaged coastal ELC subbasins (e.g. Eel River,

Mad River, Van Duzen River, and Little River) were estimated using area-ratio adjusted daily discharge values. Daily suspended sand loads at the outlets of the remaining six ungaged coastal ELC subbasins were estimated via the application of area-ratio adjusted flows from the Little River.

3.1.2.1.1 Eel River SSC Rating Curve

Preliminary exploratory data analyses suggested that the area-normalized SSC-Q relationship for the Eel River was dissimilar to that of the other smaller gaged study subbasins (Figure 3). In particular, the Eel River demonstrated far higher sediment concentrations across low–moderate flows relative to the Van Duzen River, Mad River or Redwood Creek. This is in accordance with previous studies that have concluded that the Eel River generates one of the highest suspended sediment loads in the U.S. on a per unit area basis (Brown and Ritter, 1971).

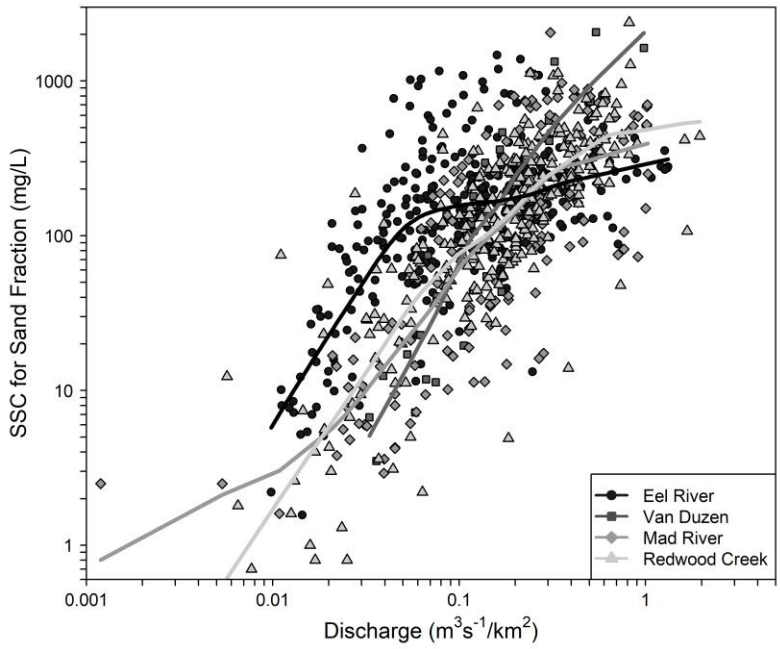

Figure 3. Relations between area-normalized river discharge and fluvial suspended sediment concentration for the sand fraction (>= 125µm) for the Eel River, Van Duzen River, Mad River and Redwood Creek.

Given the regionally unique SSC-Q relationship and the fact that the Eel River was relatively data-rich, a separate non-area-normalized LOESS SSC-Q rating curve and median residual ratio correction factors were computed for the Eel River (Figure 4). Median residual ratio values prior to the earliest SSC (sand >= 125µm) record (1956) were assumed to equal the mean of post-2000 residual ratios (i.e. consistent with the hypothesis that sediment concentrations are returning to pre-disturbance [intense mid-century logging and flooding] levels; Warrick, 2014). All median residual ratios for years with insufficient data post-1957 were imputed via an exponential decay function (Figure 4B & C).

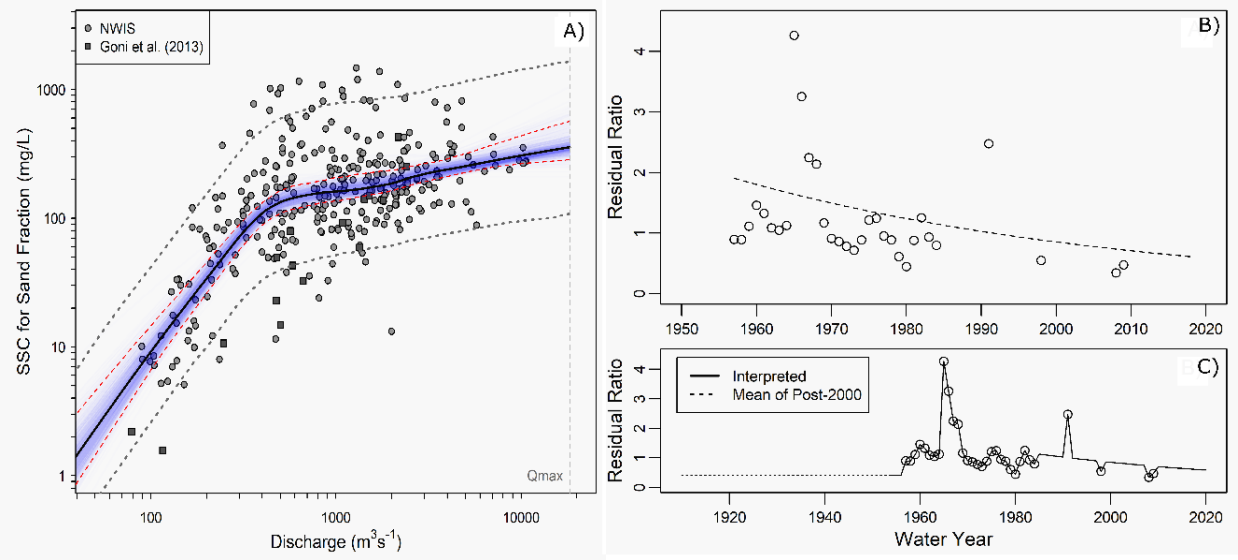

Figure 4. A) Relation between river discharge and suspended sediment concentration for the sand fraction (>=125µm) for the Eel River at the Scotia Station (11477000). Additional flow and SSC data from Goni et al. (2013) is depicted by black squares. LOESS fit curve is solid black line. Red and grey dashed lines represent block-bootstrapped 95% confidence and 90% prediction intervals, respectively. Solid light blue lines represent the 95% block-bootstrapped confidence interval iterations. Dashed grey vertical line indicates the highest observed discharge applied to the LOESS rating curve. B) Median residual ratios from the LOESS regression computed for each water year for the period 1950-2018. Dashed line represents an exponential decay model used to predict residual ratios for years with no data. C) Gap-filled residual ratios for the period 1910-2018. Dotted line represents period of no data for which residual ratios were computed as the mean of post-2000 ratios.

3.1.2.1.2 Regional SSC-Q Rating Curve

Suspended sand loads for the remaining coastal ELC subbasins were computed via a regional dynamic LOESS rating curve using data from the Mad River, Van Duzen River and Redwood Creek (Figure 5). Redwood Creek was included in the regional SSC-Q curve because: 1) preliminary analyses indicated that the littoral suspended sediment data was inadequate to build a regional rating curve for the Mad and Van Duzen Rivers alone; 2) Redwood Creek has a long period of record that captures temporal dynamics of SSC in the region (i.e. long-term decline in SSC in response to changing land use practices); 3) it exhibits a similar SSC-Q relationship relative to the Mad and Van Duzen Rivers (Figure 3); 4) it is in a similar physiographic region; and 5) it is directly adjacent to the ELC and possesses a similar drainage area relative to the other, smaller gaged and ungaged basins in the ELC watershed.

Daily sand loads (Eq. 1) for the Mad, Van Duzen, and Little Rivers were estimated by applying this regional curve to the area-normalized MOVE1-extended mean daily flows. Suspended sand loads in ungaged coastal ELC subbasins (Figure 1; Table 1) were computed using the area-ratio adjusted mean daily flows from the Little River. Similar to the Eel River, residual ratios were computed for the regional rating curve and applied to capture temporal trends in fluvial sand flux. Median residual ratio values prior to the earliest SSC record were assumed to equal the mean of post-2000 residual ratios, while all median residual ratios for years with insufficient data post-1964 were imputed via an exponential decay function (Figure 5B & C).

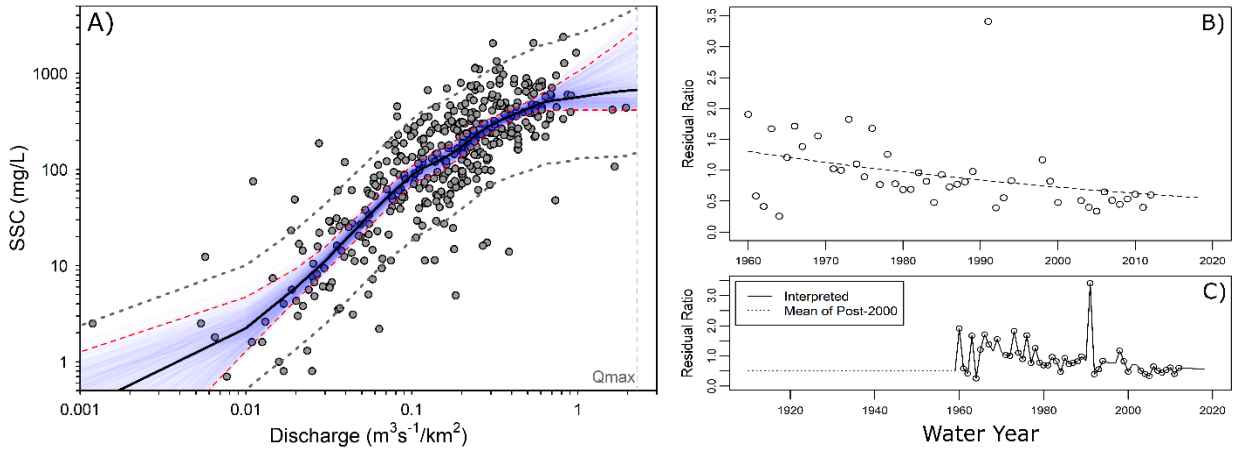

Figure 5. A) Regional relation between area-normalized river discharge and suspended sediment concentration for the sand fraction (>=125µm) for Mad River, Van Duzen River and Redwood Creek (stations: 11481000, 11478500, 11482500, respectively). LOESS fit curve is solid black line. Red and grey dashed lines represent block-bootstrapped 95% confidence and 90% prediction intervals, respectively. Solid light blue lines represent the 95% block-bootstrapped confidence interval iterations. Dashed grey vertical line indicates the highest observed discharge applied to the LOESS rating curve. B) Median residual ratios from the LOESS regression computed for each water year for the period 1960-2012. Dashed line represents an exponential decay model used to predict residual ratios for years with no data. C) Gap-filled residual ratios for the period 1910-2018. Dotted line represents period of no data for which residual ratios were computed as the mean of post-2000 ratios.

3.1.2.2 Bedload Flux

In line with our data driven approach, we investigated the feasibility of computing bedload sand flux via dynamic river-specific and regional LOESS bedload rating curves using discharge and bedload data from all USGS gages with adequate data in the ELC watershed (Table 1). Unfortunately, the construction of these bedload rating curves was greatly limited by the following constraints: 1) bedload sampling in the ELC watershed was sparse; 2) there was substantial variability in Q-Bedload relationships across gages; 3) the observed discharge domain of the rating curves were quite limited – especially for higher flows (>500 m^3), leading to potentially large extrapolation errors and uncertainties; and 4) the period of record of bedload data across the region was limited – resulting in too few residual ratios to create a time-varying rating curve.

These data constraints precluded the development of river-specific bedload rating curves and greatly reduced the suitability and reliability of a regional curve approach. As a result, we adopted the approach of Willis and Griggs (2003) for estimating bedload sand flux in Northern California rivers, where bedload is computed as 100% of the suspended sand load. As noted by Willis and Griggs (2003), the assumption that bedload was 100% of the total annual suspended sand flux is based on limited bed load data from coastal gages and has been used by previous researchers (Brownlie and Taylor 1981; Hadley et al. 1985; Inman and Jenkins 1999).

3.1.2.3 Uncertainty Estimation

Uncertainty in our estimates of suspended sand flux was quantified through the construction of 95% confidence intervals (CI) and 90% prediction intervals using the time-based block bootstrap method proposed by Hirsh et al. (2015) and implemented in the EGRETci package in R. Block bootstrapping accounts for short-term serial autocorrelation, common in paired SSC-Q data, by sampling with replacement from within time blocks (defined by block length) that approximates the correlation structure

of the dataset. Block lengths, estimated via autocovariance plots, were determined to be 300 for the SSC confidence and prediction intervals. This approach yields a more statistically rigorous quantification of uncertainty relative to the more conventional "sum of individual errors" methods (e.g. Wright and Schoellhamer, 2005).

Uncertainty intervals for the paired SSC-Q dataset were resampled with replacement 2000 times. The 95% bootstrap percentile confidence intervals (e.g. Chernick, 1999) were constructed by fitting a LOESS curve to the 2.5th and 97.5th percentiles of the 2000 bootstrap realizations. Similarly, 90% prediction intervals were constructed by fitting LOESS curves to the 5th and 95th percentiles of the bootstrap replicates. Additional uncertainty associated with residual scatter (described in Slaets et al., 2016) was included in the estimation of prediction intervals by adding a randomly selected bootstrap error term, drawn from the population of block bootstrapped replicates, to the expected SSC estimate (Rustimji and Wilkinson, 2008; Vigiak and Bende-Michl, 2013). As per Rustimji and Wilkinson, 2008 and Vigiak and Bende-Michl (2013), accounting for residual scatter via inclusion of resampled residuals removed the need for a log back-transformed bias correction factor. Additionally, bootstrapped LOESS regression fits were constrained to be monotonically increasing to prevent pronounced non-monotonic behavior when extrapolating bootstrapped LOESS regression replicates well beyond the observed Q range.

Adoption of the Willis and Griggs (2003) approach for estimating bedload flux precluded the rigorous quantification of uncertainty used for the suspended sand flux. Instead, bedload uncertainty was estimated as 100% of the upper and lower prediction interval of the suspended load.

3.2 ELC Sand Budget Analysis

3.2.1 General Sediment Budget Equation

In its simplest form, a mass balance (or sediment/sand budget) quantifies the material inputs, outputs, and accumulation or storage within a control volume (Tchobanoglous and Schroder, 1985) (Figure 6).

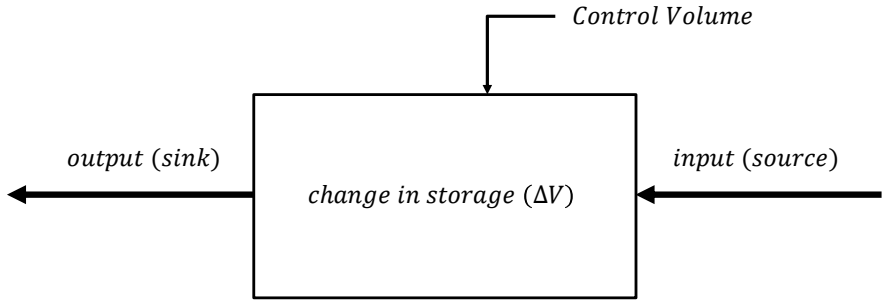

Figure 6. Sketch of materials (mass) balance.

For transferability, we used the Corps of Engineers sediment budget equation (Rosati & Kraus, 1999; CEM, 2003) expressed as:

$$\sum Q_{source} - \sum Q_{sink} - \sum \Delta V + P - \sum R = Residual \qquad \text{Eq. 2}$$

where Q_{source} and Q_{sink} are the source (input) and sink (output) to the control volume, respectively; ΔV is the control volume change; P is the material placed and R is the material removed from the control volume; and $Residual$ represents the budget balance or closure. Terms are described consistently as a volume or volumetric rate.

3.2.2 ELC Sand Budget Unit Locations and Extents

For this sand budget, we defined a unit as a distinct feature or element of the ELC, such as the shoreline. We further defined the littoral cell as a single cell that includes the shoreline and inner-shelf bounded north and south by Trinidad Head and False Cape (Figure 7). The shoreline is defined as the approximate 67 km long sandy shoreface extending from the active beach berm (~ 5.8 m NAVD88) west to the depth of closure (~ -14 m NAVD88). A small 7.2 km section of shoreline extending from False Cape north is backed by eroding bluffs, and 3.4 km of the northern end of the ELC consists of pocket beaches backed by bluffs. The sandy inner-shelf, as defined here, extends from the depth of closure east to the -50 m (NAVD88) elevation. East of the beach berm, approximately 51.2 km of sand dunes extend from the northern and southern bluffs along the littoral cell and are bisected by the Humboldt Bay entrance and the estuary mouths of the Eel, Mad and Little Rivers. We defined three sandy estuaries for the Eel River, Mad River and the interior of Humboldt Bay below the mean higher high water elevation (~ 2 m NAVD88). Three sites have been used for the disposal of dredged sandy material from Humboldt Bay. Prior to 1990 dredged sand was placed within the ELC at sites SF-3 and NDS (~ 15 to 18 m depth, Figure 7). After 1990, dredged sand has been placed at HOODS at a depth of ~ 50 m, which is considered a non-dispersive site (Scheffner, 1992; EPA, 1995; HBHCRD and COE, 1995), effectively outside of the ELC (EPA and COE, 2020).

Sand inputs from nine tributaries were accounted for in the sand budget. Seven of these tributaries (Luffenholtz Creek, Little River, Strawberry Creek, Norton Creek, Mad River, Eel River and Guthrie Creek) discharge directly into the ELC. The other two tributaries, Freshwater Creek and Elk River, discharge into Humboldt Bay and are assumed to contribute sand to the ELC sand budget. Two additional tributaries not shown on Figure 7, Jacoby Creek and Salmon Creek, discharge into the upper ends of North Bay and South Bay, respectively. Previous hydrodynamic and sediment transport modeling on the Elk River indicate that a significant fraction of the upstream sediment load is deposited into lower channel, floodplain and estuary reaches and does not transport into Humboldt Bay (Caltrout et al., 2019). Observations and similar hydraulic conditions indicate that this depositional process likely exists for the other three Humboldt Bay tributaries. Therefore, we assumed that only sand loads from Freshwater Creek and Elk River contribute sand to the ELC via Humboldt Bay.

For the ELC sand budget, we also assumed that the littoral cell is closed, and headland bypassing from longshore transport does not occur for Trinidad Head or False Cape.

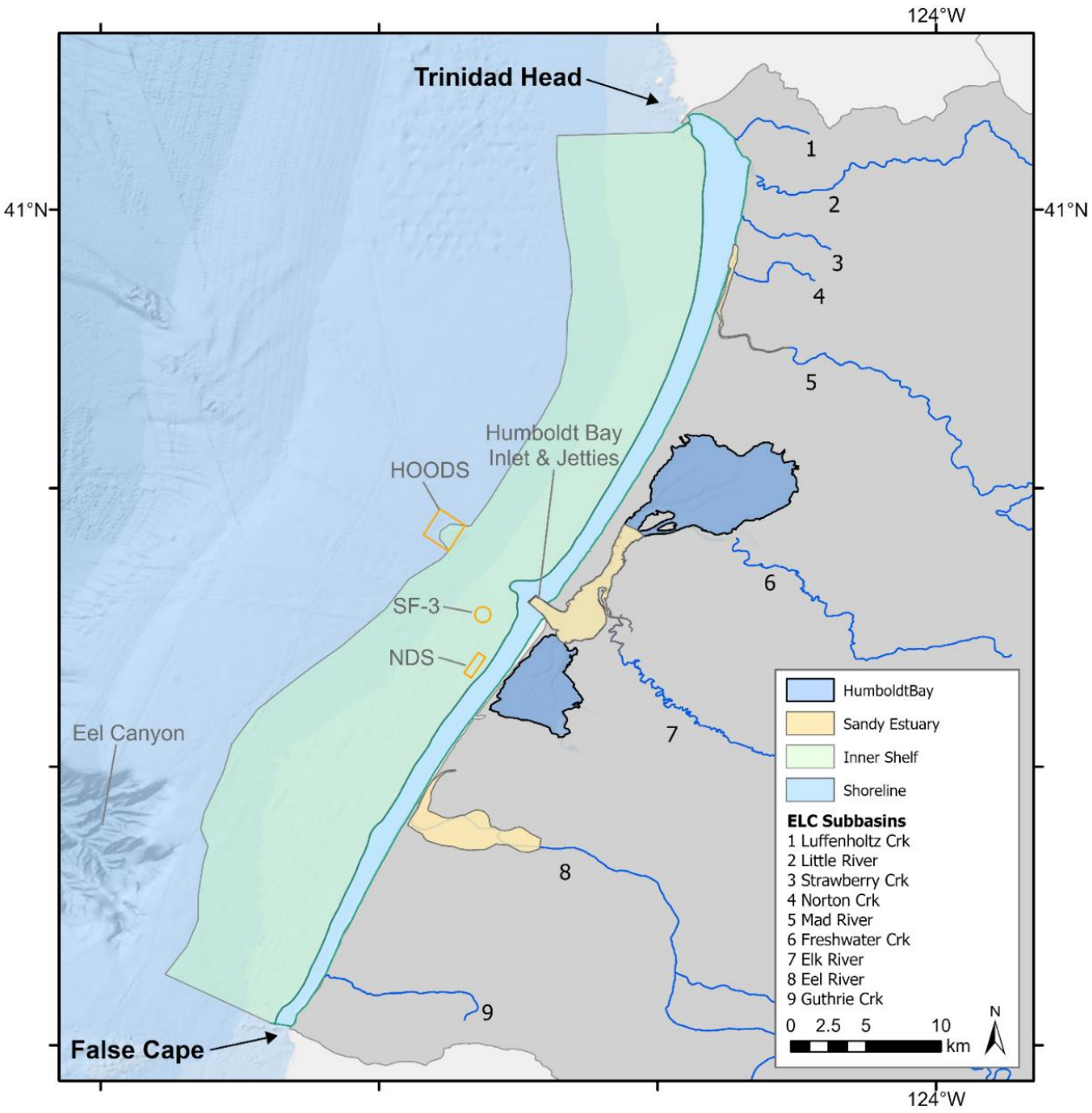

Figure 7. Location map of Eureka Littoral Cell (ELC) showing the extent of the littoral cell from Trinidad Head to False Cape; the location and extents of the shoreline, inner-shelf, and sandy estuaries; Humboldt Bay dredge disposal sites; and the nine tributaries used in the ELC sand budget.

3.2.3 ELC Sand Budget Term Definitions

For the sand budget, we defined several distinct inputs, outputs and storage mechanisms that interact within the ELC units previously described (Section 3.2.2) as follows:

- Sand inputs (sources) include the time-dependent fluvial sand loads (Q_R) described in Section 3.1 for the nine tributaries flowing into the ELC, and bluff erosion (Q_B) at the southern end of the ELC near False Cape.

- Outputs (sinks) of the ELC include shoreline loss (Q_{SLS}) and estuary loss (Q_{SLE}) of sand to sea-level rise, and sand loss to dune growth (Q_D). We defined dune loss/growth as an output term, but it could also be treated as a storage term.
- Sand storage change includes shoreline change (ΔS_S) and inner-shelf change (ΔS_{IS}).
- The placement term is defined as dredged sand placement (P_B). As described previously, dredged sand was placed within the ELC prior to 1990, and outside of the ELC after 1990 (disposal at HOODS).
- The removal terms are defined as fluvial sand/gravel extraction (R_R) and Humboldt Bay sand dredging (R_{HB}).

Each of these terms will be further described below. As mentioned earlier, we assume that all sand is beach sized sand greater than or equal to the cutoff diameter of 125μm.

3.2.4 Sand Budget Process Equations

Several process equations used in the sand budget are described below.

The shoreline volume change (ΔS_S) between the active berm and the depth-of-closure was estimated by (Rosati and Kraus, 1999; CEM, 2003):

$$\Delta S_S = \Delta y \Delta x D_A \quad \text{Eq. 3}$$

where Δy is the change in shoreline position, Δx is the longshore distance, and D_A is the active depth further defined as:

$$D_A = B + D_c \quad \text{Eq. 4}$$

where B is the active berm height, and D_c is the depth of closure.

The inner-shelf volume change (ΔS_{IS}) is described as:

$$\Delta S_{IS} = (A_{IS})\Delta_{SSR} \quad \text{Eq. 5}$$

where A_{IS} is the inner shelf area, and Δ_{SSR} is the shelf sedimentation rate.

Brunn's rule (Bruun, 1962) was used to estimate shoreline loss to sea-level change (Q_{SLS}), and can be formulated as:

$$Q_{SLS} = W_c RSL / D_A \quad \text{Eq. 6}$$

where W_c is the shoreline cross-shore distance, RSL is the relative sea-level change rate, and D_A is previously defined.

To determine estuary sand loss to sea-level rise (Q_{SLE}) we use an equation similar to the inner-shelf volume change described as:

$$Q_{SLE} = (A_E)RSL \quad \text{Eq. 7}$$

where A_E is the estuary area, and RSL is previously defined.

Sand input from bluff erosion (Q_B) was estimated as (Best and Griggs, 1991; Patsch and Griggs, 2006):

$$Q_B = C_L H_C C_E C_{SF} \quad \text{Eq. 8}$$

where C_L is the cliff length, H_C is the cliff height, C_E is the cliff erosion rate, and C_{SF} is the cliff sand fraction (>= 125μm).

During the Monte Carlo simulation (described below) it was necessary to determine the active shoreline width from the active depth (D_A) described by the random variates for B and D_C (Eq. 4). We used the Dean and Dalrymple (2002) equilibrium beach profile equation rearranged to determine the active shoreline width (W_A) as follows:

$$W_A = \left(\frac{D_A}{A}\right)^{\frac{3}{2}} \quad \text{Eq. 9}$$

where A is a constant and initially determined by rearranging Eq. 9 and solved using the mean values for W_A and D_A. An additional random error was included in each W_A estimate using the normally distributed width measurement error (see Table 2).

3.2.5 ELC Sand Budget Uncertainty

Construction of littoral cell sand budgets is a notoriously challenging task for a host of reasons, foremost among them being substantial limitations regarding data availability and quality (Komar, 1998). Accounting for uncertainty in the budget terms can enhance confidence in the sand budget results and allows the range of more uncertain values to be assessed (Kraus and Rosati, 1998).

To account for uncertainty in the sand budget, we use Monte Carlo simulation to propagate uncertainty and/or errors in the input, output, and storage terms. In estimating mean values over time (annual means) for various terms in the ELC sand budget, along with their associated uncertainties such as confidence limits, we follow a methodology consistent with other mass budgets (e.g., Yanai et al., 2010; Lester and Cebrian, 2010). Specifically, we use the standard error of the mean to describe the uncertainty or error in the mean estimates. The standard error (SE) of the mean, or standard deviation of the mean sample distribution, is computed as (Hines and Montgomery, 1990):

$$SE = \frac{S}{\sqrt{n}} \quad \text{Eq. 10}$$

where S is the standard deviation of the sample, and n is the number of observations.

In this study, certain terms, such as the annual tributary sand loads (Section3.1), were directly estimated, along with uncertainties (e.g. 95% CI of the annual mean sand load). In cases where data existed to estimate terms, such as the active berm height, we used 10,000 bootstrap samples with replacement to estimate the mean and SE. However, it was necessary to base several of the sand budget terms on literature values. In some cases, enough data was provided to define the mean or "best estimate" and/or probability distributions describing the SE. For cases when only a single estimate was available for the mean, we assumed an error distribution. Several terms, such as the inner-shelf sedimentation rates, were determined by combining several variables into a single value. In these cases, the means and SE of each variable were combined into a single value with mean and SE using an intermediate MC simulation with 10,000 replicates.

To quantify uncertainty in measures of length or area (e.g. littoral cell length), we assumed a coefficient of variation ($CV = mean/SE$) of 0.5% and 1%, respectively. In addition, we incorporated additional mapping error by assuming a random normal distribution with a mean of zero and the reported SE of the map error for each data source.

The following sections detail the various sources, uncertainties, error distributions, approaches, and assumptions concerning the input, output and storage terms used in the ELC sand budget.

3.2.6 ELC Sand Budget Analysis and Time Periods

Two sand budget analyses spanning different time periods were conducted for this work. The first sand budget spanned the years 1966 to 2001, during which estimates for all sand budget terms were available except for dune growth. The second sand budget was a time-dependent analysis from 1911 to 2018, a period when many of the terms were unknown, necessitating a shift in the interpretation of these terms. The following sections provide a brief overview of each sand budget analysis period and underlying assumptions.

3.2.6.1 Sand Budget for 1966-2001 Period

The sand budget for the 1966-2001 period (36-years) treats the ELC as a single cell (1-cell). As mentioned above, we developed estimates (mean and uncertainty) for all sand budget terms during the period, except for dune growth (Q_D), for which no data was available. For this budget, we assumed the residual term in Eq. 1 was zero and the ELC was closed (i.e. no sand by-passing of headlands). With these assumptions, and by substituting individual terms into Eq. 1 and rearranging to solve for Q_D, the following equation was derived for this sand budget:

$$Q_D = (Q_R + Q_B) + P_B - (Q_{SLS} + Q_{SLE}) - (R_R + R_{HB}) - (\Delta S_S + \Delta S_{IS}) \qquad \text{Eq. 11}$$

3.2.6.2 Time-Dependent Sand Budget for 1911-2018 Period

A time-dependent sand budget analysis was conducted for the period 1911-2018, during which only a few terms were estimated. For this analysis, we rearrange Eq. 1 to solve for the residual over time, and account for the following terms: (1) time-dependent fluvial loads, (2) Humboldt Bay dredging, (3) fluvial sand/gravel extraction, (4) dredge placement in ELC or HOODS, and (5) the volume of sand needed to offset relative sea-level rise of the shoreline, inner-shelf, and estuaries. By rearranging Eq. 1 and solving for the residual, we obtained:

$$Residual = (Q_R + Q_B) + P_B - (R_R + R_{HB}) - (Q_{SLS} + Q_{SLE} + Q_{SLIS}) \qquad \text{Eq. 12}$$

where Q_{SLIS} accounts for sand loss to the inner-shelf to RSL and is defined as

$$Q_{SLIS} = (A_{IS})RSL \qquad \text{Eq. 13}$$

The time-dependent residual term represents the annual volume of sand remaining, which can be positive or negative. A positive (+) residual indicates a sand surplus available for shoreline storage (i.e. shoreline growth), inner-shelf storage, and/or dune growth. Conversely, a negative (-) residual indicates a sand deficit, where sand is insufficient to keep pace with RSL, and excess sand is not available for shoreline and inner-shelf storage, and dune growth. We expect that a long-term negative residual would indicate significant changes, such as shoreline or dune recession.

3.2.7 Common Sand Budget Variables

Several variables were initially determined and utilized for various calculations throughout the sand budget simulation (Table 2). These variables were randomly sampled from their associated probability distributions and then held constant for each ensemble or Monte Carlo iteration. They are succinctly described below:

- Active berm height (B) was estimated from shoreline linework generated by McDonald (2017) and elevations were extracted from the USGS 2020 CoNED Topobathy DEM.

- Depth of closure (D_C) estimates (based on the Hallermeier (1981) D_C equation) for 1980 to 2011 were extracted from the Corps of Engineers Wave Information Study (WIS) for three stations (83046, 83047, 83048) located offshore of the ELC.
- Shoreline length (L_S) was determined as the average lengths of the active berm and depth of closure feature lines.
- Shoreline cross-shore distance (W_c) or shoreline width between B and D_C were measured from the NOAA (2010) NAVD88 DEM of Eureka, CA model using 63 shore normal cross-sections spaced approximately 1,000 ft on center along the ELC.

Table 2. Miscellaneous sand budget probability distribution (PD) variables used in Monte Carlo simulation.

Variable	Unit	Mean	SE	CV	PD	Comment
Active berm elevation (B)	m[1]	5.81	0.11	1.91	Normal	Bootstrap sample + normal dist. map error (SE = 0.104 m)
Depth of Closure (D_C)	m[1]	-14.01	0.18	1.29	Normal	Bootstrap sample
Shoreline Length (L_S)	km	67.049	0.3352	0.5	Normal	Measured, CV = 0.5%
Shoreline width (W_C)	km	1.1706	0.0414	3.53	Normal	Bootstrap sample + uniform dist. map error (min/max = -10/10 m)

[1] Elevation referenced to NAVD88.

3.2.8 Relative Sea-Level Change Rate and Acceleration

We estimated an ensemble of time-dependent relative sea-level (RSL) change series spanning 1900 to 2021 by combining annual rates and accelerations of regional sea-level change (ReSL) with vertical land motion (VLM) estimates from Patton et al. (2023) for six locations within the ELC (Table 3). Two data sources were combined to create the annual ReSL series for the Humboldt Bay region. The first source used sea-level data from the Crescent City, CA station (NOAA ID: 9419750) for the 1933-2021 period of record, with annual sea levels estimated from monthly data after removing the seasonal cycle. The second source relied on the annual mean sea-level data representing the East Pacific basin provided by Frederikse et al. (2020) for 1900-1932 and three missing data periods for Crescent City (1944, 1948 and 1950).

Prior to combining into a single series, each data source was adjusted to the 1.99 mm/yr Pacific Northwest regional (or absolute) rate provided by Montillet et al. (2018). Differencing the RSL and VLM rates for Crescent City (or any of the stations) in Table 3 results in a ReSL rate of 1.99 mm/yr as this rate was directly used to resolve the VLM rates in Patton et al. (2023). To adjust the Frederikse et al. (2020) data to the 1.99 mm/yr regional rate, we applied an optimized rate and offset so that the Frederikse data aligned with the Crescent City data for the overlapping 1933 to 2018 period.

We determined the rate and acceleration of the ReSL series using a second-order polynomial fit (Figure 8A), resulting in a linear rate of 1.757 mm/yr and an acceleration of 1.008e-05 m/yr^2 (2 x quadratic term). To account for residual serial autocorrelation in the $ReSL$ fit, we followed the approach of Wang et al. (2021) that uses nonparametric bootstrapping to generate synthetic sea-level series with the same serial autocorrelation. This approach employs the random-phase sampling methodology of Ebisuzaki (1997), creating random series with the same power spectra as the original residual series, and was implemented using the astrochron package in R (Meyers, 2014). Additionally, we estimated a weighted VLM probability distribution (Figure 8B) for the ELC by calculating the length weighted average of 10,000 bootstrapped samples of normally distributed VLM rates and distances for each ELC station (Table 3).

Table 3. Tide station relative sea level (RSL) and vertical land motion (VLM) rates and standard errors (SE) from Patton et al. (2023); VLM determined by differencing RSL and the regional (or absolute) sea level (ReSL) rate of 1.99 ± 0.16 mm/yr (Montillet et al., 2018); and the alongshore measured distance and SE (coefficient of variation = 0.5%) between stations in the ELC. Trinidad is at the north end of the ELC, and Crescent City is not in the ELC.

	Sea-Level Change Rates (mm/yr)				Distance between Stations (km)		
Station	**RSL**	**SE for RSL**	**VLM**	**SE for VLM**	**Stations**	**Distance**	**SE**
Crescent City (not in ELC)	-0.84	0.14	2.83	0.21			
Trinidad (TR)	2.86	1.10	-0.87	1.11	TR to MRS	20.466	0.102
Mad River Slough (MRS)	2.53	0.41	-0.54	0.44	MRS to SO	5.792	0.029
Samoa (SO)	3.92	0.35	-1.93	0.38	SO to NS	6.320	0.032
North Spit (NS)	5.20	0.17	-3.21	0.23	NS to FL	3.100	0.016
Fields Landing (FL)	4.65	0.33	-2.66	0.37	FL to HS	3.9378	0.020
Hookton Slough (HS)	6.64	0.65	-4.65	0.67	HS to SELC	24.169	0.121
South end ELC (SELC)							

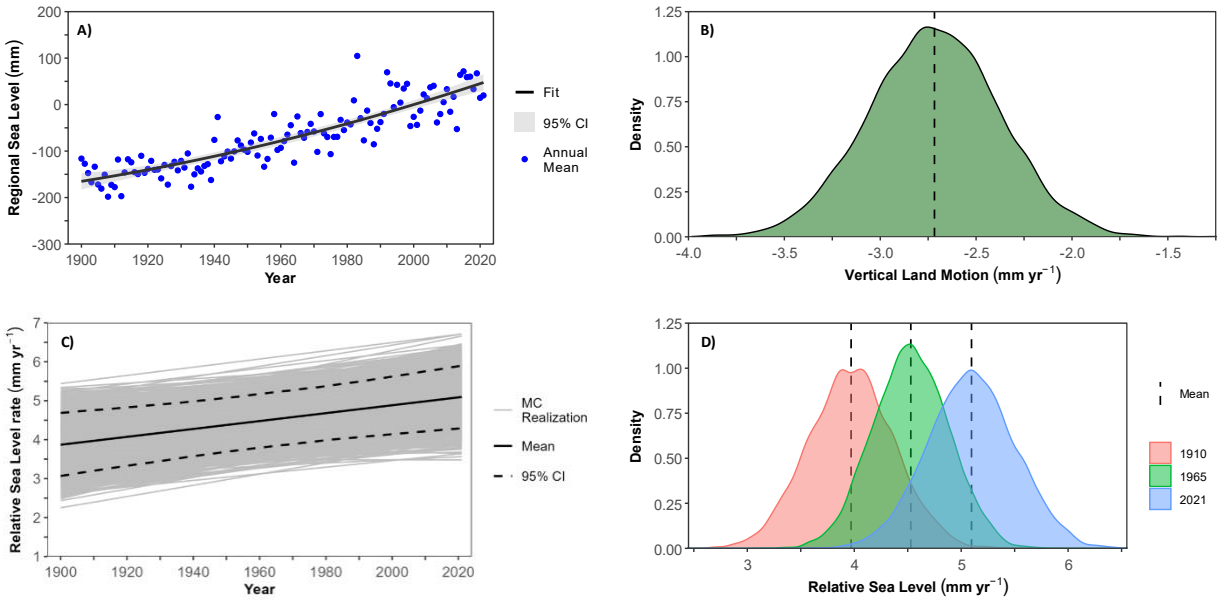

Figure 8. A) Annual regional sea level (ReSL) for the Humboldt Bay region fit with second-order polynomial resulting in a rate = 1.757 mm/yr and acceleration = 1.008E-6 m/yr^2 (2 x quadratic term). Results for single iteration of 10,000 Monte Carlo simulations for determining the relative sea-level (RSL) rate for the ELC; B) probability distribution of vertical land motion (VLM) for ELC; C) ensemble of RSL rates by combining the ReSL rate and acceleration, and VLM; and D) resulting probability distributions of RSL for 1910, 1965 and 2021.

To determine the ensemble of time-dependent RSL series, we first determined the mean and SE of 10,000 bootstrapped rates and accelerations for the ReSL series using the Ebisuzaki (1997) methodology. Subsequently, we sampled a single normal deviate for VLM and the ReSL rate and acceleration. These sampled values were then combined into a single RSL series using the following equation:

$$RSL = rate + (acc * year) - vlm \qquad \text{Eq. 14}$$

where *acc* is the acceleration, the other terms have been previously described, and the resulting RSL rate has units of mm/yr. This process was repeated 10,000 times to create an ensemble of RSL rates spanning 1900 to 2021 (Figure 8C). Figure 8D illustrates the resulting probability distributions of annual RSL rates from a MC iteration for 1910, 1965 and 2021. During these years, the RSL rates were found to be 3.971 ± 0.398 mm/yr, 4.529 ± 0.353 mm/yr, and 5.097± 0.409 mm/yr, respectively, indicating a clear upward trend in RSL over time.

As a validation step, we compared the mean rate from the RSL ensemble against a length weighted estimate of the RSL rates for the ELC stations listed in Table 3. This comparison employed the same bootstrap approach as the VLM analysis (Figure 8B). The resulting Table 3 RSL rate (4.715 ± 0.332 mm/yr) closely aligns with the stabilized RSL ensemble rate (4.716 ± 0.378 mm/yr) for the sand budget period spanning 1966-2001. Additionally, the ELC RSL rate from 1977 to 2021 (4.873 ± 0.401 mm/yr) compares favorably with the current NOAA RSL rate (5.01 ± 0.76 mm/yr) for the North Spit, CA station spanning 1977 to 2023 (accessed Feb. 2024; https://tidesandcurrents.noaa.gov/stationhome.html?id=9418767).

3.2.9 Sand Budget Input Terms

3.2.9.1 Fluvial Sand Load (Q_R)

Time-dependent annual sand loads (mean and 95% CI) were determined for each of the nine ELC tributaries (Section 3.1). The SE was estimated as the CI range divided by 3.92, a common approximation for larger sample sizes and reasonably normally distribution. Using the means and SE of the nine tributary loads, we determined a statistical distribution of the total fluvial sand load for each year (1911 to 2018) was determined by combining 10,000 bootstrapped normally distributed samples of each tributary.

For use in the MC sand budget analysis, we assumed that the resulting annual total fluvial sand loads followed a lognormal distribution. Consequently, we converted the means and standard errors into equivalent lognormal parameters (Hines and Montgomery, 1990). To validate the lognormal distribution assumption, we estimated the mean and 95% CI for the nine ELC tributary sand loads using estimated lognormal parameters derived from the reported mean and SE (assuming CI range divided by 3.92). Comparing the nine tributary loads estimated from a lognormal distribution to the loads reported in Section 3.1 revealed identical mean loads. Additionally, the lower and upper 95% CIs showed average differences of 2.9% and 1.6%, respectively. This suggests that our assumption of annual fluvial sand loads being lognormally distributed was reasonable.

To convert estimated river load mass to volume, we use a dry bulk density of 1,600 kg/m^3, consistent with other California rivers and ELC sand budgets (e.g. Best and Griggs, 1991; Slagel and Griggs, 2006; Patsch and Griggs, 2007). This value was held constant throughout the sand budget analysis.

3.2.9.2 Bluff Erosion (Q_B)

The dominant source of bluff erosion occurs at the sound end of the ELC. We used the Scripps California Coastal Cliff Erosion Viewer (https://siocpg.ucsd.edu/data-products/ca-cliff-viewer/) to identify the zone and rate of active bluff erosion. Cliff length was measured from the NOAA (2010) NAVD88 DEM of Eureka, CA, and cliff height elevations were sampled from the same DEM (Table 4). Eight cliff top and face erosion rates (m/yr) are provided for this location in the Scripps Viewer. We determined the 95% confidence interval on the mean differences of the top and face erosion rates using the bootstrap t-test (MKinfer package in R; Kohl, 2023). Since the resulting confidence interval included zero (p = 0.408), we combined the 16 top and face rates into a single erosion rate series (Table 4). The maximum sand fraction of the bluff material (>= 125μm) was assumed as 0.25 (Leroy, personal communication), and a

uniform distribution with a minimum fraction of 0.05 was used for this variable (Table 4). Due to limited data availability, we were only able to estimate an annual bluff erosion rate using Eq. 8, rather than a time-dependent rate. Any negative bluff erosion rates generated during the MC simulation were set to zero, resulting in a truncated distribution.

Table 4. Bluff erosion probability distribution (PD) variables used in Monte Carlo simulation.

Variable	Unit	Mean	SE	CV	Min	Max	PD	Comment
Cliff length (C_L)	km	7.232	.036	0.5	NA	NA	Normal	Measured, assumed SE + normal dist. map error (SE = 0.104 m)
Cliff height (H_C)	m[1]	78.84	3.76	19.94	NA	NA	Normal	Bootstrap sample + normal dist. map error (SE = 0.255 m)
Cliff erosion rate (C_E)	m/yr	0.78	0.10	13.35	NA	NA	Normal	Bootstrap sample
Cliff sand fraction >= 0.125 (C_{SF})	frac	NA	NA	NA	0.05	0.25	Uniform	Assumed

[1] Elevation referenced to NAVD88.

3.2.10 Sand Budget Output Terms

3.2.10.1 Shoreline Sand Loss from Sea-Level Rise (Q_{SLS})

We computed shoreline sand loss due from Relative Sea-Level Rise (RSL) by applying Brunn's rule (Eq. 6) and utilizing bootstrapped samples for B and D_C, (which collectively form D_A as per Eq. 4), along with the active cross-shore width (W_A) determined via Eq. 10, and the time-dependent RSL rates. The resulting Q_{SLS} values are either time-dependent mean annual values or a mean period estimate.

3.2.10.2 Estuary Sand Loss from Sea-Level Rise (Q_{SLE})

The loss of sand from RSL in the estuaries was determined using Eq. 7 and bootstrapped samples for the areas of the three estuaries (Table 5) and the time-dependent RSL rates. Similar to Q_{SLS} the resulting Q_{SLE} values represent either annual time-dependent or mean estimate of a specified period.

Table 5. Estuary area probability distribution (PD) variables used in Monte Carlo simulation.

Variable	Unit	Mean	SE	CV	PD	Comment
Eel River	km^2	12.110	0.121	1.0	Normal	Measured, CV = 1.0%
Humboldt Bay	km^2	11.896	0.119	1.0	Normal	Measured, CV = 1.0%
Mad River	km^2	1.523	0.015	1.0	Normal	Measured, CV = 1.0%

3.2.11 Sand Budget Storage Change Terms

3.2.11.1 Shoreline Volume Change (ΔS_S)

Volumetric shoreline change (ΔS_S) was determined via Eq. 9, employing bootstrapped samples for B and D_C (combine to D_A), shoreline length (L_S) used for Δx, and the shoreline change rate used for Δy. Shoreline change rates for the ELC were estimated from the historical shoreline analysis conducted by McDonald (2017) for Little River to Table Bluff, and GHD (2018) for Table Bluff to Centerville Beach. Both analyses documented shoreline changes digitized from aerial imagery dating from 1939 to 2016 using the Digital Shoreline Analysis Software (DSAS; Himmelstoss et al., 2021). For this sand budget, we were interested in the shoreline rate for the 1966 to 2001 period and not the longer-term rates reported

by McDonald and GHD for 1939 to 2016. End point rates and uncertainties for each shoreline segment (Little River to Mad River Beach, Mad River Beach to North Spit, and South Spit to Table Bluff) were provided by McDonald (2017), covering intervals from 1966 to 2001. We extracted the end point rates and uncertainties spanning 1966-2001 and computed cumulative erosion for each segment based on the reported rate and the number of years between image acquisitions, or the years between 1966 or 2001 and the nearest image date. We used a weighted linear model to determine the mean shoreline rates and SE (Table 6), with weights assigned as the inverse of the reported end point uncertainty squared.

Table 6. Shoreline rate probability distribution (PD) variables used in Monte Carlo (MC) simulation for the period 1966-2001.

Variable	Unit	Mean	SE	CV	PD	Comment[1]
Rate (Little River to Mad River Beach)	m/yr	1.48	0.28	19.10	Normal	Int MC simulation
Rate (Mad River Beach to North Spit)	m/yr	-0.83	0.11	-12.59	Normal	Int MC simulation
Rate (South Spit to Table Bluff)	m/yr	2.04	0.41	20.27	Normal	Int MC simulation
Rate (Table Bluff to Eel River)	m/yr	0.48	0.09	18.25	Normal	Int MC simulation
Rate (Eel River to Centerville Beach)	m/yr	-0.22	0.12	-52.10	Normal	Int MC simulation
Length (Little River to Mad River Beach)	km	8.609	0.043	0.5	Normal	Measured, CV = 0.5%
Length (Mad River Beach to North Spit)	km	23.510	0.118	0.5	Normal	Measured, CV = 0.5%
Length (South Spit to Table Bluff)	km	7.971	0.040	0.5	Normal	Measured, CV = 0.5%
Length (Table Bluff to Eel River)	km	6.122	0.031	0.5	Normal	Measured, CV = 0.5%
Length (Eel River to Centerville Beach)	km	8.858	0.044	0.5	Normal	Measured, CV = 0.5%

[1] Int refers to intermediate.

The GHD (2018) report provided end point rates for two segments (South Spit to Eel River and Eel River to Centerville Beach) but did not include uncertainty estimates. To account for this, we used a weighted linear model of McDonald's median reported uncertainty values against the year span between images (Figure 9). This approach provided a reasonable approximation for the SE, considering that both analyses used the same image set and analysis software (DSAS). Additionally, we added an extra error term, based on the SE of the regression prediction at each interval, to the mean SE value. After estimating the uncertainty terms, the same approach described above was used to determine the shoreline rates and SE for the two GHD segments (Table 6). The measured lengths of the shoreline segments and SE are also listed in Table 6.

A length-weighted shoreline rate for the entire ELC was determined using 10,000 bootstrap samples of the rates and lengths for each shoreline segment (Table 6). The resulting stabilized ELC shoreline rate for the 1966 to 2001 period was estimated as 0.19 ± 0.09 mm/yr (CV = 47.6%).

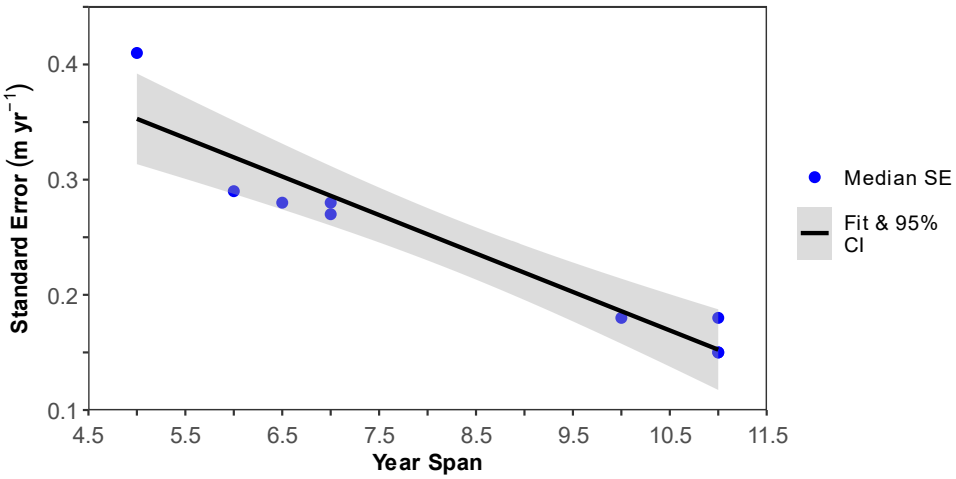

Figure 9. Linear model fit of the median end point uncertainties versus the span in years between images used in the McDonald (2017) shoreline analysis.

3.2.11.2 Inner-Shelf Volume Change (ΔS_{IS})

Crockett and Nittrouer (2004) (hereafter CN2004) conducted two cruises in 1999 and 2000, during which they collected 50 vibracores from the inner-shelf in water depths ranging from 20 to 55 m. These cores were distributed across five distinct sub-environment zones (A, D/E, H/I/L, O/P, and R/T) within the ELC's inner-shelf region (Figure 10). Through radionuclide analysis, they identified distinct mud layers deposited during the 1964 flood, and subsequently quantified the mass and volume of sediment (sand and mud fractions) deposited since 1964. This timeframe spanned approximately 36 years, encompassing the period following the 1964 flood up to the 1999 and 2000 sampling cruises. As fluvial sand loads were determined by water years (Section 2.1), and given that the 1964 flood occurred in WY 1965, we defined the 36-year period for this analysis as spanning from 1966 to 2001, aligning with one of the sand budget analyses (Section 2.2.6.1).

The data reported in CN2004 did not provide enough supporting information to directly determine the sand deposition thickness or rates in the five inner-shelf zones, and it appears that the supporting data may not be available (Crockett, personal communication). However, by making some general assumptions regarding Eel River sand and mud loads, and utilizing the data provided in Table 1 of CN2004, we were able to back calculate the sand deposition rates for sand (>= 125µm) in each of the five zones for the 1966 to 2001 period.

CN2004 estimated the mass of mud and sand discharged by the Eel River for the 36-year period using the rating curve developed by Sommerfield and Nittrouer (1999), assuming that the suspended sand fraction was 25% of the total suspended sediment load and sand bedload contributed an additional 10% of the suspended sediment load. However, it was not clear if the Van Duzen River sediment load was included in the CN2004 Eel River load estimate, as it was included as a mass per year (kg/yr) estimate in Sommerfield and Nittrouer (1999). For this work, we determined the total Eel River sediment loads for the 1966 to 2001 period using the rating curve from Sommerfield and Nittrouer (1999) with and without the Van Duzen River loads, and then determined the sand and mud fractions using the percentages described in CN2004. This approach provided a low and high estimate of the sand and mud loads discharged from the Eel River during the 1966-2001 period. For the uncertainty analysis, we assumed lognormal distributions for the low and high load estimates and assigned SEs based on an approximate CV of 8.7% estimated for the total fluvial sand loads (Section 3.2.9.1) for each Monte Carlo iteration

(Table 7). Lognormal distribution estimates (10,000 samples) were created for the low and high load estimates and then randomly sampled to create a single estimate comprising 10,000 samples.

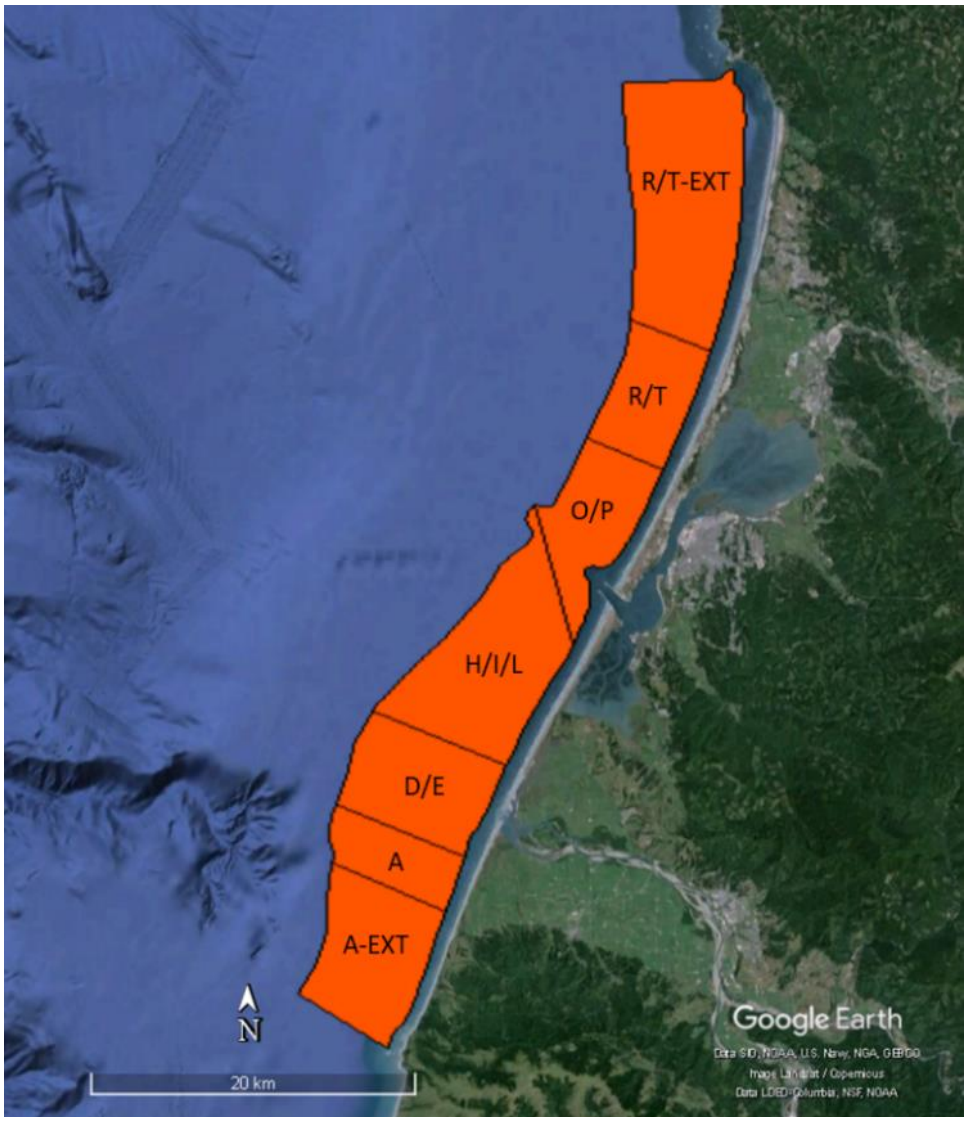

Figure 10. Location of the five inner-shelf sub-environment zones (A, D/E, H/I/L, O/P, R/T) as defined by Crockett and Nittrouer (2004). These five zones were digitized (based on Figure 10 in Crockett and Nittrouer, 2004) between the -14 m (depth of closure) and the -50 m contour lines (referenced to NAVD88), which covers the inner-shelf area defined in this work. To cover the entire ELC inner-shelf we extended zone A (A-EXT) and zone R/T (RT-EXT) to the south and north ends of the ELC, respectively.

Table 7. Inner-shelf mud and sand probability distribution (PD) variables used in Monte Carlo simulation to determine deposition rates for the 1966-2001 period (36-years). Inner-shelf zone data from Table 1 in Crockett and Nittrouer (2004). Total Eel River loads estimated from Eel River rating curve and Van Duzen River stated annual loads in Sommerfield and Nittrouer (1999), and mud/sand fractions from Crockett and Nittrouer (2004).

Variable	Unit	Mean	SE	CV	Min	Max	PD
Eel River Mud and Sand Load							
Eel River low mud load	t	4.65e+08	4.04e+07	~8.7	NA	NA	Lognormal
Eel River high mud load	t	4.97e+08	4.32e+07	~8.7	NA	NA	Lognormal
Eel River low sand load	t	2.17e+08	1.89e+07	~8.7	NA	NA	Lognormal
Eel River high sand load	t	2.32e+08	2.02e+07	~8.7	NA	NA	Lognormal
Area A Mud							
Area	km^2	40	0.4	1.0	NA	NA	Normal
Bulk density	g/cm^3	2.10	0.0088	0.42	NA	NA	Normal
Mud in deposited layer	%	NA	NA	NA	9.5	31.0	Uniform
Eel River mud on inner-shelf	%	NA	NA	NA	0.3	1.1	Uniform
Area D/E Mud							
Area	km^2	70	0.7	1.0	NA	NA	Normal
Bulk density	g/cm^3	2.10	0.0088	0.42	NA	NA	Normal
Mud in deposited layer	%	NA	NA	NA	5.0	27.6	Uniform
Eel River mud on inner-shelf	%	NA	NA	NA	0.3	1.7	Uniform
Area H/I/L Mud							
Area	km^2	135	1.35	1.0	NA	NA	Normal
Bulk density	g/cm^3	2.10	0.0088	0.42	NA	NA	Normal
Mud in deposited layer	%	NA	NA	NA	24.4	37.3	Uniform
Eel River mud on inner-shelf	%	NA	NA	NA	5.5	8.3	Uniform
Area O/P Mud							
Area	km^2	61	0.61	1.0	NA	NA	Normal
Bulk density	g/cm^3	2.10	0.0088	0.42	NA	NA	Normal
Mud in deposited layer	%	NA	NA	NA	5.1	12.4	Uniform
Eel River mud on inner-shelf	%	NA	NA	NA	0.2	0.5	Uniform
Area R/T Mud							
Area	km^2	40	0.4	1.0	NA	NA	Normal
Bulk density	g/cm^3	2.10	0.0088	0.42	NA	NA	Normal
Mud in deposited layer	%	NA	NA	NA	1.7	27.7	Uniform
Eel River mud on inner-shelf	%	NA	NA	NA	0.08	1.2	Uniform
Area A Sand							
Area	km^2	40	0.4	1.0	NA	NA	Normal
Bulk density	g/cm^3	2.10	0.0088	0.42	NA	NA	Normal
Sand in deposited layer	%	NA	NA	NA	69.0	90.5	Uniform
Eel River sand on inner-shelf	%	NA	NA	NA	4.5	5.9	Uniform
Area D/E Sand							
Area	km^2	70	0.7	1.0	NA	NA	Normal
Bulk density	g/cm^3	2.10	0.0088	0.42	NA	NA	Normal
Sand in deposited layer	%	NA	NA	NA	72.4	95.0	Uniform
Eel River sand on inner-shelf	%	NA	NA	NA	8.9	11.9	Uniform
Area H/I/L Sand							
Area	km^2	135	1.35	1.0	NA	NA	Normal
Bulk density	g/cm^3	2.10	0.0088	0.42	NA	NA	Normal
Sand in deposited layer	%	NA	NA	NA	62.7	75.6	Uniform
Eel River sand on inner-shelf	%	NA	NA	NA	26.3	31.8	Uniform

We estimated mud and sand deposition rates using an intermediate MC simulation, which integrated the available data for each inner-shelf zone summarized in CN2004, along with our assigned uncertainties and probability distributions (Table 7). First the total thickness of deposited mud/sand was estimated by multiplying the Eel River load by the percent mud/sand from the Eel River on the inner-shelf, and then dividing by area, bulk density, and precent mud/sand in the sediment deposit. This total thickness was then divided by 36 years to provide the sedimentation rate in cm/yr.

CN2004 did not provide enough data to directly determine sand deposition rates for zones O/P and R/T. To overcome this limitation, we estimated the mean sand rates for these two zones using a linear model fit of the sand and mud rates for zones A, D/E and H/I/L (Figure 11). Additionally, SEs for zones O/P and R/T were assigned using the maximum CV from zones A, D/E and H/I/L. The resulting sand deposition rate means and SEs for each inner-shelf zone are summarized in Table 8.

The estimated sand deposition rates ranged from a minimum of 0.31 (0.22 – 0.40) cm/yr (mean and 95% CI) to a maximum of 0.93 (0.71 – 1.15) cm/yr. These estimates align reasonably well with the maximum sedimentation (mud and sand) rates of 1.3 to 3.3 cm/yr reported by CN2004 for three cores located at 45 to 55 m depths.

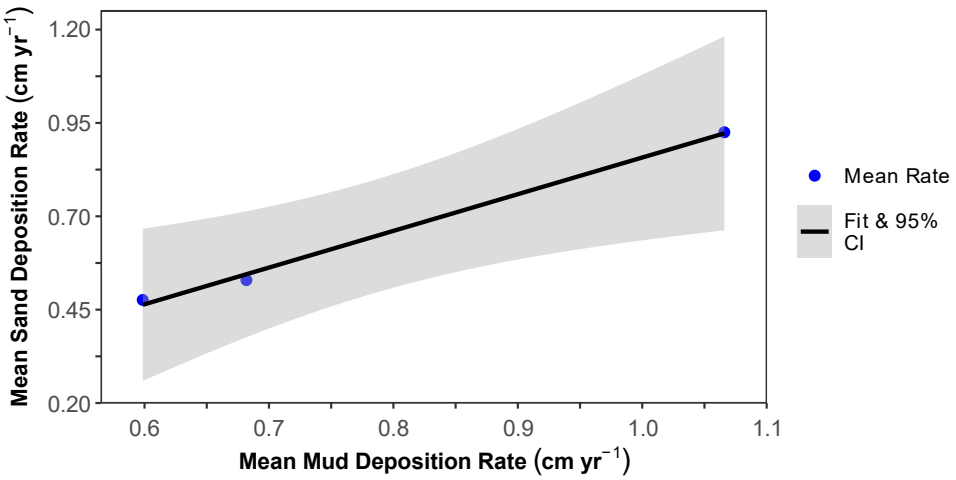

Figure 11. Linear model fit of the mean sand deposition rate (cm/yr) versus the mean mud deposition rate (cm/yr) for the inner-shelf zones A, D/E and H/I/L.

The inner-shelf volume change (ΔS_{IS}) of sand was ultimately determined using Eq. 5 and 10,000 bootstrapped samples from Table 8. To cover the entire ELC inner-shelf we extended zone A and zone R/T at the south (A-EXT) and north (R/T-EXT) ends of the ELC, respectively (Figure 10). The estimated sand deposition rates for zones A and R/T were used as the rates for zones A-EXT and R/T-EXT, respectively. Zone areas were digitized from the NOAA (2010) NAVD88 DEM of Eureka, CA. During the volume change calculations, we accounted for the zone area changes associated with the active cross-shore width (W_A) estimated in Section 3.2.10.1.

The estimated deposition rates pertain to the total sand load. To estimate the amount of sand greater than or equal to 125μm (sand cutoff diameter) stored on the inner-shelf we assumed a mean inner-shelf sand diameter of 125μm (3ϕ, where ϕ represents phi units). This approximates the middle (2.9ϕ = 0.134 mm) of the mean sand diameter range of 2.2 to 3.6ϕ reported by CN2004 for the surface sand fraction. Nearshore bed sampling in depths between 19 to 31 m indicated mean grain sizes of 3ϕ (125μm) north of the Humboldt Bay entrance (Pequegnat et al., 1993 and 1995, as summarized in GHD, 2021). Dean and Dalrymple (2002) note that sand reasonably follows a lognormal distribution with phi (ϕ) units, resulting

in a 50% probability that a grain size is greater than the mean grain size. Thus, using a mean inner-shelf sand diameter of 125μm indicates that half of the sand on the shelf is greater than 125μm, and half is less than 125μm. For the sand budget analysis, we used a constant fraction of 0.5 to determine the inner-shelf sand volume greater than or equal to 125μm.

Table 8. Inner-shelf sand storage probability distribution variables used in the Monte Carlo (MC) simulation for the period 1966-2001. Sand deposition rates were determined from an intermediate MC simulation using data from Table 7. Inner-shelf zone areas A and R/T were expanded (A-EXP, R/T-EXP) to cover the entire ELC (Figure 10).

Variable	Unit	Mean	SE	CV	PD	Comment[1]
Sand deposition rate (Zone A, A-Ext)	cm/yr	0.47	0.07	14.46	Normal	Int MC simulation
Sand deposition rate (Zone D/E)	cm/yr	0.53	0.08	14.76	Normal	Int MC simulation
Sand deposition rate (Zone H/I/L)	cm/yr	0.93	0.11	12.16	Normal	Int MC simulation
Sand deposition rate (Zone O/P)	cm/yr	0.31	0.05	14.76	Normal	Int MC simulation
Sand deposition rate (Zone R/T, R/T-EXT)	cm/yr	0.63	0.09	14.76	Normal	Int MC simulation
Zone A-Ext area	km^2	65.95	0.66	1.0	Normal	Measured, CV = 1.0%
Zone A area	km^2	31.96	0.32	1.0	Normal	Measured, CV = 1.0%
Zone D/E area	km^2	60.69	0.61	1.0	Normal	Measured, CV = 1.0%
Zone H/I/L area	km^2	93.48	0.94	1.0	Normal	Measured, CV = 1.0%
Zone O/P area	km^2	59.07	0.59	1.0	Normal	Measured, CV = 1.0%
Zone R/T area	km^2	47.48	0.48	1.0	Normal	Measured, CV = 1.0%
Zone R/T-EXT area	km^2	131.8	1.32	1.0	Normal	Measured, CV = 1.0%

[1] Int refers to intermediate.

3.2.12 Sand Budget Removal/Extraction Terms

3.2.12.1 Fluvial Sand/Gravel Extraction (R_R)

The primary fluvial sand and gravel extraction operations in the ELC watershed are concentrated on the lower reaches of the Mad, Eel and Van Duzen Rivers. Historical gravel extraction has been documented on the Eel River since about 1911 for road construction, and residential and commercial projects (Humboldt County, 1992). Significant gravel extraction volumes on the Mad River were documented back to the 1940s for large County projects (Humboldt County, 1993), but earlier extraction likely occurred to support smaller construction activities. The County of Humboldt established the County of Humboldt Extraction Review Team (CHERT) in 1992 to provide scientific oversight on Mad River gravel extraction (CHERT, 2019). In 1997, the scope of CHERT was expanded to include most fluvial extraction sites throughout Humboldt County. Annual CHERT reports have documented extraction volumes for the Mad River beginning in 1992, and the Eel and Van Duzen Rivers since 1997. However, quantitative historical gravel extraction data prior to 1992 are not available for all rivers.

To support the sand budget analysis, we developed an annual fluvial sand/gravel extraction time series for the Mad, Eel and Van Duzen Rivers spanning from 1911 to 2018. For the Mad River, historical extraction volumes for 1952 to 1991 were obtained from Klein (personal communication), and for 1992 to 2019 from CHERT (2019). Gravel extraction prior to 1952 was computed by assuming gravel mining rates decayed exponentially from 1952 to 1911, where the 1911 extraction rates were assumed to be 10% of the 1952 rates. Gravel volumes for the Eel and Van Duzen Rivers for the period 1997 to 2018 were obtained from CHERT (2019). Extraction volumes for the 1952 to 1996 period were estimated by separate power regressions of gravel mining rates in the Mad River versus Eel and Van Duzen River rates for the overlapping periods of 1997 to 2018 (Figure 12). Similar to the Mad River, we used an exponential curve

to define rates from 1952 to 1911. The individual extraction time series for the Mad, Eel and Van Duzen Rivers were combined to provide a single fluvial sand/gravel extraction time-series for the ELC (Figure 13).

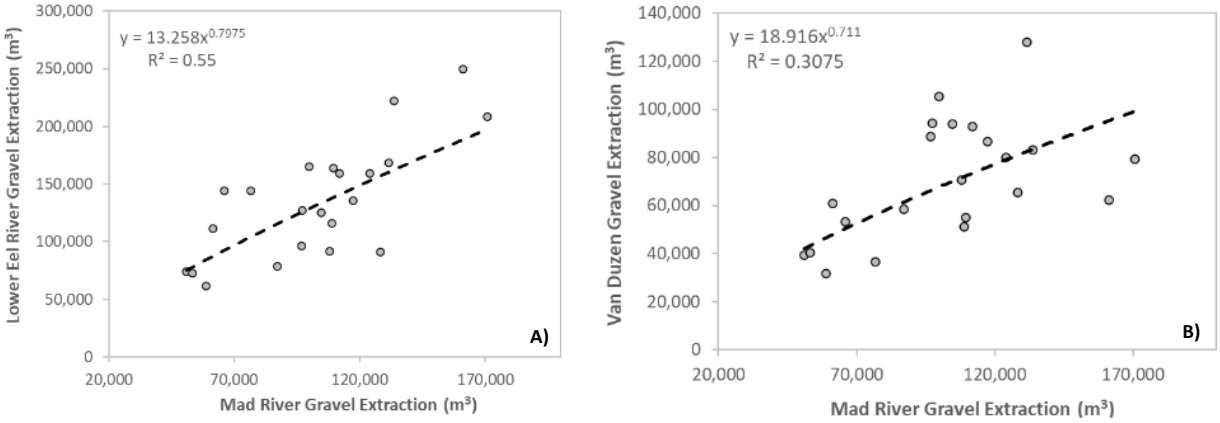

Figure 12. Power regression model fits of annual sand/gravel extraction volume fits for the Eel River and Mad River (A), and the Van Duzen River and Mad River (B) for the 1997 to 2018 period.

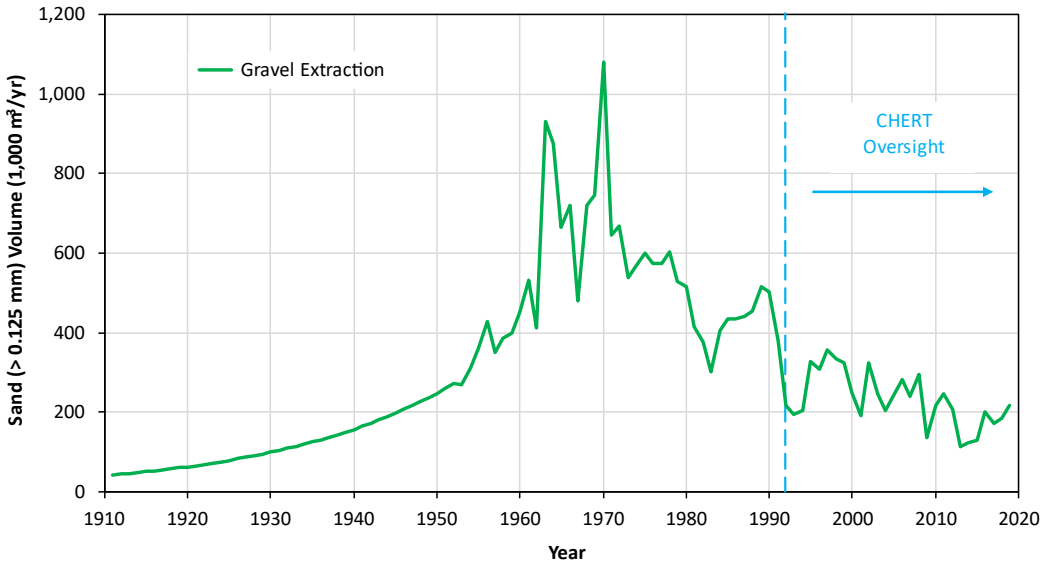

Figure 13. Annual fluvial sand/gravel extraction volumes (>= 125µm) for the Mad, Eel and Van Duzen Rivers for the 1997 to 2018 period, with CHERT oversight beginning in 1992.

For the uncertainty analysis, we assumed triangle distributions for each annual sand/gravel extraction volume. In this approach, the middle value corresponds to the reported volume, while the minimum and maximum values are computed as the reported volume ± 50% of the reported volume (Table 9). To define the fraction of extracted sand/gravel greater than the littoral cutoff diameter of 125µm, we used 25 surface and 25 subsurface grain size distributions sampled from four different Mad River gravel extraction bars (Reid, 2011). Similar grain size data for the Eel River or Van Duzen River were not available. A bootstrap t-test (MKinfer package in R) indicated that the 95% CI on the mean differences of the surface

and subsurface samples (>= 125μm) contained zero (p = 0.07). Thus, we combined the grain size data into a single series to define the probability distribution of fluvial extracted sand/gravel volume (<= 125μm) (Table 9).

Table 9. Fluvial sand/gravel extraction volume probability distribution (PD) variables used in Monte Carlo simulation.

Variable	Unit	Mean	SE	CV	Min	Max	PD	Comment
Fluvial sand/gravel extraction	m^3/yr	Value	NA	NA	-50%	+50%	Triangle	Middle (mean) value is reported value; min/max value is reported value ± 50% reported value
Fluvial sand >= 125um	frac	0.985	0.002	0.18	NA	NA	Normal	Bootstrap sample

3.2.12.2 Humboldt Bay Sand Dredging (R_{HB})

As the sole deep-water port between San Francisco and Coos Bay, Oregon, Humboldt Bay is an important marine port that requires dredging to maintain navigable channel depth for commercial and recreational vessels. Dredging operations in the ELC are primarily focused on maintenance dredging of federal, district and private navigation channels in Humboldt Bay. The bulk of the dredging is conducted by the Corps of Engineers, which is responsible for annual maintenance of the Bar and Entrance Channel, as well as periodic dredging of other federally maintained interior channels. (EPA, 1995; EPA and COE, 2020). Prior to 1999, dredging efforts focused on maintaining the bar and entrance channel at a depth of -12.1 m (-40 ft) and interior channels at approximately -9.1 m (-30 ft). However, in 1999, bar and entrance dredging were deepened to its current depths of -14.6 m (-48 ft) and interior channels to -11.6 m (-38 ft).

For the sand budget analysis, we developed an annual Humboldt Bay dredging time series for the bar and entrance channels, and the interior channels for the period 1911 to 2018. The primary sources of the annual dredge volumes were Costa and Glatzel (2002) for years prior to WY 1977, and the COE Ocean Dredged Material Disposal Site (ODMDS) database (COE, 2022) beginning in WY 1977. The ODMDS dredged volumes were compared to annual dredging data obtained from a variety of government agencies and researchers (i.e. COE 1989, 2012, 2017; EPA 1995; EPA and COE, 2020; CCC Feb 2017, Oct 2017, Dec 2018; Ross, personal communication). The ODMDS values were approximately 13% higher than the other sources for the period 1977 to 2018, with the difference likely from ODMDS reporting actual dredged volumes and some of the other sources reporting permitted values. The bar/entrance and interior channel dredge volumes were combined to provide a single Humboldt Bay sand dredging time-series for the ELC (Figure 14). We assumed no dredging occurred prior to the earliest year of record (1931).

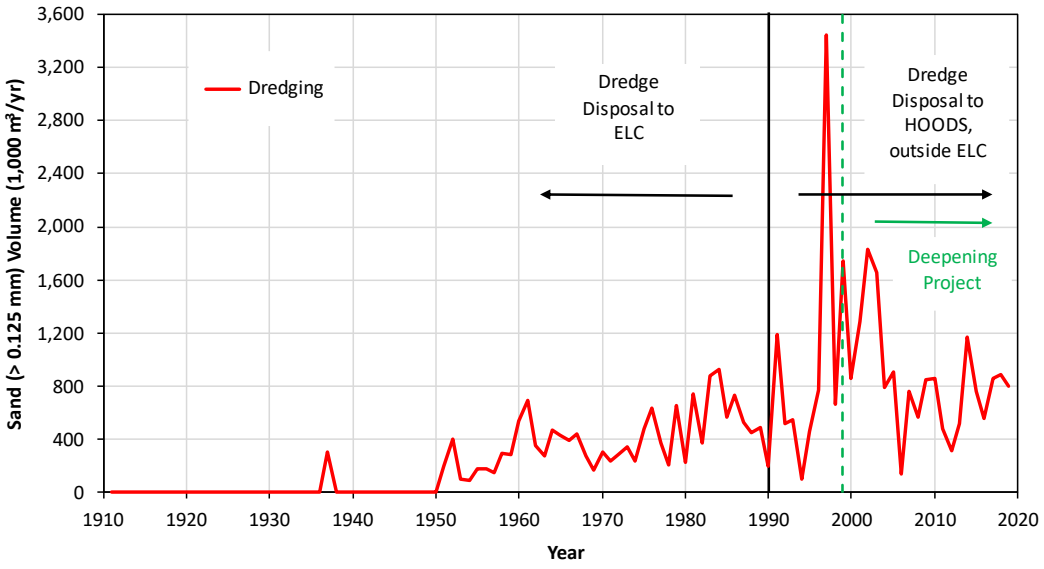

Figure 14. Annual Humboldt Bay dredging volumes for sand (>= 125µm) for the 1911 to 2018 period. Dredge disposal to HOODS began in 1990, and the dredge deepening project started in 1999.

It was necessary to determine the sand fraction of dredged material greater than or equal to 125µm for two locations: (1) Bar/Entrance and North Bay Channels, and (2) the interior channels consisting of the North Bay Channel, Samoa Channel and Turning Basin, Eureka Outer Channel, and the Fields Landing Channel and Basin. Notably, the North Bay Channel was utilized in both sand fraction estimates as dredge volumes for this location were reported alongside the Bar/Entrance Channel and the interior channels. Sand fractions (>= 125µm) were extracted from pre-dredging particle size distributions (KLI, 2016, attachment in COE, 2017).

For the Bar/Entrance and North Bay Channels, a bootstrap t-test (MKinfer package in R) indicated that the 95% CI on the mean differences of the sand fraction (>= 125µm) contained zero (p = 0.23). Thus, we combined the sand fractions into a single series. For the interior channels we computed a volume-weighted sand fraction using 10,000 bootstrapped samples of particle size (>= 125µm) and the annual average dredged volume reported by EPA and COE (2020) for the four interior channel locations (Table 10). Given that the Fields Landing Channel only contained one sample, we adopted the maximum SE (0.119) from the Samoa Channel.

For the MC simulation uncertainty analysis, we estimated separate sand volumes (>= 125µm) dredged from Bar/Entrance and North Channels, and the interior channels. We then combined these estimates into a single annual Humboldt Bay dredged sand volume. Triangle probability distributions were assumed for each annual dredged volume with the middle value being the reported volume and the minimum and maximum values being the reported volume ± 50% of the reported volume, and the sand fraction (>= 125µm) distributions represent the stabilized values from the aforementioned sand fraction analysis (Table 11).

3.2.13 Sand Budget Placement Terms

3.2.13.1 Sand Placement (P_B)

As described earlier, disposal of sand dredged from Humboldt Bay has occurred at three locations. Prior to 1990, dredged sand was placed at two sites located in the ELC (SF-3 and NDS). After 1990 dredged sand was placed at HOODS located outside of the ELC.

Table 10. Interior channel probability distribution variables for an intermediate Monte Carlo (MC) simulation to determine the interior channel's sand fraction greater than 125µm.

Variable[1]	Unit	Mean	SE	CV	Min	Max	PD	Comment[1]
Sand >= 125µm (North Channel)	frac	0.958	0.004	0.456	NA	NA	Normal	Bootstrapped sample
Sand >= 125µm (Samoa Channel)	frac	0.641	0.119	18.5	NA	NA	Normal	Bootstrapped sample
Sand >= 125µm (EO Channel)	frac	0.390	0.118	30.25	NA	NA	Normal	Bootstrapped sample
Sand >= 125µm (FL Channel)	frac	0.514	0.119	23.1	NA	NA	Normal	Bootstrapped sample
Dredged volume (North Channel)	m^3/yr	7.65e+04	NA	NA	-50%	+50%	Triangle	Middle (mean) value is reported value; min/max value is reported value ± 50% reported value
Dredged volume (Samoa Channel)	m^3/yr	1.53e+04	NA	NA	-50%	+50%	Triangle	Middle (mean) value is reported value; min/max value is reported value ± 50% reported value
Dredged volume (EO Channel)	m^3/yr	1.91e+04	NA	NA	-50%	+50%	Triangle	Middle (mean) value is reported value; min/max value is reported value ± 50% reported value
Dredged volume (FL Channel)	m^3/yr	4.59e+03	NA	NA	-50%	+50%	Triangle	Middle (mean) value is reported value; min/max value is reported value ± 50% reported value

[1] EO is Eureka Outer; FL is Fields Landing.

Table 11. Humboldt Bay dredged sand volume probability distribution (PD) variables used in Monte Carlo simulation.

Variable[1]	Unit	Mean	SE	CV	Min	Max	PD	Comment[1]
Humboldt Bay sand dredging	m^3/yr	Value	NA	NA	-50%	+50%	Triangle	Middle (mean) value is reported value; min/max value is reported value ± 50% reported value
BEN channels sand >= 125um	frac	0.953	0.004	0.46	NA	NA	Normal	Bootstrap sample
Interior channels sand >= 125um	frac	0.804	0.026	3.25	NA	NA	Normal	Int MC simulation

[1] BEN refers to Bar, Entrance and North; Int refers to intermediate.

4 RESULTS AND DISCUSSION

4.1 Fluvial Sand Loads

Gross fluvial sand flux (>= 125µm) from all coastal ELC subbasins was variable over the period of record (Figure 15). Plots of sand flux for the remaining smaller tributaries are not provided as they are scaled to the Little River discharge by watershed area, and thus mirror the Little River sand flux except the magnitudes are smaller. Peak sand loads generally occurred in the 1960s and 1970s, coinciding with a series of large flood events coupled with road building and mechanized logging practices. Mean annual sand loads were roughly 6-10 times greater in the Eel River relative to the Van Duzen and Mad Rivers. Over the period 1911-2018, the combined Eel and Van Duzen Rivers contributed 86% of the total fluvial sand load to the ELC, while the Mad River and the sum of all remaining smaller coastal subbasins contributed roughly 9.6% and 4.6%, respectively (Table 12). The individual river contributions to the total fluvial load remained generally the same for the more recent period of 2009 to 2018.

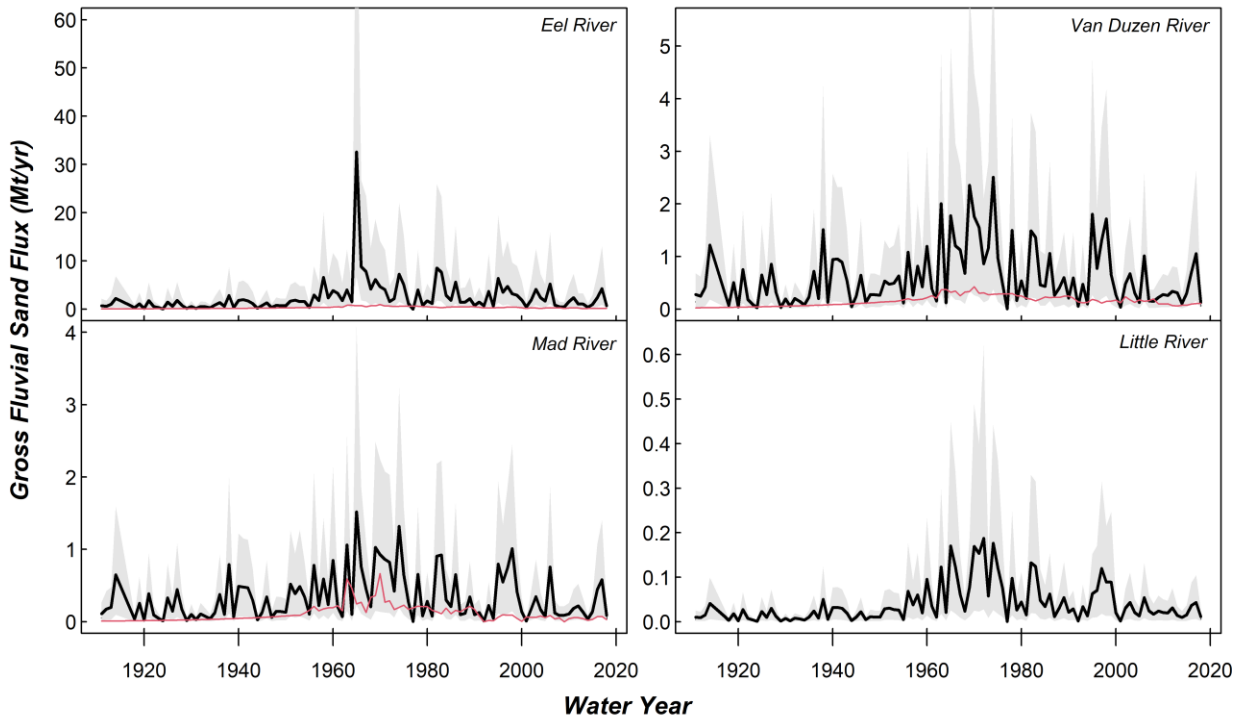

Figure 15. Gross fluvial sand flux (>= 125µm) to the Eureka Littoral Cell from the Eel, Van Duzen, Mad and Little Rivers from water years 1911-2018. Red line represents the gravel extraction rates (no extraction on Little River). Shaded region represents 90% prediction interval uncertainty bounds. Note the different vertical axis scales.

Table 12. Percent of total mean annual sand flux (>= 125µm) for tributary subbasins draining to the Eureka Littoral Cell during the periods 1911-2018 and 2009-2018.

Subbasin	Percent of Total Mean Annual Sand Flux	
	1911-2018	2009-2018
Eel & Van Duzen Rivers	85.8	86.6
Mad River	9.6	9.2
All remaining rivers	4.6	4.2

Translating the fluvial sand load estimates to total yields on a per unit area basis indicated that average annual yields ranged from 258 – 339 tons/km^2/yr in the gaged study basins over the period 1911-2018 (Table 13). Although not directly comparable, our estimates of total sand yield are generally in line with the findings of other researchers for coastal California watersheds. For example, CGS (2003) and Warrick et al. (2015) estimated total suspended sediment yields for a host of coastal California watersheds ranging from 5 – 2,100 t/km^2/yr and 105 – 1,051 t/km^2/yr, respectively. Assuming the sand fraction was 25% of the total suspended load and that bedload could be reasonably estimated as 100% of the sand load, this translates to sand yields ranging from 2.5 – 1,050 t/km^2/yr and 25 – 525.5 t/km^2/yr, respectively. Moreover, application of these assumptions to the findings of Barrett (2004), who computed suspended sediment yields for Elk River and Freshwater Creek, indicates total sand yields ranging from 70 – 175 t/km^2/yr. This suggests that our estimates of sand yield for the Little River (a proxy for all smaller ungaged basins in the ELC) during the most recent and most directly comparable decade (2009-2018) are similar, albeit more conservative.

Table 13. Average sand yields (>= 125µm) during select periods for the Eel, Van Duzen, Mad and Little Rivers from this study, as well as CRSMP (2017). CRSMP reported annual volumes converted to mass using 1,600 kg/m^3.

Subbasin	Sand Yield (CRSMP 2017) (t/km^2/yr)	Sand Yield from this Study (t/km^2/yr)						
		1911-2018	1954-2000	1965-1976	1979-1988	1989-1998	1999-2008	2009-2018
Eel River + Van Duzen River	326	316	501	890	414	366	271	199
Mad River	467	258	369	591	280	303	176	155
Little River	432	339	571	997	453	425	269	194

4.1.1 Trends in Fluvial Sand Loads

Examination of Figure 15 suggests two principal trends in sand flux within the ELC: 1) substantial increases in gross sand loading across all coastal subbasins from 1911 to the mid-century; and 2) pronounced decreases in loading subsequent to the mid-1960s and 1970s. Indeed, mean annual sand loads to the ELC for the period 2009-2018 were only 20 to 26% of the 1965-1976 period (Table 13). These temporal trends are in accordance with the LOESS residual ratios for the Eel River and regional SCC rating curves (Figure 4 and Figure 5), which indicated statistically significant declines in suspended sediment concentration with respect to flow since the mid-1960s (Mann Kendall tests, $p << 0.05$). The pronounced decrease in total load is also in agreement with Klein and Anderson (2012) and Warrick et al. (2014) who observed similar trends in sediment discharge in Redwood Creek and the Eel River, respectively. The time-dependent patterns of littoral sand discharge are largely driven by the Eel River, not only because the Eel is the largest source of sand in the ELC, but also because the residual ratios (Figure 4B and Figure 5B) exhibited a much steeper decline from 1965-2018 (~4.3 to 0.5) relative to the regional SSC rating curve (~1.25 to 0.5).

4.1.2 Dynamic vs. Static Rating Curves

Comparing sediment discharge estimates from the static and dynamic SSC rating curves suggests: 1) the time-dependent approach yields substantially different loads; and 2) the relative difference between the two methods varies considerably over time (Table 14). For instance, the mean annual fluvial sand load computed from the dynamic rating curve was 56% higher during WY 1965-1976, but 38% lower during WY 2009-2018. For the 1966 to 2001 sand budget period, there was only a minor difference (2%) between the static and dynamic rating curves, indicating that for this period either rating curve approach would provide similar load inputs. However, differences increase substantially post-2000, suggesting static curves result in a growing overestimation of sand loads that will likely have important implications for the ELC sand budget.

Table 14. Total mean annual sand loads (>= 125µm) to the Eureka Littoral Cell computed using static vs. dynamic rating curves over select time periods. Percent (%) difference is relative to dynamic curve.

	Mean Annual Sand Load (Mt/yr)						
Rating Curve	**1911-2018**	**1965-1976**	**1979-1988**	**1989-1998**	**1999-2008**	**2009-2018**	**1966-2001**
Dynamic	3.516	9.744	4.534	4.090	2.947	2.194	4.890
Static	4.374	6.265	5.032	4.592	4.130	3.567	5.011
% Difference	24.4	-35.7	11.0	12.3	40.1	62.6	2.5

This is in accordance with Warrick (2014) who examined fine-grained (< 63µm) suspended sediment loads in the Eel River using time-constant vs. time-dependent techniques and found similar relative differences and temporal patterns. Interestingly, Warrick (2014) concluded that time-independent approaches had overestimated fine-grain sediment loads by a factor of 1.6 for the period 1911-2000 – significantly higher than computed here for the 1911-2018 period (factor of 1.24). We note, however, that for the period 2009-2018, our data indicate that the static curve overestimates by a similar magnitude as found by Warrick (2014). Disparities between our results and Warrick (2014) are likely attributable to the fact that we focused on the larger grain size fractions for sand (>= 125µm) and bedload was estimated to be two times the suspended sand load.

4.1.3 Uncertainty in Fluvial Sand Loads

The 90% prediction intervals suggest a high degree of uncertainty in the estimates of fluvial sediment discharge (Figure 4A and Figure 5A). Such wide uncertainty bounds are unsurprising because: 1) our estimates of total fluvial sand loads represent compounded uncertainty of both the bedload and suspended load components; 2) we utilized regional rating curves that did not account for seasonal or stage effects; and 3) the sample size and observed discharge domain of the SSC rating curves was limited. The magnitude of uncertainty is consistent with a number of other studies that have quantified uncertainty in sediment flux estimates using Bayesian and frequentist approaches (e.g. Rustomji and Wilkinson, 2008; Schmelter et al., 2012).

While the block bootstrap approach provides a more statistically rigorous means of quantifying uncertainty relative to the conventional sum of errors method, it does not necessarily capture all sources of uncertainty (e.g. error in discharge or SSC measurement). Nevertheless, the lack of paired sediment-flow data resulted in relatively large 90% prediction intervals which may provide a reasonable estimate of cumulative error.

4.1.4 **Comparison of Bedload Approaches**

For comparison, we calculated cumulative total sand loads using our static regional bedload rating curve and the approach of Slagel and Griggs (2006) for estimating bedload in Northern California rivers, where bedload is computed as 4% of the total suspended load. As evidenced in Figure 16, total sand loads computed via the static regional bedload curve tracked well with the Willis and Griggs (2003) approach. General agreement between these two methods lends credence to the Willis and Griggs (2003) assumption because total loads computed with the bedload curve represent our best guess using available (albeit sparse) bedload data. It is also evident from Figure 16 that the Slagel and Griggs (2006) method deviates significantly from the other techniques – appearing to significantly underestimate total sand loads. The time-independent rating curve, by contrast, yields comparatively high and likely unrealistic fluvial sand flux estimates.

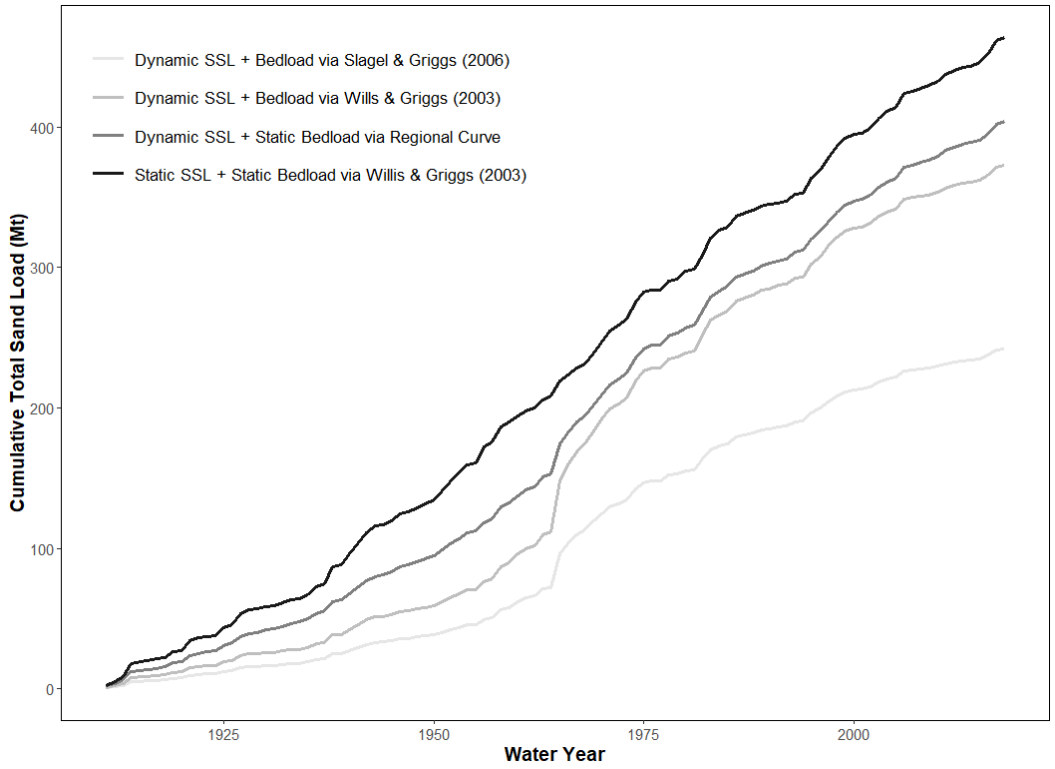

Figure 16. Cumulative sand loads (>= 125µm) from all nine coastal subbasins in the ELC watershed computed using static and dynamic rating curves (both suspended sand load and bedload); as well as the bedload approach of 4% of the total suspended load (Slagel and Griggs, 2006), and the bedload as 100% of the total suspended sand load (Willis and Griggs, 2003).

To provide further insight into the suitability of the Wills and Griggs (2003) approach (bedload is 100% of the suspended sand load), we compared mean annual sand loads computed via the combined dynamic SSC rating curve and static regional bedload curve (based on limited data). As Table 15 suggests, mean annual sand flux for the period 1911 – 2018 computed via the simple assumption that bedload was 100% of the sand load yielded estimates that were within roughly 10% of a regional (albeit poorly constrained) curve based on observed data. General agreement among these methods adds additional support to the approach of Willis and Griggs (2003) and suggests future studies may adopt a similar strategy in the absence of reliable bedload data.

Table 15. Comparison of total mean annual sand loads (>= 125µm) from select subbasins for the period 1911 – 2018, where bedload was computed via regional bedload rating curve vs. 100% of the suspended sand load (Willis and Griggs, 2003).

Subbasin	Mean Annual Sand Load (Mt)		Percent Difference Relative to 100% Sand Load
	Bedload Computed via Regional Curve	Bedload Computed via 100% Sand Load	
Eel River	2.734	2.421	12.9
Mad River	0.367	0.336	9.2
Van Duzen River	0.547	0.597	-8.4

4.2 Fluvial Sand/Gravel Extraction and Humboldt Bay Dredging

Humboldt Bay dredging and fluvial sand/gravel extraction are the only significant sand (>= 125µm) removal activities from the ELC. Figure 17 shows the annual mean Humboldt Bay dredging, fluvial extraction, and the combined dredging and extraction which represents the total potential sand removal from the ELC. Table 16 summarizes the total mean fluvial extraction volume, and the total dredge volume for different time periods. It should be noted that fluvial sand/gravel extraction volumes only include extraction downstream of stream gaging stations used in the construction of the sediment rating curves as we assumed upstream extraction effects were already accounted for in the rating curves. Actual total fluvial extraction volumes are higher than reported here.

Fluvial sand/gravel extraction rates were variable over the period of record and highest in the 1960s and 1970s, remained relatively constant from 1980 to 1990, and then steadily declined following CHERT oversight in 1992. In fact, total sand/gravel extraction was roughly four times lower in the most recent decade relative to the peak extraction period (1965-1976; Table 16). Humboldt Bay dredging, while somewhat variable, has generally increased over time from the 1950s to 1990s. Following the deepening project in 1999, annual dredge volumes increased (Figure 17), with volumes over the most recent decadal period (2009-2018) more than double those in WY1965-1976 (Table 16). The annual volumes for the 1999-2008 period are almost twice the most recent decadal period (2009-2018), which is due to the elevated dredged quantities during the deepening project and the years immediately after. It should be noted that dredge disposal to HOODS and outside of the ELC began in 1990, coinciding with the higher dredge volumes.

A point worth noting is that since the 1960s the combined extraction and dredge volumes have remained somewhat constant, so as sand/gravel extraction decreased it was offset by increased dredge volumes. Furthermore, this combined extraction/volume rate represents two different periods regarding loss of sand from the ELC. Prior to 1990, the dredged sand (about half of the combined volume) was disposed of within the ELC, and fluvial extraction was the only sand loss from the ELC. However, following 1990 and dredge disposal at the HOODS, which is outside of the ELC, the entire combined volume of fluvial extracted and dredged sand is lost to the ELC. Since 2000, the average rate of combined sand (>= 125µm) removal is 1,090,483 m^3/yr (1,426,298 cy/yr). Fluvial sand/gravel extraction made up 19.4% of the combined volume (211,556 m^3/yr (276,704 cy/yr)), and the dredged sand makes up the remaining 80.6% (878,927 m^3/yr (1,149,593 cy/yr)).

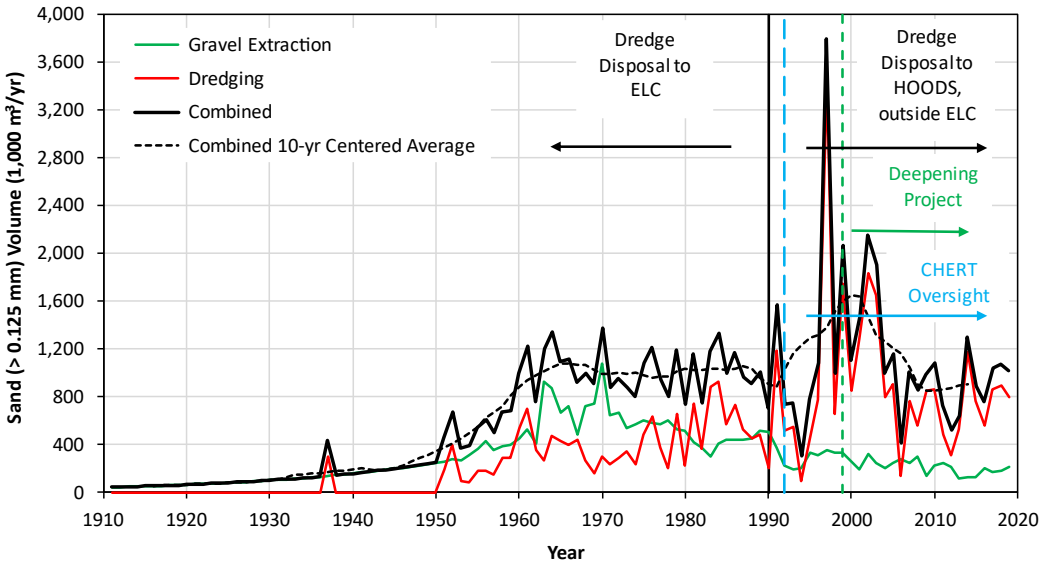

Figure 17. Annual fluvial (fluvial) sand/gravel extraction, Humboldt Bay dredging, and combined extraction and dredging volumes for sand (>= 125µm) for the 1911 to 2018 period. The black dashed lines is the running 10-yr centered average for the combined volumes. Also shown are key dates for CHERT oversight of fluvial extraction (1992), dredge disposal to HOODS and outside the ELC (1990), and the dredge deepening project (1999) which increased annual dredge volumes.

Table 16. Total fluvial (Mad, Eel and Van Duzen Rivers) extraction volume per year, and the Humboldt Bay dredged sand volume per year for sand (>= 125µm) for select time periods.

	Sand Volume (m³/yr)						
Item	**1911-2018**	**1954-2000**	**1965-1976**	**1979-1988**	**1989-1998**	**1999-2008**	**2009-2018**
Total Fluvial Extraction	301,901	486,256	667,184	431,360	334,234	260,751	173,819
Humboldt Bay Dredging	374,790	493,478	318,657	566,725	524,501	1,330,468	683,973

4.3 ELC Sand Budget

4.3.1 Sand Budget for 1966-2001 Period

Probability distributions describe each term in the single cell (1-cell) sand budget for the 1966-2001 period (36-years) except dune growth (Q_D). This sand budget assumes the residual term in Eq. 2 is zero and solves Eq. 11 for Q_D (mean and uncertainty). Results for this sand budget (>= 125µm) are presented in several different formats. Table 17 provides tabular results of the individual sand budget terms showing the mean annual volume, SE, CV, the 90% and 95% CI of the mean estimate, and the mean percent of the total positive or negative terms. Figure 18 is a schematic showing the ELC as a control volume, and the various input, output, storage, and removal and placement terms. In the following sections, the results for the various sand budget terms will generally be presented as the mean ± SE.

Although the fluvial input for the 1966-2001 period was determined from time-dependent ratings described in Section (3.1), the difference between the static and time-dependent sand loads for this period was only 2.5% (Table 14). In other words, results for the 1966-2001 sand budget would generally be the same rather static or time-dependent sand load estimates were used for the fluvial input term.

Table 17. Eureka littoral cell sand budget (sand >= 125µm) results for the 1966 to 2001 period for each term. Results are provided for the mean annual volume, standard error (SE), coefficient of variation (CV), the 90% and 95% confidence intervals (CI), and the mean percent of each term to the total positive or negative terms.

Budget Terms[1]	Volume of Sand >= 125µm (1,000 m³/yr)					
	Mean	SE	CV	90% CI	95% CI	% Mean
Inputs, Placed Material (+ terms)						
Fluvial input (Q_R)	3,132	237.0	7.57	2,758 - 3,536	2,693 - 3,621	89.5
Bluff erosion (Q_B)	66.68	27.41	41.1	21.21 – 112.0	12.52 – 120.7	1.9
Humboldt Bay dredge disposal (P_B)	301.6	12.81	4.25	280.6 – 322.7	276.6 – 326.7	8.6
Total	**3,500**	**239.0**	**6.83**	**3,107 – 3,893**	**3,032 – 3,969**	**100.0**
Outputs, Material Removed, Volume Change (- terms)						
Shoreline change from RSL (Q_{SLS})	370.0	31.58	8.54	318.9 – 422.7	309.4 – 433.2	10.6
Estuary change from RSL (Q_{SLE})	120.3	9.20	7.65	105.2 – 135.5	102.4 – 138.4	3.4
Dune growth (Q_D)	513.9	289.6	56.4	47.78 – 999.7	-37.37 - 1,098	14.7
Humboldt Bay dredging (R_{HB})	595.2	26.51	4.45	551.5 – 638.9	543.7 – 646.7	17.0
Fluvial extraction (R_R)	470.6	17.18	3.65	442.3 – 498.9	437.0 – 504.2	13.5
Shoreline change (ΔS)	249.2	118.8	47.7	53.90 – 444.5	16.57 – 482.0	7.1
Inner-shelf change (ΔIS)	1,181	100.8	8.54	1019 - 1351	990.0 - 1,384	33.7
Total	**3,500**	**332.0**	**9.48**	**2,954 – 4,046**	**2,849 – 4,151**	**100.0**

[1] RSL is relative-sea level.

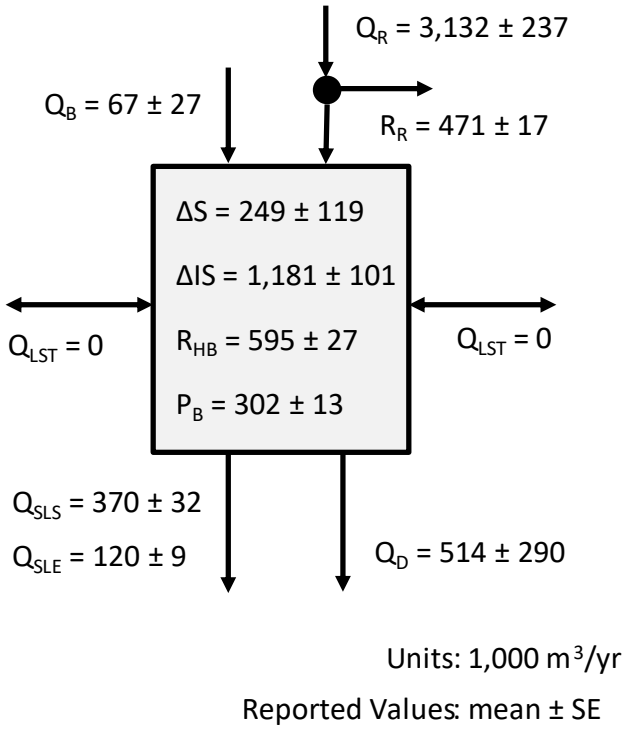

Figure 18. Schematic diagram of Eureka littoral cell sand budget terms (sand >= 125µm) for mean annual volumes ± standard error (SE) for the 1966 to 2001 period.

4.3.1.1 Sand Budget Inputs and Placed Material (+ Terms)

For the 1966-2001 period, the dominant sand input to the littoral cell is the fluvial load (3,132,000 ± 237,000 m^3/yr), which comprises 89.5% of the total input. Humboldt Bay dredged material placement (301,600 ± 12,810 m^3/yr) within the ELC makes up the next largest sand input of 8.6%, which only occurred from 1966 to 1990. The smallest input is bluff erosion (66,680 ± 27,410 m^3/yr) at only 1.9% of the total.

4.3.1.2 Sand Budget Outputs, Material Removed, and Volume Change (- Terms)

The largest negative sand budget term for the 1966-2001 period is the inner-shelf volume change (1,181,000 ± 100,800 m^3/yr), which represents 33.7% of the total output. The volume of sand removed via Humboldt Bay dredging (595,200 ± 26,510 m^3/yr) and fluvial extraction (470,600 ± 17,180 m^3/yr) are similar and represent 17.0% and 13.5% of the total output, respectively. Shoreline volume change (249,200 ± 118,800 m^3/yr) represents 7.1% of the total output and was similar in magnitude to the shoreline sand loss to RSL (370,000 ± 31,580 m^3/yr) at 10.6%. The smallest output term is sand loss to RSL in the estuaries (120,300 ± 9,200 m^3/yr), which comprises only 3.4% of the total output.

Dune growth, calculated from Eq. 11, represents the residual term balancing positive input against the negative output. Known output terms in the sand budget account for 85.3% of the sand input, with dune growth (249,200 ± 118,800 m^3/yr) comprising 14.7%. To validate this estimate, we compared the estimated linear dune growth rate in the ELC to literature values. Assuming an approximate dune length of 51.2 km, the calculated linear growth rate of 10.0 $m^3/(m \cdot yr)$ compares well with the range of rates (2.5 to 25 $m^3/(m \cdot yr)$) reported in the SPM (1984) and the rate of 13.8 $m^3/(m \cdot yr)$ for Clatsop Spit, Oregon (Meyer and Chester, 1977, as reported in SPM, 1984). For the period 1950 to 1999, Kaminsky et al. (2010) reported sand accumulation rates between 16.4 and 110.6 $m^3/(m \cdot yr)$ for the upper shoreface, strand plains and barriers in the Columbia River littoral cell. Additionally, Ruggiero et al. (2016) reported backshore sand accumulation rates of 10 $m^3/(m \cdot yr)$ during the 1999 to 2011 period for the Long Beach sub-cell of the Colombia River littoral cell.

4.3.1.3 1966-2001 Sand Budget Uncertainty

For this sand budget, we use the reported CV and the 90% and 95% CI (Table 17) to address the uncertainty determined from the Monte-Carlo analysis for the input (positive) and output (negative) terms. To aid in interpretation of the sand budget results and uncertainties, we provide bar charts showing the annual mean sand volume and 95% CI for each budget term (Figure 19).

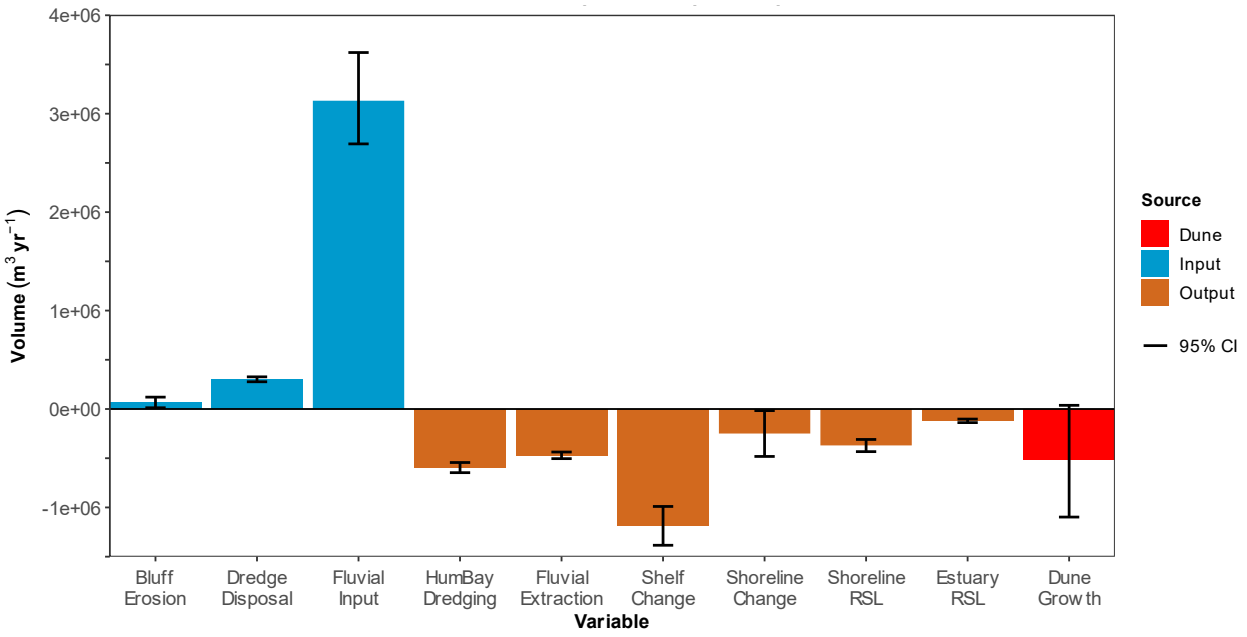

Figure 19. Bar chart of the 1966-2001 the Eureka littoral cell sand budget (sand >= 125µm) showing mean annual volumes and 95% confidence intervals (CI) for all budget terms. Blue bars represent input or positive terms; brown are output or negative terms; and dune growth (red) is the residual from the sum of the input and output terms.

Although the mean annual bluff erosion is the smallest sand input term, it has the largest uncertainty with a CV of 41.1% (Table 17), largely due to the assumptions and unknown values in estimating this term (Section 3.2.9.2). In contrast, the uncertainty for the fluvial sand load and dredged material placement are significantly lower with CV at 7.6% and 4.3%, respectively (Table 17). The 95% CI for each of the input terms does not contain zero, indicating reasonably strong evidence that all input terms are positive and greater than zero (Table 17).

Regarding the output (negative) terms, the uncertainty for shoreline change from *RSL*, estuary change from *RSL*, Humboldt Bay dredging, fluvial extraction, and inner-shelf storage are all relatively modest, with CVs ranging from 3.7% to 8.5% (Table 17). However, the shoreline change term exhibits a notably high CV of 47.7%, primarily due to the intermediate MC simulated estimate of the ELC shoreline rate of 0.19 ± 0.09 m/yr (CV = 47.6%) described in Section 3.2.11.1. This elevated CV is attributed partly to the necessity of estimating the shoreline rate error terms not reported in the GHD (2018) shoreline DSAS analysis. However, a more significant cause relates to the low estimated ELC mean shoreline rate of 0.19 m/yr, which is the denominator in the CV calculation. For example, a higher mean rate of 1 m/yr with the same SE would give a CV value of 9%. Similar to the input terms, all of the 95% CI for the known output terms exclude zero providing strong evidence that all output terms represent negative values.

The estimated dune growth term (residual from Eq. 11) has the highest CV of 56.4%, and the 95% CI contains zero. Regarding the 95% CI, the 95% interval is almost entirely positive, providing reasonable evidence that the estimated dune growth is a positive value. Furthermore, the 90% CI excludes zero reinforcing dune growth as a positive value. The high dune growth CV value is directly related to the high SE (289,600 m^3/yr) estimate from propagating the input and output errors through the MC simulation. The only way to reduce the dune growth SE would be to reduce or refine the known input/output SEs. We can estimate the dune growth SE by taking the root mean square error of the known input/output SE terms from Table 17. This yields an SE of 288,800 m^3/yr, a value almost identical to the SE determined from the MC simulation (289,600 m^3/yr). Reducing all the known SE terms by 25% results in a dune growth

SE of 216,655 m^3/yr (17.4% SE reduction). However, reducing only the three highest SE terms (fluvial input, shoreline change, and inner-shelf change) by 25% gives a SE of 219,700 m^3/yr (16.3% SE reduction) indicating the other six terms have a minor effect on the dune growth SE.

It seems unlikely that we can significantly improve the uncertainty estimate of the fluvial sand load given the available input data and the robust methodology outlined in Section 3.1. Unless the additional data not reported in CN2004 can be provided, we further feel that improving the uncertainty for the inner-shelf change is unlikely. This leaves the uncertainty associated with shoreline change.

As described above, obtaining the errors of the DSAS shoreline analysis, not reported in GHD (2018), may lower the overall uncertainty associated with the estimated shoreline rate. This potential reduction may also lower the dune growth SE and perhaps remove the zero value from the 95% CI. However, barring potential improvements to the shoreline rate SE, we feel that the sand budget assumptions, input/output terms, and the MC simulation provide robust estimates of mean annual values and associated uncertainty.

In addition, it is worth noting that the uncertainty in the total input values (CV = 6.8%) is lower than the uncertainty related to the total output values (CV = 9.5%), with the input SE (239,000 m^3/yr) being approximately 28% lower than the output SE (332,000 m^3/yr). The lower uncertainty in the total input volume is due to fewer budget terms (3 terms) contributing to the combined error compared to the total output with seven terms.

4.3.1.4 Comparison to Other ELC Sand Budgets

Patsch and Griggs (2007), hereafter referred to as PG2007, developed a sand budget for the ELC to support the California Regional Sediment Management Plan. As part of the ELC Coastal Regional Sediment Management Plan (CSMW, 2017), additional sand losses from fluvial gravel extraction were discussed, along with updating Humboldt Bay dredging and disposal information, but an updated tabulated ELC sand budget was not provided. We combined the PG2007 and CSMW (2017) information into a single sand budget, referred to as the PG-CSMW budget, and compared it to the 1966-2001 sand budget developed in this study (Table 18).

The following describes key differences between the two sand budgets.

- The PG-CSMW budget only contained 6 terms (2 sources and 4 sinks), and the updated budget contains 10 terms (3 input and 7 output).
- The estimated fluvial load in the PG-CSMW budget was significantly lower than the updated budget, but both river loads made up significant portions of the total source or input. The fluvial 95% CI of the updated budget did not contain the PG-CSMW budget fluvial input, indicating that these estimates are different at the 95% level.
- Humboldt Bay dredging in the PG-CSMW budget is higher than the updated budget dredging value, and the 95% CI indicates the dredging estimates are different.
- The dune sink in the PG-CSMW budget was estimated from the sand volume change on the beaches and dunes from 1992 to 1998 for a portion of the north and south spits (Winkleman et al., 1999). This value is lower than the dune growth term determined in the updated sand budget (513,900 m^3/yr), but falls within the 95% CI.
- The total annual sand budget sink/source term from the PG-CSMW budget is 2,304,000 m^3/yr, which is 34.2% lower than the updated budget input/output annual sand volume of 3,500,000 m^3/yr.

- The PG-CSMW sand budget did not close, and it was assumed that 1,010,000 m^3/yr of sand was lost offshore to the continental shelf, deposited into the Eel Canyon, supplied beaches to the north, or transports south out of the ELC past Cape Mendocino to balance the sand budget. This unknown term made up 43.7% of the total sand input. The updated sand budget had a residual term of 14.7% of the total input, which we assumed represented dune growth.

Table 18. Comparison of Eureka Littoral Cell sand budgets for sand >= 125µm. Left side sand budget (white columns) is a combination of the Patsch and Griggs (2007) (PG2007) and CSMW (2017) (CSMW) information. Right side (grey columns) is the sand budget developed in this study (subset of Table 17).

PG2007 and CSMW2017 Sand Budget Volume (1,000 m^3/yr)				**Updated 1966-2001 Sand Budget (this study) Volume (1,000 m^3/yr)**			
Budget Terms	**Source**	**Estimate**	**% Total**	**Budget Terms**	**Mean**	**95% CI**	**% Total**
Sources (+)				**Inputs, Placed Material (+ terms)**			
Fluvial input (Eel, Mad, Little Rivers)	PG2007	2,171	94.2	Fluvial input	3,132	2,693 - 3,621	89.5
				Bluff erosion	66.68	12.52 – 120.7	1.9
Dunes	PG2007	133.8	5.8	Dredge disposal	301.6	276.6 – 326.7	8.6
Total		**2,304**	**100.0**	**Total**	**3,500**	**3,032 – 3,969**	**100.0**
Sinks (-)				**Outputs, Material Removed, Volume Change (- terms)**			
Humboldt Bay dredging	CSMW	696.5	30.2	Shoreline change from RSL	370.0	309.4 – 433.2	10.6
Fluvial extraction	CSMW	391.0	17.0	Estuary change from RSL	120.3	102.4 – 138.4	3.4
				Dune growth	513.9	-37.37 - 1,098	14.7
Dunes	PG2007	206.4	9.0	Humboldt Bay dredging	595.2	543.7 – 646.7	17.0
Offshore losses (estimated in order to balance sand budget)		1,010	43.8	Fluvial extraction	470.6	437.0 – 504.2	13.5
				Shoreline change	249.2	16.57 – 482.0	7.1
				Inner-shelf change	1,181	990.0 - 1,384	33.7
Total		**2,304**	**100.0**	**Total**	**3,500**	**2,849 - 4,151**	**100.0**

With the inclusion of nine known sand budget terms, the updated sand budget was able to reasonably close with a residual of only 14.7%. We assumed the residual term represents dune growth, and as described above, the resulting dune growth rate of the 10.0 m^3/(m/yr) aligns well with literature values.

Notably, the inner-shelf storage, shoreline volume change, and losses of sand to RSL collectively account for approximately 55% of the annual average sand input, indicating that these terms are important in the ELC sand budget. Previous ELC sand budgets did not directly account for these terms.

4.3.1.5 Sand Loss from the ELC

To better understand the significance of permanent sand loss from the ELC due to extraction and RSL, we combined the Humboldt Bay dredging and fluvial extraction terms into a single Dredging/Extraction term, and further created a single Shoreline/Estuary RSL term that combined shoreline and estuary change to RSL terms (Table 19, Figure 20). These combined terms provide a better context for comparing permanent sand loss in the ELC to other budget terms. It should be noted that not all the Humboldt Bay dredged sand was lost from the ELC in the 1966-2001 sand budget, as dredged sand was placed back into the ELC from 1966 to 1990 (P_B input term). However, after 1990, the dredged sand was disposed of at

HOODS and removed from the ELC. For this discussion we use the dredged sand volume to represent a fraction of the permanent sand loss post 1990.

Table 19. Eureka littoral cell sand budget (sand >= 125µm) results for the 1966 to 2001 period (Table 17) that combined shoreline change from RSL and estuary change from RSL into a single Estuary/Shoreline *RSL* term; and combined Humboldt Bay dredging and fluvial extraction to Dredging/Extraction term. Results are provided for the mean annual volume, standard error (SE), coefficient of variation (CV), the 90% and 95% confidence intervals (CI), and the mean percent of each term to the total positive or negative terms.

	Volume of Sand >= 125µm (1,000 m^3/yr)					
Budget Terms[1]	**Mean**	**SE**	**CV**	**90% CI**	**95% CI**	**% Mean**
Inputs, Placed Material (+ terms)						
Fluvial input (Q_R)	3,132	237.0	7.57	2,758 - 3,536	2,693 - 3,621	89.5
Bluff erosion (Q_B)	66.68	27.41	41.1	21.21 – 112.0	12.52 – 120.7	1.9
Humboldt Bay dredge disposal (P_B)	301.6	12.81	4.25	280.6 – 322.7	276.6 – 326.7	8.6
Total	**3,500**	**239.0**	**6.83**	**3,107 – 3,893**	**3,032 – 3,969**	**100.0**
Outputs, Material Removed, Volume Change (- terms)						
Shoreline/Estuary RSL	490.3	32.89	6.71	436.2 – 544.4	425.9 – 554.8	14.0
Dune growth (Q_D)	513.9	289.6	56.4	47.78 – 999.7	-37.37 - 1,098	14.7
Dredging/Fluvial extraction	1,065	31.59	3.0	1,014 – 1,118	1,004 – 1,128	30.5
Shoreline change (ΔS)	249.2	118.8	47.7	53.90 – 444.5	16.57 – 482.0	7.1
Inner-shelf change (ΔIS)	1,181	100.8	8.54	1019 - 1351	990.0 - 1,384	33.7
Total	**3,500**	**332.0**	**9.48**	**2,954 – 4,046**	**2,849 - 4,151**	**100.0**

[1] *RSL* is relative-sea level.

The largest sand output (negative term) is the inner-shelf change in storage at 33.7% of the total input. The next largest output term is the dredging/extraction term at 30.5% of the total input, followed by similar volumes for dune growth and shoreline/estuary RSL loss at 14.7% and 14.0%, respectively. After combining terms, shoreline change represents the smallest output volume at 7.1%.

Patsch and Griggs (2007) and CSMW (2017) both describe ELC sand loss, particularly Eel River sand, to the continental shelf and Eel River submarine canyon However, these studies do not explicitly delineate the lateral extent of the continental shelf. In our sand budget analysis for the 1966-2001 period, we do not classify inner-shelf storage as sand loss; instead, we regard it as a storage compartment within the ELC (i.e., a control volume).

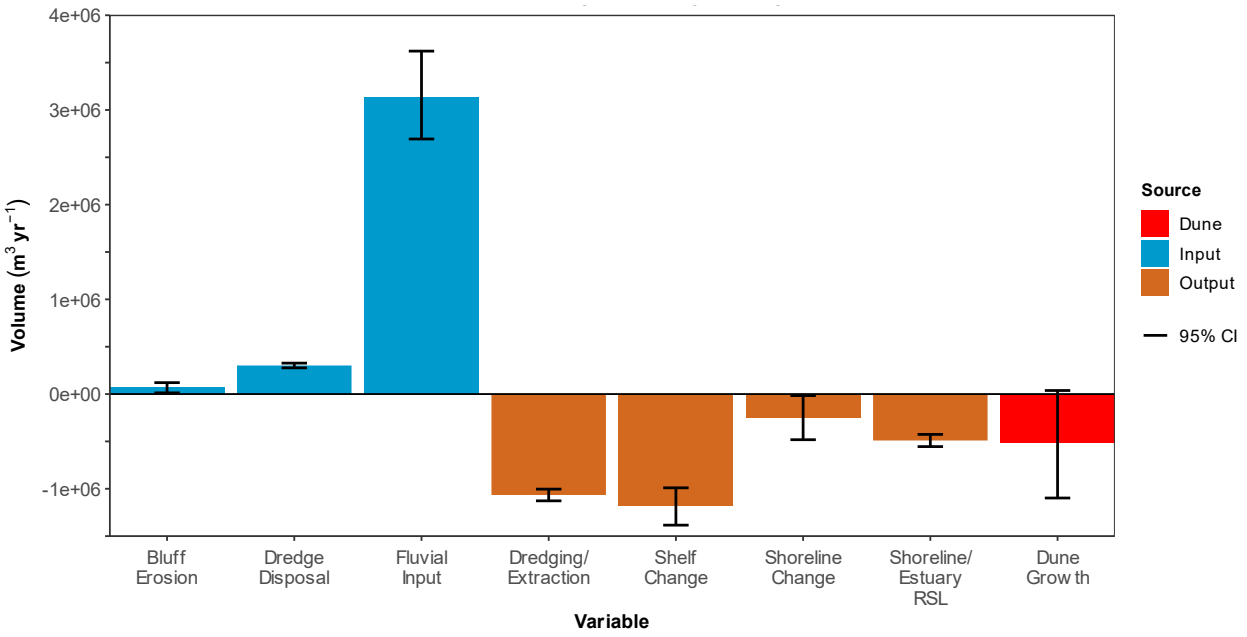

Figure 20. Simplified bar chart of Figure 19 for the 1966 to 2001 Eureka littoral cell sand budget (sand >= 125µm) showing mean annual volumes and 95% confidence intervals (CI). In this plot, Humbold Bay Dredging (HumBay Dredging) and River Extraction were combined into Dredging/Extraction; and Shoreline and Estuary relative sea-level (RSL) were combined into Shoreline/Estuary RSL. Blue bars are input or positive terms; brown is output or negative terms; and dune growth (red) is the residual from the sum of the input and output terms.

The cross-shore transport of sand between the inner-shelf and shoreline within the ELC is not documented. However, insights from the STRATAFORM study, which focused on the Eel margin (Nittrouer et al., 2007; and supporting literature, e.g. Borgeld, 1985; Wheatcroft and Borgeld, 2000; Wiberg, 2000; Harris and Wiberg, 2002; Crockett and Nittrouer, 2004), shed light on this phenomenon. The study highlights how extreme wave energy on the shelf creates a sediment continuum, with coarser sands prevailing at the shoreline and shallower depths of the inner shelf, transitioning to finer sands in deeper inner-shelf areas, and ultimately to muddier sediment on the outer shelf (~60 m depth). This continuum of sand clearly indicates cross-shore transport between the shoreline, inner-shelf, and outer-shelf.

Using wave data from NDBC Bouy 46022 – Eel River, Wiberg (2000) estimated that bottom wave velocities on the Eel shelf could transport sediment finer than 2Ø (250µm) an average of 270 days per year in 30 m of water, and approximately 150 days per year at a 50 m depth. Additionally, Ogston and Sternberg (1999) collected wave, current and suspended sediment concentration measurements at a 60 m depth on the Eel shelf from September 1995 to September 1996. Throughout the sampling period encompassing 41 identified sediment suspension events, along-shore currents exhibited an equal distribution north and south, while cross-shore currents predominantly flowed seaward for 35 events and shoreward for 6 events. Between events, the dominant across-shelf flux direction was shoreward. Recently, Harley et al. (2022) described the onshore transport of sand from beyond the depth of closure during extreme storm events. Based on these observations, we hypothesize that during large wave events, and possibly between large wave events, the ELC inner-shelf could supply sand to the shoreline at interannual to decadal time scales.

We assume that dredging/extraction and shoreline/estuary change from RSL represent permanent sand losses. Combining these two terms means that approximately 44.5% of the annual sand input is lost each

year from the ELC, with the largest losses attributed to Humboldt Bay dredging and fluvial gravel extraction. If we assume that the inner-shelf storage represents a loss from the ELC, then the total sand loss is approximately 78% of the total input, which seems excessive given the expansive beach and dune system found in the ELC. With sea-level-rise projected to increase and accelerate in the future, the permanent loss of sand from the ELC will increase if other management actions are not taken. For instance, reintroducing dredged sand back into the ELC, as previously practiced prior to disposal at HOODS, could mitigate this trend.

4.3.2 Time-Dependent Sand Budget for 1911-2018 Period

A single cell (1-cell) time-dependent sand budget analysis was conducted for the 1911-2018 period, in which an annual sand residual (>= 125μm) was estimated over time using Eq. 12. For this analysis, temporal estimates for shoreline change (ΔS_S), inner-shelf change (ΔS_{IS}), and dune growth (Q_D) terms were not known. Instead, this analysis accounted for the annual changes over time for (1) fluvial loads, (2) Humboldt Bay dredging, (3) fluvial sand/gravel extraction, (4) dredge placement in ELC or HOODS, and (5) the volume of sand needed to offset RSL rise of the shoreline, inner-shelf, and estuaries. Bluff erosion was also included as an input term, but it was estimated as an annual average term that varied due to uncertainty within the MC simulation.

The residual term represents the annual volume of sand remaining, where a positive (+) residual indicates a sand surplus available for shoreline change (i.e. shoreline growth), inner-shelf change (storage), and/or dune growth. Conversely, a negative (-) residual indicates a deficit where sand is not available to keep pace with RSL, or for shoreline and inner-shelf change, and dune growth. As mentioned earlier, we anticipate that a long-term negative residual would be an indicator of significant adverse change, such as shoreline or dune recession.

Two time-dependent sand budget analyses were conducted. The first analysis accounted for existing Humboldt Bay dredged sand disposal practices with sand placement within the ELC prior to 1990 and HOODS disposal out of the ELC after 1990. The second analysis, representing a hypothetical condition, assumed that all Humboldt Bay dredged sand was placed within the ELC, and disposal out of the ELC to HOODS did not occur. The resulting time-dependent sand residual provides a temporal snapshot of the long-term effects of changing fluvial loads and permanent sand losses from the ELC due to the history of Humboldt Bay dredging/disposal and fluvial sand/gravel extraction management, and the increasing rate of RSL over time.

4.3.2.1 Time-Dependent Sand Budget Analysis with Sand Disposal at HOODS (Existing Conditions)

The annual sand residual for the existing Humboldt Bay dredge disposal practices (existing condition) shows significant year to year variability (Figure 21) and generally tracks the fluvial input, especially the Eel River (Figure 15). The large sediment input from the December 1964 flood is apparent in the 1965 sand residual (~2.0 x 10^7 m^3/yr), which is almost 40 times greater than the next highest residuals in 1974 and 1983. To better describe the underlying trends in the annual sand residual, we use the 10-year centered average and 95% CI (Figure 21) for the following discussion. Table 20 summarizes individual and combined terms of the time-dependent 1911-2018 sand budget residual for specific time periods.

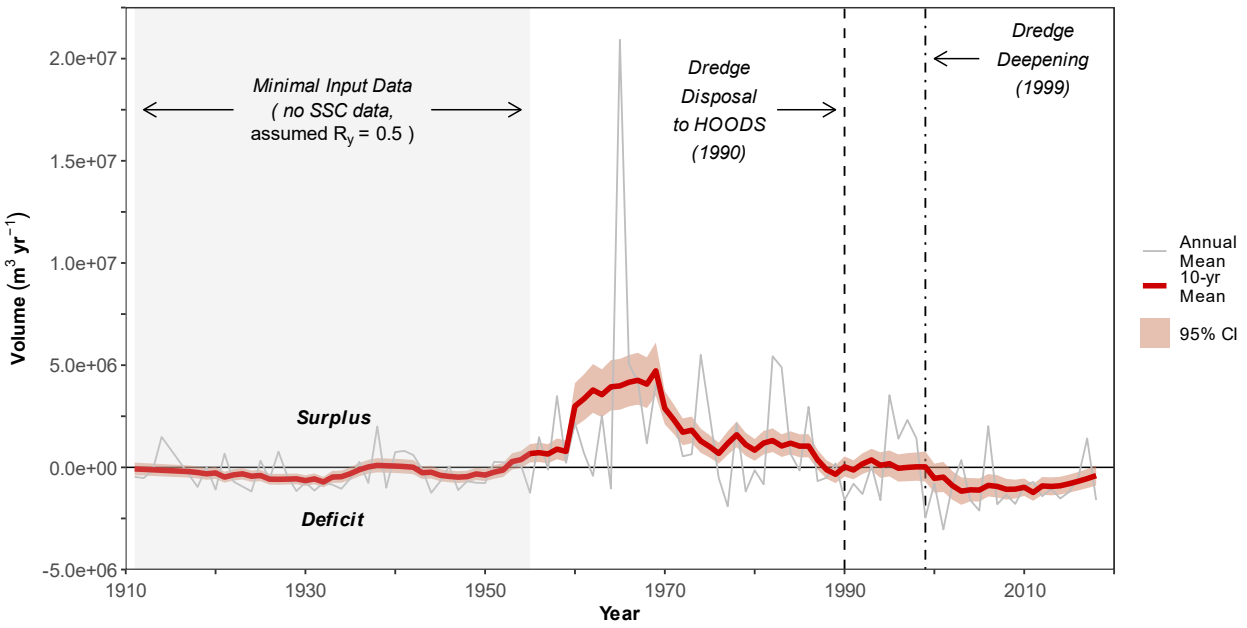

Figure 21. Time-dependent annual mean sand residual for the 1911-2018 sand budget analysis with the existing Humboldt Bay dredged sand disposal practices. The grey line is the annual mean residual, the red line is the 10-year centered average annual mean residual, and the 95% CI on the annual mean residual is the light red band. Also shown is the period of minimal SSC data (1911 to 1954), when dredge disposal to HOODS (out of the ELC) begins (1990), and the Humboldt Bay dredge deepening project (1999).

Table 20. Time-dependent annual mean sand residual (>= 125µm) for specific/combined terms from the 1911-2018 sand budget analysis for select time periods with the existing Humboldt Bay dredged sand disposal practices.

	Volume of Sand >= 125µm (1,000 m^3/yr)							
Budget Terms1	**1911-2018**	**1911-1953**	**1954-1964**	**1965-1976**	**1979-1988**	**1989-1998**	**1999-2008**	**2009-2018**
Inputs, Placed Material (+ terms)								
Fluvial input (Q_R)	2,198	1,033	2,492	6,090	2,834	2,556	1,842	1,371
Bluff erosion (Q_B)	66.69	66.69	66.69	66.69	66.69	66.69	66.69	66.69
Humboldt Bay dredge disposal (P_B)	140.2	12.08	294.3	318.7	566.7	52.39	0.0	0.0
Total	**2,405**	**1,111**	**2,853**	**6,476**	**3,467**	**2,676**	**1,909**	**1,438**
Outputs, Material Removed, Volume Change (- terms)								
Dredging/Fluvial extraction	676.7	143.3	788.6	985.68	998.1	858.7	1,591	857.8
Inner-shelf, shoreline, estuary loss from RSL	1,369	1,269	1,349	1,384	1,424	1,454	1,484	1,515
Total	**2,045**	**1,412**	**2,138**	**2,370**	**2,422**	**2,313**	**3,076**	**2,373**
% of input	**85.1**	**127.1**	**74.9**	**36.6**	**69.8**	**86.4**	**161.2**	**165.0**

[1] *RSL* is relative-sea level; % is percent.

Prior to 1955, the mean sand residual and 95% CI was near zero and slightly in deficit, indicating a period when permanent sand losses to sand management and RSL were about 127% of the total sand inputs. This also suggests a potential period when excess sand would not be available for inner-shelf storage, or shoreline and dune growth. It should be noted that the 1911 to 1954 period did not have SSC data, and we assumed a sand rating residual ratio (R_y) of 0.5 (Section 3.1.2.1). This period of residual balance is somewhat supported by the end-point shoreline rates reported by McDonald (2017) with an overall study area erosional rate of -2.68 ± 0.04 m/yr for the 1939-1942 period (earliest period analyzed), followed by accretional rates of 2.65 ± 0.16 m/yr and 0.67 ± 0.11 m/yr for the 1942-1948 and 1948-1958 periods, respectively. However, the McDonald (2017) shoreline rates for the 1939 to 1958 period indicates net accretion or shoreline growth for a portion of the 1911-1954 period of residual deficit, and similarly Hapke (2006) reported a long-term (~1850s to 2002) positive shoreline rate for the Eureka Region. This contradiction between the reported shoreline accretion and the sand residual deficit for the 1911 to 1954 period indicates: (1) our rating curve residual ratio assumption of 0.5 for the 1911 to 1954 period was too low, and a higher residual ratio would create a positive sand residual (surplus) for this period; and (2) this supports our hypothesis that cross-shelf transport of sand from the inner-shelf to the shoreline could have occurred during this neutral period, supplying sand for shoreline growth.

Beginning in 1955, there was consistent increase in the positive residual (surplus) rate within the ELC until approximately 1970, which coincides with the large increases in sand loads from all coastal basins during the 1950s and 1970s (Figure 15; Table 13). This positive residual occurred during the highest rates of fluvial sand/gravel extraction, and lower rates of Humboldt Bay sand dredging (Figure 17). However, during this period, dredge material was disposed of within the ELC, which offsets some of the permanent sand loss from dredging/fluvial extraction (Table 16). The total output ranged from 75% to 37% of the total sand input for the time periods 1954-1964 and 1965-1976, respectively.

As fluvial sand loads begin to decrease in the mid to late 1970s (Figure 15; Table 13), the positive sand residual shows a steady 20-year decline from 1970 to the end of the 1980s, but remains positive. During this period fluvial sand extraction declines from the peak extraction in 1970 to a relatively constant rate in the 1980s (Figure 17). Although Humboldt Bay dredging steadily increased during this period, dredge disposal continued to be placed within the ELC. Total output was approximately 70% of the total input during this period.

At no time during the 1950s through late 1980s did the 10-yr average or 95% CI fall below zero, indicating a 35 to 40 year period when a significant surplus of sand existed within the ELC for inner-shelf storage, and shoreline and dune growth. This surplus sand period coincides with an almost continual interval of shoreline expansion within the ELC that occurred from approximately 1948 to 1988 (McDonald, 2017; GHD, 2018). However, during this time frame McDonald (2018) reported a small amount shoreline erosion (0.15 ± 0.09 m/yr) from 1970 to 1981.

For an approximate 10-year period from 1989 to 1999, the sand residual was near zero but remained in surplus, with the 95% CI showing small but continuous surplus or deficit values. Although fluvial sand loads continued to decrease during this 10-yr period, the decrease was relatively small (~10%) compared to the prior decade (Table 13). However, two significant management actions/changes occurred during this period. First, CHERT oversight of fluvial extraction begins in 1992, coinciding with a drop in extraction rates (Figure 17). Second, disposal of Humboldt Bay dredged sand to HOODS begins in 1990 which, for the first time, permanently removes dredged sand from the ELC. As mentioned in Section 4.2, although fluvial extraction decreased, it was offset by increased dredging, and the combined extraction and dredge volumes have remained constant since the 1960s. However, during the 1990s, the combined

extraction/dredging volume increased due to two large dredge events (Figure 17). Throughout this period the total sand output averaged 86% of the total sand input.

Beginning in 1999, the mean sand residual drops below zero and has remained in deficit for 20-years until the end of the sand budget analysis period (2018). The 95% CI has also remained below zero during this period, except for one to two years immediately after 1999 when it was slightly positive. During this period fluvial sand loads steadily decreased to levels that are approximately 77% lower than the peak loads of the 1960s to 1970s. Furthermore, the Humboldt Bay deepening project occurred in 1999, in which annual sand dredge volumes significantly increased compared to previous period volumes.

The permanent loss of sand for this 20-year period from dredged/fluvial extraction and losses from RSL has exceeded the total sand input by over 160%. As summarized previously, the total combined dredged/fluvial sand extraction for this period is approximately 1,090,483 m^3/yr, with fluvial extraction and HOODS disposal accounting for 19.4% and 80.6%, respectively. Additionally, inner-shelf, shoreline, and estuary sand losses from RSL have steadily increased over time, and for the period from 2009-2018 RSL sand losses alone have exceeded fluvial inputs.

During this deficit period, McDonald (2017) reported periodic erosion of North Spit from North Jetty to Mad River, and persistent erosion from North Jetty to Fairhaven since 1980s; and an overall small negative shoreline erosion rate (-0.01 ± 0.15 m/yr) for 1999-2005, and then overall accretion of 1.29 ± 0.08 m/yr from 2005-2016 for the shorelines south of South Spit. GHD (2017) reported that the shoreline north of the Eel River showed an interval of erosion followed by accretion during this period, with a low to moderate net accretion. However, the shoreline south of the Eel River showed net erosion, with an interval of neutral change followed by erosion. As discussed earlier, the segments of shoreline accretion during this 20-year sand residual deficit period could support our hypothesis of onshore cross-shore transport of sand from the inner-shelf to the shoreline.

The 20-year period of sand deficit is a direct result of several factors: (1) decreased fluvial sand loads, (2) management decisions regarding Humboldt Bay dredge disposal to HOODS (out of ELC) and fluvial extraction, and (3) increasing sand losses due to higher and accelerating rates of RSL rise. We hypothesize that this 20-year negative residual could be an indicator of significant shoreline recession or dune losses, such as those occurring between North Spit and Mad River (McDonald, 2017), and south of the Eel River (GHD, 2018) during this period.

4.3.2.2 Time-Dependent Sand Budget Analysis with No HOODS Disposal (Hypothetical Case)

This time-dependent analysis assumes the hypothetical case where Humboldt Bay dredge disposal continued to be placed in the ELC after 1990, and disposal at HOODS did not occur (Figure 22). Table 21 is an update to Table 20 with all Humboldt Bay dredged material placed within the ELC.

Prior to 1990, the temporal sand residual is the same as Figure 21, and no additional discussion is provided. However, after 1990 the response of the sand residual is quite different from the existing conditions analysis described above showing the significance of the management decision to dispose of dredged sand at HOODS and out of the ELC.

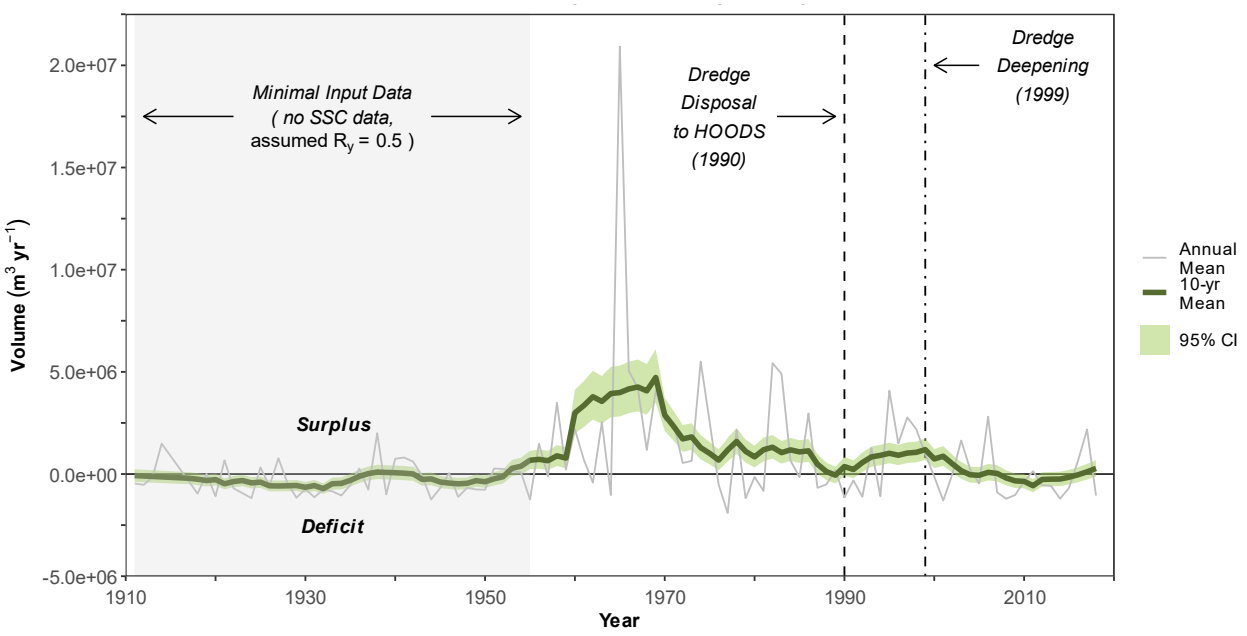

Figure 22. Time-dependent annual mean sand residual for the 1911-2018 sand budget analysis for the hypothetical case of Humboldt Bay dredged sand placement within the ELC after 1990 and no HOODS disposal. The grey line is the annual mean residual, the green line is the 10-year centered average annual mean residual, and the 95% CI is the light green band. Also shown is the period of minimal SSC data (1911 to 1954), when dredge disposal to HOODS (out of the ELC) begins (1990), and the Humboldt Bay dredge deepening project (1999).

Table 21. Time-dependent annual mean sand residual (>= 125µm) for specific/combined terms from the 1911-2018 sand budget analysis for select time periods with the hypothetical case of Humboldt Bay dredged sand placement within the ELC after 1990 and no HOODS disposal.

	Volume of Sand >= 125µm (1,000 m^3/yr)							
Budget Terms1	**1911-2018**	**1911-1953**	**1954-1964**	**1965-1976**	**1979-1988**	**1989-1998**	**1999-2008**	**2009-2018**
Inputs, Placed Material (+ terms)								
Fluvial input (Q_R)	2,198	1,033	2,492	6,090	2,834	2,556	1,842	1,371
Bluff erosion (Q_B)	66.69	66.69	66.69	66.69	66.69	66.69	66.69	66.69
Humboldt Bay dredge disposal (P_B)	374.8	12.08	294.3	318.7	566.7	524.5	1,330	684.0
Total	**2,639**	**1,111**	**2,853**	**6,476**	**3,467**	**3,148**	**3,239**	**2,122**
Outputs, Material Removed, Volume Change (- terms)								
Dredging/Fluvial extraction	676.7	143.3	788.6	985.68	998.1	858.7	1,591	857.8
Inner-shelf, shoreline, estuary loss from RSL	1,369	1,269	1,349	1,384	1,424	1,454	1,484	1,515
Total	**2,045**	**1,412**	**2,138**	**2,370**	**2,422**	**2,313**	**3,076**	**2,373**
% of input	**77.5**	**127.1**	**74.9**	**36.6**	**69.8**	**73.5**	**95.0**	**111.8**

[1] *RSL* is relative-sea level; % is percent.

With the hypothetical placement of dredged sand within the ELC, the sand residual and 95% CI remained above zero from 1990 to approximately 2003, compared to near zero for the existing condition (Figure 21). The total sand output decreased from 86% to 74% of the total input for the hypothetical case compared to the existing condition, respectively, during this period.

The most significant effect of continuous sand placement within the ELC occurred during the 20-year period since 1999, with the sand residual hovering near zero with only a few years around 2010 when the mean and 95% CI were in deficit (Figure 22). This contrasts with existing conditions where the sand residual and 95% CI remained below zero for same 20-year period (Figure 21). By refraining from disposing dredged sand at HOODS and instead depositing it within the ELC, the hypothetical scenario would have mitigated cumulative impacts. Specifically, for the 1999-2008 period, this would have reduced the dredged/fluvial extraction and RSL sand losses from exceeding 160% to 95%, and for the subsequent 2009-2018 period, it would have decreased it to 112%.

4.3.2.3 Comparison of Cumulative Mean Annual Sand Residual

The time-dependent cumulative sand residual for existing conditions with dredged sand placement in the ELC prior to 1990 and then disposal at HOODS after 1990, and the hypothetical case of all dredged sand placement within the ELC clearly demonstrates the effects of sand disposal at HOODS and out of the ELC (Figure 23). Prior to 1999, the cumulative residual for existing conditions and the hypothetical case are the same as all dredged sand disposal was within the ELC.

From 1911, the cumulative residual was in deficit, although the rate of negative accumulation was low. Beginning in the early 1950s, the sand residual becomes positive, and the negative cumulative residual begins to decrease until the 1964 flood rapidly shifts the residual to surplus (positive) in 1965. The positive cumulative residual continued to increase at a high rate through the mid-1970s due to the high positive sand residual (Figure 21 and Figure 22), and then continued to increase at a lower rate until 1999.

Beginning in 1990, there has been a steady decrease in the accumulation rate of the positive cumulative residual which coincides with dredge disposal at HOODS (out of the ELC) and the dredge deepening project. The steady rate of decreasing sand accumulation since 1999 is a function of decreased fluvial sand loads, dredge disposal at HOODS, fluvial extraction, and increasing rates of sand loss from RSL.

For the hypothetical case of all dredged sand placement within the ELC (no HOODS disposal), the cumulative residual would have continued to increase from 1990 to 2000 and then the rate of accumulation would have decreased until about 2008. From 2008 to 2018 the cumulative rate for the hypothetical case slightly decreased. The difference between the two cumulative residuals is the volume of sand that has been disposed of at HOODS and out of the ELC during this period.

The large surplus of sand that has accumulated within the ELC from the mid-1950s to 1999 has contributed to shoreline growth documented during this period (McDonald, 2017; GHD 2018), inner-shelf sand storage, and dune growth. However, as described earlier, the 20-year period of decreased cumulative sand residual beginning in 1999 may be contributing to the documented periods of shoreline erosion between North Spit and Mad River (McDonald, 2017) and south of the Eel River (GHD, 2018) during this period.

As rates of sea-level rise continue to escalate, inner-shelf, shoreline, and estuary sand losses to RSL will inevitably increase. Presently, the most significant management action capable of slowing the rate of surplus cumulative sand loss is the strategic placement of dredged sand within the ELC, rather than continuing disposal at HOODS (outside of the ELC). While ongoing reductions in fluvial sand/gravel extraction would also contribute to offsetting the current negative sand residual (Figure 21) and slowing

the decline in surplus cumulative residual (Figure 23), it is crucial to acknowledge that fluvial extraction merely accounts for 19.4% of the total annual dredging/fluvial extraction volume. This further underscores the critical importance of placing Humboldt Bay dredged sand within the ELC.

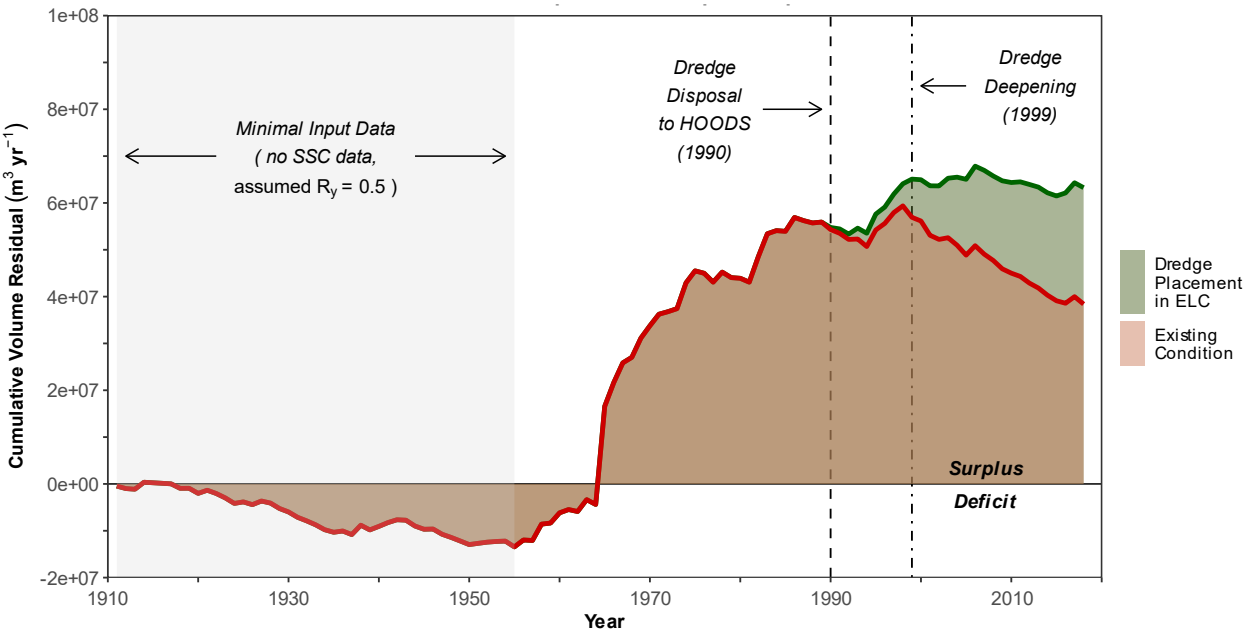

Figure 23. Cumulative time-dependent annual mean sand residual for the 1911-2018 sand budget analysis for the two cases: (1) existing conditions with dredged sand placement within the ELC prior to 1990 and disposal at HOODS out of the ELC after 1990 (green line and fill), and (2) hypothetical case of Humboldt Bay dredged sand placement within the ELC after 1990 and no HOODS disposal (red line and brown fill). Also shown is the period of minimal SSC data (1911 to 1954), when dredge disposal to HOODS (out of the ELC) begins (1990), and the Humboldt Bay dredge deepening project (1999).

5 SUMMARY

Owing to substantial land use and climate change, as well as coastal and fluvial engineering, the Eureka Littoral Cell watershed has experienced significant alterations in key hydrologic and geomorphologic processes that shape sediment transport and influence the littoral sediment budget. Development of an updated and refined sand budget for the ELC has provided a better understanding of temporal changes in fluvial sand loads, the repercussions of management decisions regarding Humboldt Bay dredging/disposal and fluvial sand/gravel extraction, the importance of different sand compartments (units) within the ELC sand budget, and the effects of rising sea-levels.

Our results strongly suggest that conventional static sediment rating curves do not adequately characterize the effect of these time-dependent alterations on fluvial transport of sand-size sediments. Indeed, our static vs. dynamic sand flux estimates diverge over time, such that the time-dependent estimates for the most recent decade (2009-2018) overestimate sand flux by 63%. Moreover, net loading of littoral sand to the ELC has been steadily declining since the mid-1960's and may be returning to pre-disturbance levels (e.g. on average, only 18% of the gross fluvial sand was delivered to the ELC since WY1999, whereas over 81% was delivered during 1965-1976).

The timelines of Humboldt Bay dredging, dredge placement/disposal, and fluvial sand/gravel extraction demonstrate that the management of these resources has a direct and potentially irreversible effect on the ELC sand supply. Pre-1990, dredged sand from Humboldt Bay was placed within the ELC, while post-1990, dredge disposal began at HOODS, out of the ELC. Beginning in 1992, CHERT oversight of fluvial sand/gravel extraction has resulted in steady decreases in fluvial extraction volumes. Since 2000 the combined dredge and fluvial extraction volumes of sand (>= 125μm) have averaged 1,090,483 m^3/yr, with dredging accounting for 80.6% of the annual average and fluvial extraction for 19.4%.

The 1966 to 2001 sand budget (sand >= 125μm) consisted of three input terms and seven output terms. The average total sand input for this period was 3,500,000 ± 239,000 m^3/y (mean ± SE), with fluvial inputs contributing ~89.5%, Humboldt Bay dredge placement within the ELC accounting for ~8.9%, and bluff erosion only providing ~ 1.9% of the total input. For the balanced sand budget, the largest output term was the inner-shelf storage which represents 33.7% of the total input. The combined Humboldt Bay dredging and fluvial sand/gravel extraction make up the second largest output term at 30.5%, followed by dune growth at 14.7%, then shoreline and estuary sand loss from *RSL* at 14.0%, and shoreline change at 7.1%.

Previous ELC sand budgets accounted for fewer input and output terms and the residual needed to close the sand budget was approximately 43.7% of the total input. Prior sand budgets also assumed that this sand was lost offshore to the continental shelf, deposited into the Eel Canyon, supplied beaches to the north, or transported south out of the ELC. In contrast, the 1966-2001 sand budget developed in this study, included nine known sand budget terms and was able to close within 14.7% of the total input. We assigned this residual term to dune storage, and the resulting dune growth rate of 10.0 m^3/(m·yr) aligned well with literature rates. Consequently, we feel that all sand outputs and storage terms were reasonably accounted for in the 1966-2001 sand budget. Inner-shelf storage, shoreline volume change, and losses of sand from RSL account for approximately 55% of the total sand input, underscoring their significance in the ELC sand budget. Previous ELC sand budgets did not explicitly account for these terms.

To better understand how changes in sand management and potential losses of sand to RSL affect the sand supply to the ELC, we conducted two time-dependent sand budgets covering the period 1911-2018. One budget represents existing conditions, reflecting actual Humboldt Bay dredge disposal and fluvial

sand/gravel extraction practices, while the other explores a hypothetical scenario where all dredged sand is placed within the ELC.

Results for existing conditions indicate that 1955 to 1990 was a period of positive sand residual, driven by the high fluvial loads during the 1960s to 1970s, where excess sand was available for inner-shelf storage, and shoreline and dune growth. However, beginning in 1990, the surplus sand residual was significantly reduced to near zero for a decade, coinciding with the start of dredged sand disposal to HOODS (out of ELC) and CHERT oversight of fluvial extraction. Since 1999, the ELC has been in a continuous 20-year period of sand deficit indicating that dredge disposal to HOODS, fluvial gravel extraction, and losses to RSL have outpaced sand inputs. We believe that this 20-year span of negative sand residual could be a driver of shoreline recession or dune loss, such as those occurring between North Spit and the Mad River, and south of the Eel River.

Findings from the hypothetical sand budget, where dredged sand was placed within the ELC and not disposed at HOODS, revealed that this change in dredged sand management significantly affects the sand residual. The period of positive sand residual within the ELC would have extended from 1955 to about 2005, and then would have remained near zero or balanced, effectively removing the 20-yr period of sand deficit.

As fluvial sand loads continue to decrease, and sand losses from RSL increase into the future with sea-level rise, we feel the primary management action to mitigate ELC sand loss is to place dredged sand within the ELC, instead of disposing it at HOODS (out of the ELC). While reductions in fluvial sand/gravel extraction would also help to offset the current loss of sand, it is important to note that fluvial extraction accounts for only 19.4% of the total annual dredging/fluvial extraction volume. This further highlights the critical importance of placing Humboldt Bay dredged sand within the ELC and underscores the need for data-driven adaptive sediment management strategies that prioritize coastal resilience and ecosystem health.

6 REFERENCES

Barrett (2004): https://escholarship.org/content/qt6000h2dc/qt6000h2dc.pdf?t=lnmran.

Best, T. C. and G.B. Griggs. 1991. A sediment budget for the Santa Cruz littoral cell, California. From Shoreline to Abyss. SEPM (Society for Sedimentary Geology), Special Publication No. 46, 35–50.

Borgeld, J.C. 1985. Holocene stratigraphy and sedimentation on the northern California continental shelf. Ph.D. Thesis, University of Washington, 177pp.

Brown, W.M., III and J.R. Ritter. 1971. Sediment transport and turbidity in the Eel River basin, California. U.S. Geological Survey Water Supply Paper 1986, 70 p.

Brownlie, W. R. and B.D. Taylor. 1981. Sediment management for the southern California mountains, coastal plains, and shoreline, Part C: coastal sediment delivery by major rivers in southern California. California Institute of Technology, Environ. Qual. Lab Rep. 17-C, 314 p.

Brunn, P. 1962. Sea level rise as a cause of shore erosion. Journal of Waterways and Harbors Division, American Society of Civil Engineers, 88, 117-130.

California Coastal Commission (CCC). Dec 2018. Corps Consistency Determination for 2019 Maintenance Dredging in Humboldt Bay, CD-0005-18. CCC file F 13c. San Francisco, CA.

California Coastal Commission (CCC). Feb 2017. Corps Consistency Determination for 2017 Maintenance Dredging in Humboldt Bay, CD-0002-17. CCC file W 14b. San Francisco, CA.

California Coastal Commission (CCC). Oct 2017. Corps Consistency Determination for 2018 Maintenance Dredging in Humboldt Bay, CD-0005-17. CCC file W 18a. San Francisco, CA.

California Geologic Society (CGS). 2002. Review of July 2002 EPA Analysis of Impacts of Timberland Management on Water Quality. Department of Conservation–California Geological Survey, Eureka, CA. November 2002.

California Trout (Caltrout), Stillwater Sciences, and Northern Hydrology & Engineering. 2018. Elk River Recovery Assessment: Recovery Framework. Prepared by California Trout, Arcata, California; Stillwater Sciences, Arcata, California; and Northern Hydrology & Engineering, McKinleyville, California for North Coast Regional Water Quality Control Board, Santa Rosa, California.

Chernick, M.R. 1999. "Bootstrap Methods, A Practitioner's Guide," Wiley, New York.

Cleveland, W.S. and J.D. Devlin. 1988. Locally Weighted Regression: An Approach to Regression Analysis by Local Fitting. Journal of the American Statistical Association, vol. 83, no. 403, pp. 596–610. JSTOR, www.jstor.org/stable/2289282.

Coastal Engineering Manual. 2003. Part V, Chapter 6: Sediment management and inlets. U.S. Army Corps of Engineers, Washington, D.C. Engineer Manual, EM 1110-2-1100.

California Coastal Sediment Management Workgroup (CSMW). August 2017. Eureka Littoral Cell, California, Coastal Regional Sediment Management Plan. Drafts through December 2013. Prepared by Moffatt & Nichol under contract to the U.S. Army Corps of Engineers, Los Angeles District.

Cohn, T. A. 1995. Recent advances in statistical methods for the estimation of sediment and nutrient transport in rivers. U.S. National Report to International Union of Geodesy and Geophysics, 1991-1994. Review of Geophysics, Supplement, p. 1117-1123.

Costa, S.L. and K.A. Glatzel. 2002. Humboldt Bay, Entrance Channel Report 1: Data Review. Report ERDC/CHL CR-02-1. U.S. Army Engineer Research and Development Center, Coastal and Hydraulics Laboratory, Vicksburg, MS.

County of Humboldt (Humboldt County). 1992. Final Program EIR (Environmental Impact Report) on gravel removal from the lower Eel River. Humboldt County Public Works Department, Natural Resource Division, Eureka, CA.

County of Humboldt (Humboldt County). 1993. Final Program Environmental Impact Report on gravel removal from the lower Mad River. Humboldt County Planning and Building Department, Planning Division, Eureka, CA.

County of Humboldt Extraction Review Team (CHERT). 2019. 2018 Post-Extraction Report. Prepared for County of Humboldt Board of Supervisors. Prepared by Randy Klein, Doug Jager, and Andre Lehre. https://humboldtgov.org/Archive/ViewFile/Item/1334.

Crockett, J.S. and C.A. Nittrouer. 2004. The sandy inner shelf as a repository for muddy sediment: an example from Northern California. Continental Shelf Research 24, 55-73.

Crockett, J.S. San Diego State University, personal communication.

De Cicco, L.A., Lorenz, D., Hirsch, R.M. and W. Watkins. 2018. dataRetrieval: R packages for discovering and retrieving water data available from U.S. federal hydrologic web services. doi: 10.5066/P9X4L3GE, https://code.usgs.gov/water/dataRetrieval.

Dean, R.G. and R.A. Dalrymple. 2002. Coastal processes with engineering applications. Cambridge University Press, New York, NY.

Duan, N. 1983. Smearing estimate: a nonparametric retransformation method. Journal of the American Statistical Association, Vol. 78, No. 383, pp. 605-610.

Ebisuzaki, W. 1997. A method to estimate the statistical significance of a correlation when the data are serially correlated. J. Clim. 10, 2147–2153.

Edwards, T.K. and G.D. Glysson. Field methods for measurement of fluvial sediment U.S. Geological Survey, Techniques of Water-Resources Investigations (1999) (Book 3, Chapter C2, 97 pp.).

Frederikse, T., Landerer, F., Caron, L., Adhikari, S., Parkes, D., Humphrey, V. W., Dangendorf, S., Hogarth, P., Zanna, L., Cheng, L. and Y.-H. Wu. 2020. The causes of sea level rise since 1900. Nature, 584, 393–397. https://doi.org/10.1038/s41586-020-2591-3.

George, D.A. and P.S. Hill. 2008. Wave climate, sediment supply and the depth of the sand-mud transition: A global survey. Marine Geology 254, 121-128.

GHD, 2018. Coastal dune and vulnerability and adaption study, Eel River shoreline trends. Prepared for the Humboldt Coastal Resilience Project (formally Dunes Climate Ready Project), Friends of the Dunes. GHD, Eureka, CA.

GHD, 2021. Marine Resources Biological Evaluation Report, Samoa Peninsula Land-based Aquaculture Project. Prepared for Nordic Aquafarms, California. GHD, Eureka, CA.

Glogoczowski, M. and P. Wilde. 1971. River Mouth and Beach Sediments, Russian River, California to Rogue River, Oregon, Part A: Introduction and Grain Size Analysis. Berkeley, California: University of California Hydraulic Engineering Laboratory, Report HEL 2-36, 73

Goñi, M.A., Hatten, J.A., Wheatcroft, R.A. and J.C. Borgeld. 2013. Particulate organic matter export by two contrasting small mountainous river systems from the Pacific Northwest, U.S.A. J. Geophys. Res. Biogeosci. 118, http://dx.doi.org/10.1002/jgrg.20024.

Graham Matthews & Associates (GMA). 2007. Mad River Sediment Source Analysis. Report to Tetra Tech, Inc. GMA, Weaverville, CA.

Hadley, R. F.; Lal, R.; Onstad, C. A.; Walling, D. E. and A. Yair. 1985. Recent developments in erosion and sediment yield studies. UNESCO Tech. Doc. Hydrol., 125 p.

Hallermeier, R. J. 1981. Seaward Limit of Significant Sand Transport by Waves: An Annual Zonation for Seasonal Profiles. Coastal Engineering Technical Aid No. 81-2. U.S. Army Corps of Engineers, Coastal Engineering Research Center, Fort Belvoir, VA.

Hapke, C.J., Reid, D., Richmond, B.M., Ruggiero, P. and J. List. 2006. National assessment of shoreline change: Part 3: Historical shoreline changes and associated coastal land loss along the sandy shorelines of the California coast: U.S. Geological Survey Open-file Report 2006-1219.

Harley, M. D., Masselink, G., Ruiz de Alegría-Arzaburu, A., Valiente, N. G. and T. Scott. 2022. Single extreme storm sequence can offset decades of shoreline retreat projected to result from sea-level rise. Communications Earth & Environment, 3(1), 112.

Harris, C.K. and P.L. Wiberg. 2002. Across-shelf sediment transport, interactions between suspended sediment and bed sediment. J. Geophys. Res., 107(C1), 3008.

Helsel, D.R., Hirsch, R.M., Ryberg, K.R., Archfield, S.A. and E.J. Gilroy. 2020. Statistical methods in water resources: U.S. Geological Survey Techniques and Methods, book 4, chapter A3, 458 p., https://doi.org/10.3133/tm4a3.

Hicks, D.M. and L.R. Basher. 2008. The signature of an extreme erosion event on suspended sediment loads: Motueka River Catchment, South Island, New Zealand. Sediment Dynamics in Changing Environments, 325. IAHS Publication, pp. 184–191.

Hicks, D.M., Gomez, B. and N.A. Trustrum. 2000. Erosion thresholds and suspended sediment yields: Waipaoa River basin, New Zealand. Water Resour. Res. 36, 1129–1142.

Himmelstoss, E.A., Henderson, R.E., Kratzmann, M.G. and A.S. Farris. 2021. Digital Shoreline Analysis System (DSAS) version 5.1 user guide: U.S. Geological Survey Open-File Report 2021–1091, 104 p., https://doi.org/10.3133/ofr20211091.

Hines, W.W. and D.C. Montgomery. 1990. Probability and Statistics in Engineering and Management Science, third edition. John Wiley & Sons, Inc. New York.

Hirsch, R.M. 1982. A comparison of four streamflow record extension techniques. Water Resources Research, 18 (4), 1081–1088.

Hirsch, R.M., Archfield S.A. and L.A. De Cicco. 2015. A bootstrap method for estimating uncertainty of water quality trends, Environmental Modelling & Software, 73:148-166.

Humboldt Bay Harbor Recreation and Conservation District (HBHRCD) and U.S. Army Corps of Engineers, San Fracisco District (COE). 1995. Final Feasibility Report and Environmental Impact Statement/Report for Navigation Improvements, Humboldt Harbor and Bay (Deepening), Humboldt County, CA. Prepared HBHRCD and U.S. Army Corps of Engineers, San Francisco District.

Inman, D. L. and S.A. Jenkins. 1999. Climate change and the episodicity of sediment flux of small California rivers. J. Geol. 107:251–270.

Kaminsky, G.M., Ruggiero, P., Buijsman, M.C., McCandless, D. and G. Gelfenbaum. 2010. Historical evolution of the Columbia River littoral cell. Mar. Geol. 273 (1-4), 96–126.

Kelsey, H. M. 1980. A sediment budget and an analysis of geomorphic process in the Van Duzen River basin, north coastal California, 1941–1975. Geological Society of America Bulletin, 91(4_Part_II), 1119-1216.

Kinnetic Laboratories Incorporated (KLI). 2016. Humboldt Harbor and Bay O&M dredging grain size verification and Tier III evaluation sampling and analysis results. Prepared for U.S. Army Corps of Engineers, San Francisco District. KLI, Santa Cruz, CA.

Klein, R. personal communication.

Klein, R.D. and J.K. Anderson. 2012. Declining sediment loads from Redwood Creek and the Klamath River, north coastal California. Proceedings of the Coastal Redwood Forests in a Changing California: A Symposium for Scientists and Managers, U.S. Department of Agriculture, Forest Service General Technical Report PSW-GTR-238, p. 79-88.

Kohl, M. 2023. MKinfer: Inferential Statistics. R package version 1.1. https://www.stamats.de.

Komar, P. D. 1988. Beach processes and sedimentation, second edition. Prentice-Hall Inc., Upper Saddle River, NJ.

Kraus, N.C. and J.D. Rosati. 1998. Formulation of sediment budgets at inlets. Coastal Engineering Technical Note CETN IV-16. U.S. Army Corps of Engineers, Waterways Experiment Station, Coastal and Hydraulics Laboratory, Vicksburg, MS.

Lehrter, J.C. and J. Cebrian. 2009. Uncertainty propagation in an ecosystem nutrient budget. Ecological Applications, 20 (2), pp. 508-524.

Leroy, T. Pacific Watershed Associates, personal communication.

Limber, P.W, Patsch, K.B. and G.B. Griggs. 2008. Coastal sediment budgets and the littoral cutoff diameter: a grain size threshold for quantifying active sediment Inputs. Journal of Coastal Research - J COASTAL RES. 24. 122-133. 10.2112/06-0675.1.

Mackey, B. H. and J.J. Roering. 2011. Sediment yield, spatial characteristics, and the long-term evolution of active earthflows determined from airborne LiDAR and historical aerial photographs, Eel River, California. Bulletin, 123(7-8), 1560-1576.

McDonald, K. 2017. Historical shoreline analysis for Humboldt Bay, California, shoreline change along coastal dunes from Table Bluff to Trinidad, 1939-2016. Prepared for the Humboldt Coastal Resilience Project (formally Dunes Climate Ready Project), Friends of the Dunes. U.S. Fish and Wildlife Service, Arcata, CA.

Meyer, A.L and A.L. Chester. 1977. The stabilization of Clatsop Plains, Oregon. Shore and Beach, Vol. 45, No. 4, pp. 34-41.

Meyers, S.R. 2014. Astrochron: An R Package for Astrochronology. https://cran.r-project.org/package=astrochron.

Montillet, J.-P., Melbourne, T. I. and W. M. Szeliga. 2018., GPS vertical land motion corrections to sea-level rise estimates in the pacific northwest. Journal of Geophysical Research: Oceans, 123(2), 1196–1212.

Nittrouer, C.A., Austin, J.A., Field, M.E., Kravitz, J.H, Syvitski, J.P.M. and P.L. Wiberg (Editors). 2007. Continental Margin Sedimentation: From Sediment Transport to Sequence Stratigraphy. International Association of Sedimentologists, Special Publication Number 37, Blackwell Publishing; Malden, MA.

Ogston, A.S. and R.W. Sternberg. 1999. Sediment-transport events on the norther California continental shelf. Marine Geology, Vol. 154, p. 69-82.

Patsch, K.B. and G.B. Griggs. 2006. Littoral Cells, Sand Budgets, and Beaches: Understanding California's Shoreline. Institute of Marine Sciences, University of California, Santa Cruz, and California Coastal Sediment Management Work Group. 39 p.

Patsch, K.B. and G.B. Griggs. 2007. Development of Sand budgets for California's Major Littoral Cells. Institute of Marine Sciences, University of California, Santa Cruz, and California Sediment Management Work Group. 115 p.

Patton, J. R., Williams, T.B., Anderson, J.A., Hemphill-Haley, M., Burgette, R.J., Weldon, R. II, McPherson, R.C., and T.H. Leroy. 2023. 20th to 21st Century Relative Sea and Land Level Changes in Northern California: Tectonic Land Level Changes and their Contribution to Sea-Level Rise, Humboldt Bay Region, Northern California in Tektonika, v. 1, no. 1, https://doi.org/10.55575/tektonika2023.1.1.6.

Pequegnat, J. E., Mondeel-Jarvis, D., Bott, L. and J. Matos. 1995. Sediment characteristics, benthic infauna, demersal fish and macroinvertebrates sampled September 1994 - Volume 1.

Pequegnat, J.E., Mondeel-Jarvis, D., Borgeld, J.C. and L. Bott. 1990. Sediment characteristics, benthic infauna, demersal fish and macroinvertebrates: Analysis of communities found offshore in water between 18 and 73 meters deep west of Humboldt Bay, California, and at the nearshore disposal site (August 1989, November 1989, and March 1990). San Francisco, CA. U.S. Army Corps of Engineers.

Reid, K. 2011. An assessment of ravel bar texture and composition following in-channel mining in the Mad River, California. Master's thesis. Natural Resources, Watershed Management. Humbold State University, Arcata, CA.

Rosati, J.D. and N.C. Kraus. 1999. Formulation of sediment budgets at inlets. Coastal Engineering Technical Note CETN IV-15. U.S. Army Corps of Engineers, Waterways Experiment Station, Coastal and Hydraulics Laboratory, Vicksburg, MS.

Ross, B. U.S. Environmental Protection Agency, personal communication.

Ruggiero, P., Kaminsky, G.M., Gelfenbaum, G. and N. Cohn. 2016. Morphodynamics of prograding beaches: A synthesis of seasonal- to century-scale observations of the Columbia River littoral cell. Marine Geology, Vol. 376, p. 51-68.

Rustomji, P. and Wilkinson, S. N. 2008. Applying bootstrap resampling to quantify uncertainty in fluvial suspended sediment loads estimated using rating curves, Water Resour. Res., 44, W09435, doi:10.1029/2007WR006088.

Scheffner, N. W. 1992. Dispersion analysis of the Humboldt Bay, California, interim offshore disposal site. Prepared for U.S. Army Corps of Engineers, San Francisco District. Prepared by Coastal Engineering Research Center, Waterways Experiment Station, Corp of Engineers, MS.

Schmelter, M. L., S. O. Erwin, and P. R. Wilcock. 2012. Accounting for uncertainty in cumulative sediment transport using Bayesian statistics. Geomorphology 175, p. 1-13.

Shore Protection Manual (SPM). 1984. Volume I, Chapter 4, Littoral Processes; Volume II, Chapter 6, Structural Features. U.S. Army Corps of Engineers, Coastal Engineering Research Center, Waterways Experiment Station, Vicksburg, Mississippi.

Slaets, J. I. F., Piepho, H.-P., Schmitter, P., Hilger, T., and Cadisch, G.. 2017. Quantifying uncertainty on sediment loads using bootstrap confidence intervals, Hydrol. Earth Syst. Sci., 21, 571–588, https://doi.org/10.5194/hess-21-571-2017.

Slagel, M. and G.B. Griggs. 2006. Cumulative Losses of sand to the California coast by dam impoundment. Final Report to the California Coastal Sediment Management Workgroup and the California Department of Boating and Waterways. Institute of Marine Sciences, University of California, Santa Cruz. 41 p.

Sommerfield, K.C. and C.A. Nittrouer. Modern accumulation rates and sediment budget for the Eel shelf: a flood-dominated depositional environment. Marine Geology 154, 227-241.

Tchobanoglous, G. and E.D. Schroder. 1985. Water quality characteristics, modeling, and modification. Addison-Wesley, Reading, MA.

Thorne, K., MacDonald, G., Guntenspergen, G., Ambrose, R., Buffington, K., Dugger, B., Freeman, C., Janousek, C., Brown, L., Rosencranz, J., Holmquist, J., Smol, J., Hargan, K. and J. Takekawa. 2018. U.S. Pacific coastal wetland resilience and vulnerability to sea-level rise. Sci. Adv. 4, o3270, 10.1126/sciadv.aao3270.

U.S. Army Corps of Engineers (COE). 1989. Zone of Siting Feasibility Analysis for the Humboldt Harbor and Bay Ocean Dredged Material Disposal Site. San Francisco District of COE. Attached to EPA (1995).

U.S. Army Corps of Engineers (COE). 2012. Five-Year Programmatic Environmental Assessment and 404 (b)(1) Analysis, Humboldt Harbor and Bay Operation and Maintenance Dredging (FY 2012 -FY 2016). COE San Francisco District.

U.S. Army Corps of Engineers (COE). 2017. Environmental Assessment and Draft FONSI, Humboldt Harbor and Bay Operation and Maintenance Dredging. COE San Francisco District.

U.S. Army Corps of Engineers (COE). 2022. Ocean Dredged Material Disposal Site Database. Environmental Laboratory, U.S. Army Engineer Research and Development Center. Retrieved (1/27/ 2023) from http://odd.el.erdc.dren.mil/.

U.S. Environmental Protection Agency, Region 9 (EPA) and U.S. Army Corps of Engineers, San Fracisco District (COE). 2020. Evaluation and Environmental Assessment for Expansion of the Existing Humboldt Open Ocean Disposal Site (HOODS) Offshore of Eureka, California. Prepared by EPA Region 9 and U.S. Army Corps of Engineers, San Francisco District.

U.S. Environmental Protection Agency, Region IX (EPA). 1995. Designation of an ocean dredged material disposal site off Humboldt Bay, California. Final environmental impact statement. July. San

Francisco, CA. Prepared in association with Jones & Stokes Associates, Inc. (JSA 93-197 and 94-253.) Bellevue, WA.

U.S. Global Change Research Program. (2018). National Climate Assessment 2018: Chapter 8: Coastal Effects. Retrieved from https://nca2018.globalchange.gov/chapter/8/.

United Nations Atlas of the Oceans. (n.d.). Retrieved from https://www.oceansatlas.org/subtopic/en/c/114/.

Vasilopoulos. G., Quan, Q.L., Parsons, D.R., Darby, S.E., Tri, V.P.D., Hung, N.N., Haigh, I.D., Voepel, H.E., Nicholas, A.P. and R Aalto. 2021. Establishing sustainable sediment budgets is critical for climate-resilient mega-deltas. Environmental Research Letters, Volume 16, Number 6.

Vigiak, O. and U. Bende-Michl. 2013. Estimating bootstrap and Bayesian prediction intervals for constituent load rating curves, Water Resour. Res., 49, 8565–8578.

Wang, J., Church, J.A., Zhang, X. and C. Xianyao. 2021. Reconciling global mean and regional sea level change in projections and observations. Nat Commun 12, 990.

Wang, X. and X. Ji. 2020. fANCOVA: Nonparametric Analysis of Covariance. R package version 0.6-1. https://CRAN.R-project.org/package=fANCOVA.

Warrick, J. A., Madej, M. A., Goñi, M. A. and R.A. Wheatcroft. 2013. Trends in the suspended-sediment yields of coastal rivers of northern California, 1955–2010. Journal of hydrology, 489, 108-123.

Warrick, J.A. 2014. Eel River margin source-to-sink sediment budgets: Revisited. Marine Geology 351, 25–37.

Warrick, J.A, Melack, J.M. and B.M. Goodridge. 2015. Sediment yields from small, steep coastal watersheds of California. Journal of Hydrology: Regional Studies, Volume 4, Part B, p. 516-534. https://www.sciencedirect.com/science/article/pii/S2214581815000981.

Wheatcroft, R.A. and J.C. Borgeld. 2000. Oceanic flood deposits on the norther California shelf: large-scale distribution and small-scale physical properties. Continental Shelf Research 20, p. 2163–2190.

Wiberg, P.L. 2000. A perfect storm, formation and potential from preservation of storm beds on the continental shelf. Oceanography, Vol. 13, No. 3, p. 93-99.

Willis, C.M. and G.B. Griggs. 2003. Reductions in Fluvial Sediment Discharge by Coastal Dams in California and Implications for Beach Sustainability. Journal of Geology. 111, 167-182.

Winkelman, J., Schaaf, D. and T.R. Kendall. 1999. Humboldt Beach and Dune Monitoring. In: Ewing, L., Magoon, O.T. and S. Robertson, editors; Sand Rights ‘99, Bringing Back the Beaches, September 23-26, 1999, Ventura, California. ASCE, p. 176-190.

Wright, S. A., and D. H. Schoellhamer. 2005. Estimating sediment budgets at the interface between rivers and estuaries with application to the Sacramento–San Joaquin River Delta, Water Resour. Res., 41, W09428, doi:10.1029/2004WR003753.

Yanai, R.D., Battles, J.J., Richardson, A.D., Blodgett, C.A., Wood, D.M. and E.B. Rastetter. 2010. Estimating uncertainty in ecosystem budget calculations. Ecosystems 13, 239-248.